Studies on Expression and Function of *Vsig1* Gene

Dissertation

zur Erlangung des Doktorgrades

der Mathematisch-Naturwissenschaftlichen Fakultäten

der Georg-August-Universität zu Göttingen

vorgelegt von

Maiada Moustafa

aus Kairo, Ägypten

Göttingen, 2011

D7

Referent: **Prof. Dr. W. Engel**

Korreferentin: **Prof. Dr. S. Hoyer-Fender**

Tag der mündlichen Prüfung:

Abbreviations

ABI	Applied Biosystem Instrument
ATP	Adenosintriphosphate
bp	base pair
BSA	Bovine serum albumin
°C	Degree Celsius
cDNA	complementary DNA
Cy3	indocarbocyanine
dATP	Desoxyriboadenosintnphosphate
dH2O	distil Water
DAPI	Diamidino-2-phenylindoledihydrochloride
DMSO	Dimethyl sulfoxide
DEPC	Diethylpyrocarbonate
DNA	Deoxyribonucleic acid
DNase	deoxyribonuclease
dNTP	deoxynucleotidetriphosphate
dpc	day post coitus
dT	deoxythymidinate
DTT	Dithiothreitol
EDTA	Ethylene diamine tetraacetic acid
ES	Embryonic stem
g	gravity
gm	gram
HEPS	N-(-hydroxymethyl)piperazin,N'-3-propansulfoneacid
HPLC	High performance liquid chromatograpy
hr(s)	hour(s)IGL
IgG	Immunoglobulin G
JL	Jackson Laboratory
kb	kilobase
LB	Luria-Bertrani
M	molarity
MOPS	3 - [N-Morpholino] -Propaneslilfate
mRNA	messenger Ribonucleic acid
mg	milligram
ml	millileter
µl	microliter
min	minute
NaAc	Sodium acetate
NBT	Nitro-blue tetrazolium
NCBI	National Center for Biotechnology Information
Neo	Neomycin
ng	nanogram
nm	nanometer
NTP	Nucleotidetriphospate
OD	Optimal density

ORF	Open Reading Frame
PAGE	Polyacrylamide Gel Electrophoresis
PCR	Polymerase chain reaction
pH	Preponderance of hydrogen ions
PBS	Phosphatebuffersaline
PMSF	Phenylmethylsulfonyl fuoride
RNA	Ribonucleic acid
Rnase	Ribonuclease
rpm	revolution per minute
RT	Room temperature
RT-PCR	Reverse transcriptase-PCR
SDS	Sodium Dodecylsulfate
SDS-PAGE	SDS-Polyacrylamide Gel Electrophoresis
sec	Second
TBE	Tris-Borate-EDTA-Elecrrophoresis buffer
TE	Tris-EDTA buffer
Tris	Trihydroxymethylaminomethane
U	Unit
UV	Ultra violet
V	Voltage

Table of Contents

1-Introduction:

1.1- Immunoglobulin Superfamily

The adhesion molecules have essential roles in many events including tissue patterning, morphogenesis and organizing cell-cell adhesion (Gumbiner, 1996). Cell adhesion molecules are divided into four major families: the cadherins, integrins, selectines and members of the immunoglobulin superfamily (IgSF).

IgSF is a large group of cell surface and soluble proteins that are involved in the recognition, binding, or adhesion processes of cells. IgSF was reported to be the most popular superfamily of proteins in the human genome with 765 identified members (Lander *et al*., 2001). Members of this superfamily are characterized by the presence of immunoglobulin-like domains (Ig-like) with amino acid sequence similar to immunoglobulins (Barclay, 2003). Ig-like domains are located in the extracellular N-terminal region of molecules, which can interact with other molecules of the opposite cell membranes in homotypic or heterotypic manner. These domains consist mainly of about 100 amino acids that could be split into two categories based on function and size of variable-domain (V-domain) and constant-domain (C-domain) (Barclay, 2003).

The number of Ig-like domains in each member of this family varies from one in CD7, CD8, CD47 (Barclay, 2003), two in JAM-A (Bazzoni, 2003), three in Nectin (Takai *et al*, 2003), five in N-Cadherin (Semb and Christofori, 1998) and 17 in sialoadhesin (Barclay, 2003). Most proteins, which have Ig-like domains, are type I membrane proteins with a single transmembrane region (Barclay, 2003, Andreeva *et al*, 2009). Beside the exracellular N-terminal region, members of IgSF contain a transmembrane domain and cytoplasmic tail at C-terminus. The cytoplasmic tail of many adhesion proteins is linked to the actin cytoskeleton through many peripheral membrane

proteins, such as catenin, partitioning defective (PAR) and Zona occludens (ZO), which strengthens the cell-cell adhesion and establishes the epithelial cell polarization (Gumbiner, 2000).

Vsig1 gene is a novel member of the IgSF, localized at X-chromosome and consists of 7 exons. Analysis of the primary structure of murine VSIG1 revealed that the protein has an extracellular domain with two immunoglobulin-like domains at positions 29-139 and 154-220, a single transmembrane domain at position 237-259, and a short cytoplasmic tail at position 322-388 (Fig. 1.1) (Oidovsambuu, 2009). Analysis of the hydrophobicity of the mVSIG1 sequence indicates that the protein contains two hydrophobic domains at positions 1-12 and 237-259, and this hydrophobic domain which is at the N-terminus is similar to that of other signal peptide sequences (Oidovsambuu, 2009). The signal peptide of mVSIG1 consists of 12 amino acids and contains 9 hydrophobic amino acids. The extracellular region of VSIG1 contains 6 sites of potential N-linked glycosylation. The predicted molecular weight of VSIG1 is 47-kDa, while the affinity purified VSIG1 antibody recognizes an approximately 55-kDa protein in stomach. Enzymatic digestion of stomach extract with N-Glycosidase-F enzyme which removes N-linked oligosaccharides, revealed the presence of large amounts of N-linked glycosyl residues in VSIG1 (Oidovsambuu, 2009).

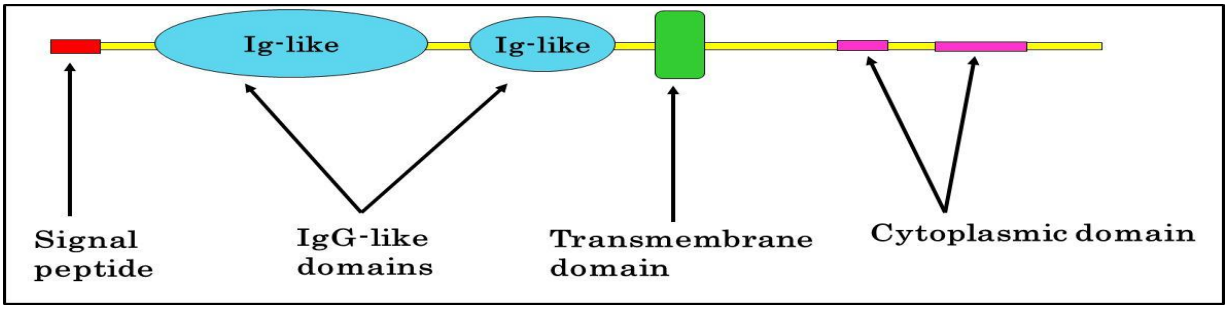

Figure 1.1: *Simple diagram showing the predicted structure of murine VSIG1 protein. There are five predicted domains which are signal peptide (red), two Ig-like domains (blue), transmembrane domain (green) and cytoplasmic domain (pink).*

VSIG1 belongs to CTX/JAM subclass of the immunoglobulin superfamily. Members of the CTX (cortical thymocyte marker in Xenopus) family are localized at the tight junctions (Tj) and adhesion junctions (Aj) of epithelial and endothelial cells, and mediate cell-cell adhesion (Bazzoni et al., 2003). CTX/JAM subfamily proteins contain a conserved extracellular domain, while the cytoplasmic domain is the least conserved region of the protein. A phylogenetic tree based on a multiple sequence alignment of the amino acid of CTX family members revealed that the closest relative to CAR (coxsackie- and adenovirus receptor) is CLMP (CAR-like membrane protein), followed by brain- and testis-specific immunoglobulin superfamily (BT-IgSF) and endothelial cell-selective adhesion molecule (ESAM), and these molecules form a new group within the larger CTX family. Since CAR was the first one to be identified, this group of proteins was tentatively named the CAR group. Likewise, JAM-1, -2, and -3, and CTX and A33, were phylogenetically separated from the CAR group, which have been called JAM and CTX groups, respectively (Fig. 1.2A) (Raschperger et al., 2004). Alignment of the amino acid sequences of VSIG1 and other members of CTX/JAM subfamily shows that the amino acid sequence of the VSIG1 is 31%, 27%, 29%, 26%, 27%, 24%, 31%, 28% and 30% identical to CTX, JAM-1, -2, -3, ESAM, CAR, IgSF11, Gpa33 and CLMP, respectively. It was also reported that the extracellular domain of the CTX/JAM subfamily proteins is conserved, while the cytoplasmic domain is the least conserved region of the protein (Fig. 1.2B) (Oidovsambuu, 2009).

The sequence of *Vsig1* cDNA contains two predicted polyadenylation sites that are spanning 0.7 kb. Northern blot analysis using a cDNA probe containing the coding sequence of cytoplasmic domain revealed that this cDNA probe detected a 2.7kb transcript in stomach and two transcripts of 2.7kb and 1.5kb in testis of adult mice. Expression level of the 1.5kb transcript in testis was higher than that of the 2.7kb. No *Vsig1* transcript could be detected in other tissues.

Analysis of *Vsig1* expression pattern during pre- and postnatal development revealed that, *Vsig1* is initially expressed in E13.5 and the expression level is increased in E14.5 E17.5 and postnatal stomach (Oidovsambuu, 2009).

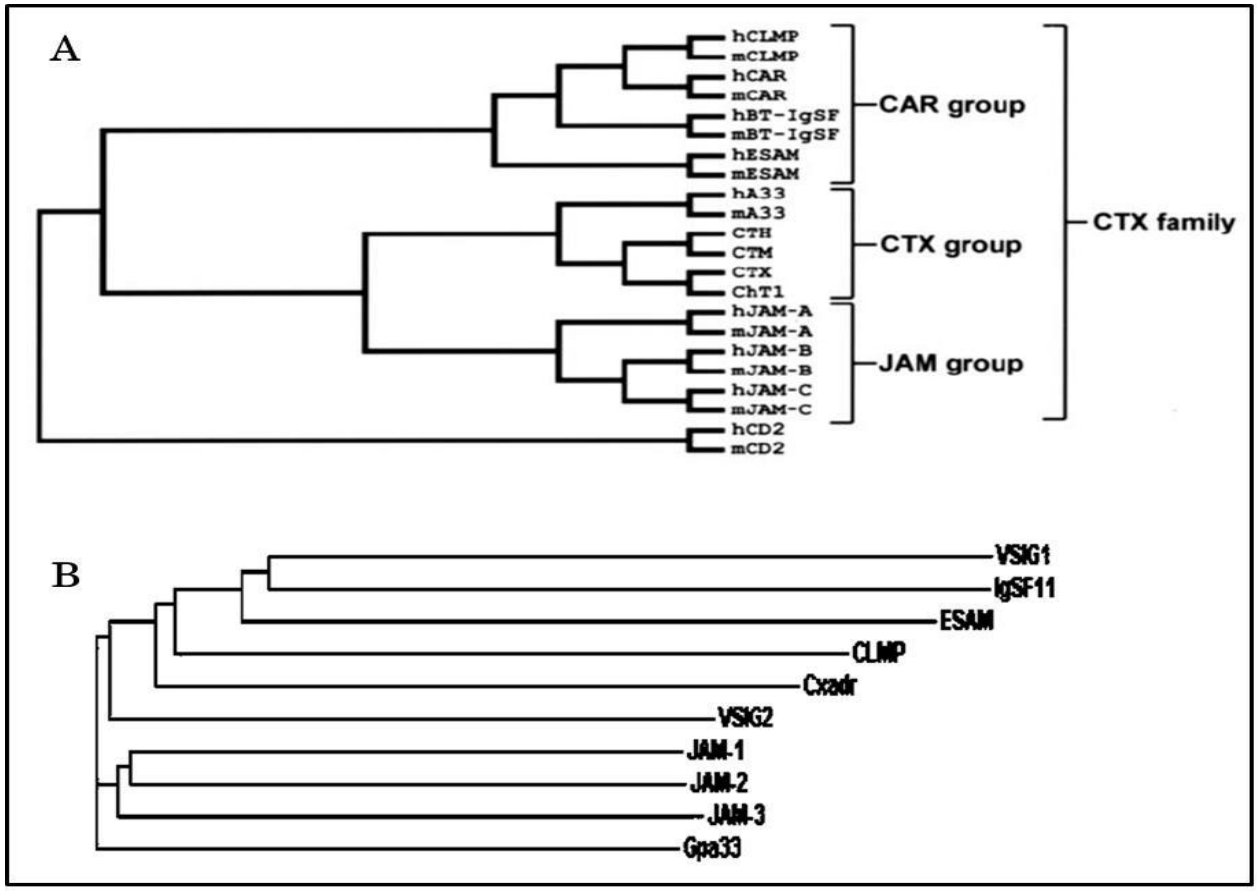

Figure 1.2: *Phylogenetic trees show (A) the classification of CTX family into groups based on a multiple sequence alignment of the amino acid sequences (Raschperger et al., 2004). (B) Relationship between VSIG1 protein and the other CTX family members (Oidovsambuu, 2009).*

A murine stomach consists of two distinct regions, the anterior and the posterior region. The anterior region (forestomach) is lined with a multilayer of squamous epithelium, which shows cornification and is almost identical to the esophageal epithelium. The posterior region of stomach is lined with a monolayer of columnar epithelium, which forms gastric units. The stomach posterior region can be subdivided into two regions: corpus and antrum, which are different as their unique features of gastric glands. The immunohistochemistry analysis showed that VSIG1 is

specifically expressed in glandular epithelium of posterior region of stomach. No VSIG1 expression could be detected in squamous epithelium in anterior stomach (Oidovsambuu, 2009). The VSIG1 protein is localized in the plasma membrane of all cells of gastric glands and is most intense in the basolateral membrane of epithelial cells in pit region (Oidovsambuu, 2009).

Vsig1-EGFP transgenic mice were generated in Institute of Human Genetics, Göttingen, in which the expression of EGFP gene is under the control of the 5´-region of *Vsig1*gene. The analysis of E18.5 and adult stomachs from *Vsig1*-EGFP transgenic mice showed that GFP fluorescence was restricted to the corpus and atrium region of E18.5 stomach (Oidovsambuu, 2009).

1.2- The phenotype of *Vsig1* knockout mice

To determine the physiological function of murine *Vsig1* function in mammals, a conventional *Vsig1* knockout construct was generated (Oidovsambuu, 2009). Following electroporation of embryonic stem cells (ESCs) with the targeting construct and drug selection, homologous recombinant ESC clones were isolated ($Vsig1^{-/Y}$). Injection of two $Vsig1^{-/Y}$ ESC clones into blastocysts resulted in 28 male chimeras. All of the generated chimeric mice had low chimerism and targeted allele was not transmitted to their offspring. These results suggested that a high contribution of $Vsig1^{-/Y}$ cells to the embryos causes lethality of chimeric embryos. Immunohistochemical analysis of the stomachs from adult chimeric mice showed that some regions of glandular epithelium in the hind stomach contain VSIG1-negative cells. In contrast to the neighboring $Vsig1^{+/Y}$ epithelium, the VSIG1-deficient epithelium did not express H^+/K^+-ATPase, which is a marker of the parietal cells in the glandular epithelium. Furthermore, immunohistological analysis revealed that the cytokeratin 5, a marker of squamous epithelium of forestomach, is highly expressed in the VSIG1-deficient epithelium. These results indicated that

the deficiency of VSIG1 leads to transdifferentiation of glandular epithelium in distal stomach to squamous epithelium (Oidovsambuu, 2009).

1.3-Expression of human VSIG1 in gastric cancer

Recently, Scanlan *et al*. (2006) have analyzed VSIG1 (hVSIG1) expression in a variety of human cancers. They reported that human *VSIG1* is expressed in gastric cancer (31%), esophageal carcinomas (50%) and ovarian cancers(23%), but not in lung, breast or colon carcinomas (Scanlan et al, 2006). In our group, immunohistological analysis of sections of gastric carcinoma representing early, middle and late stage of tumor differentiation revealed that human VSIG1 protein is strongly detected in cell clusters containing poorly differentiated compact tumor cells in early stage of gastric carcinoma, and the expression is decreased in middle stage, while no expression was found in the late stage of gastric carcinoma (Oidovsambuu, 2009).

1.5- Objectives of this study:

To study the expression and functional analysis of *Vsig1* gene, scientific approaches undertaken were as follows:

- Expression pattern of *Vsig1* splice variants.
- Expression analysis of *Vsig1* in early embryonic stages.
- Expression analysis of murine *Vsig1* in testis.
- *In vitro* study of *Vsig1* expression.
- Analysis of conditional *Vsig1*-deficient mice.

- Analysis of Cyto-*Vsig1*transgenic mice, in which the *Vsig1*is ectopically expressed in squamous epithelium.

- Analysis of Villin-*Vsig1*transgenic mice, in which the *Vsig1*is ectopically expressed in intestinal epithelium.

2-Materials and Methods:

2.1- Materials:

2.1.1- Chemicals:

Acetic acid	Merck, Darmstadt
Agar	Difco, Detroit, USA
Agarose	Peqlab, Erlangen
Ammonium acetate	Fluka, Neu Ulm
Ampicillin	Sigma, Deisenhofen
Ampuwa	Fresenius, Bad Homburg
Aprotinin	Sigma, Deisenhofen
Aqua Poly/Mount	Polysciences, Inc, USA
Bacto-Peptone	Roth, Karlsruhe
Bacto-Yeast-Extract	Roth, Karlsruhe
Blocking powder	Roth, Karlsruhe
Boric acid	Roth, Karlsruhe
BSA	Biomol, Hamburg
Cell culture media	PAN-Systems, Nürnberg
Chemiluminescent Substrate	Pierce, Rockford, IL
Chloroform	Baker, Deventer, NL
Coomasie G-250	Sigma, Deisenhofen
DAPI (Vectashield)	Vector, Burlingame
Diethyl pyrocarbonate (DEPC)	Sigma, Deisenhofen
Dimethyl sulfoxid (DMSO)	Merck, Darmstadt
Dithiothreitol	Sigma, Deisenhofen

dNTPs (100mM)	Invitrogen, Karlsruhe
DNA ladders	Invitrogen, Karlsruhe
Dulbecco's Modified Eagle Medium (DMEM)	PAN, Aidenbach
Dye Terminator Mix	Applied Biosystems
Ethanol	J.T.Baker, Deventer, Niederlande
Ethidium bromide	Carl-Roth, Karlsruhe
Ethylenediaminetetraacetic acid (EDTA)	ICN Biomedicals, Eschwege
Eukitt-quick hardening mounting medium	Fluka, Neu Ulm
FCS	Gibco/BRL, Karlsruhe
Formaldehyde	Invitrogen, Karlsruhe
Formamide	Sigma, Deisenhofen
Glutaraldehyde	Sigma, Deisenhofen
Glycerol	Invitrogen, Karlsruhe
Glycine	Biomol, Hamburg
Goat serum	Sigma, Deisenhofen
HCl	Merck, Darmstadt
Isopropanol	J.T.Baker, Deventer, Niederlande
KCl	Merck, Darmstadt
Leupeptin	Sigma, Deisenhofen
Lipofectamine^{TM}2000	Invitrogen, Karlsruhe
M2 medium	Sigma, Deisenhofen
M16 medium	Sigma, Deisenhofen

MgCl2	Merck, Darmstadt
β-Mercaptoethanol	Serva, Heidelberg
MgCl2	Merck, Darmstadt
Milk powder	Roth, Karlsruhe
MOPS	Applichem, Darmstadt
NaCl	Applichem, Darmstadt
Na_2HPO_4	Merck, Darmstadt
NaH_2PO_4	Merck, Darmstadt
NaOH	Merck, Darmstadt
Nonidet P40	Fluka, Neu Ulm
NuPAGE Novex Bis-Tris 4-12% Gel	Invitrogen, Karlsruhe
NuPAGE MOPS SDS running buffer	Invitrogen, Karlsruhe
NuPAGE SDS sample buffer	Invitrogen, Karlsruhe
OPTI-MEM I	Invitrogen, Karlsruhe
Paraformaldehyde	Merck, Darmstadt
Penicillin/Streptomycin	PAN, Aidenbach
peqGOLDTriFast	Peqlab, Erlangen
Phalloidin	Sigma, Deisenhofen
Phenol	Biomol, Hamburg
Phosphate buffered saline PBS	PAN-Systems, Nürnberg
Picric acid	Fluka, Neu Ulm
Proteinase K	Roche, Penzberg
Protein marker	Biorad, Sigma
[32P]-dCTP	Amersham Pharmalia, Braunschweig

Rapid-hybridization Puffer	Amersham, Freiburg
RIPA buffer	Pierce, Rockford, IL
RediprimeTM II	Amersham Pharmacia, Freiburg
RNase Inhibitor	Boehringer, Mannheim
RNA length standard	Invitrogen. Karlsruhe
Saccharose	Roth, Karlsruhe
Salmon sperms DNA	Sigma, Deisenhofen
SeeBlue® plus2 Pre-Stained Standard	Invitrogen, Karlsruhe
S.O.C Medium	Invitrogen, Karlsruhe
Sodium acetate	Merck, Darmstadt
Sodium citrate	Merck, Darmstadt
sodium dodecyl sulfate (SDS)	Serva, Heidelberg
SuperScript II	Invitrogen, Karlsruhe
Tris	Sigma, Deisenhofen
T4 DNA ligase	Promega, Mannheim
Tamoxifen	Sigma, Deisenhofen
TRI reagent	Sigma, Deisenhofen
Triton X-100	Serva, Heidelberg
Trypsin	PAN-Systems, Nürnberg
Tween-20	Promega, Mannheim
Xylene	Merck, Darmstadt

All those chemicals, which are not mentioned above, were ordered from Merck, Darmstadt, or Roth, Karlsruhe.

2.1.2 Solutions, buffers and media

All those chemicals, which are not mentioned below, were ordered from Merck,

Darmstadt or Roth, Karlsruhe.

Blocking buffer (10x)	40.913 g NaCl 6.057 g Tris in 500 ml dH20 adjust pH to 7.5
Blocking buffer B1 (1x)	50 ml 10 x blocking puffer 500 µl Tween-20 450 ml dH20
Bouin's solution	15 volumes of Picric acid (in H2O) 5 volumes Formaldehyde (37%) 1 volume Acetic acid
Blocking solution (immunostaining)	5% BSA 1% Tween-20 in dPBS
Denaturation solution	1.5 M NaCl 0.5 M NaOH
DEPC-H2O	0.1% (v/v) Diethylpyrocarbonate
E-buffer (10x)	300 mM NaH2PO4 50 mM EDTA
Formalin Fixative Solution	4% Paraformaldehyde in dPBS
Hypotonic buffer	0.1 g HEPES (pH 7.2) 0.042 g $MgCl_2$ 2.5 ml Nonidiet P-40 0.5 ml 1M DTT
Ligation buffer (10x)	600 mM Tris/HCl (pH 7.5) 80 mM $MgCl_2$ 100 mM DTT
Lysis buffer I	100 mM Tris/HCl (pH 8.0) 100 mM EDTA 0.5% SDS.
Lysis buffer II (DNA)	100 mM Tris-HCl (pH8) 5 mM EDTA 0.2% SDS 200 mM NaCl 100 µg/ml Proteinase K
Lysis buffer (protein)	10 ml RIPA buffer

	1 mM PMSF 1 mM aprotinin 1 mM leupeptin 1 Protease inhibitor cocktail tablet/10ml buffer
MOPS Buffer (10x)	41.8 g MOPS 16.6 ml 3 M Sodium acetate 20 ml 0.5 M EDTA in 1 liter of DEPC water adjust pH to 6.75
Neutralisation solution	1.5 M NaCl 1 M Tris/HCl (pH 7.0)
Semi-dry transfer buffer (1x)	25 mM Tris pH 8.3 150 mM Glycin 10 % Methanol
SSC (20 x)	3 M NaCl 0.3 M Na3 citrate (pH 7.0)
TBE buffer (5x)	450 mM Tris base 450 mM Boric acid 20 mM EDTA (pH 8)
TE-buffer	5 mM Tris/HCl (pH 7.4) 1 mM EDTA

2.1.3 Laboratory materials:

The laboratory materials, which are not listed here, were bought from Schütt and Krannich (Gottingen).

Cell culture flask	Greiner, Nürtingen
Culture slides	BD Falcon, Heidelberg
Filter paper 0858	Schleicher and Schüll, Dassel
Hybond C	Amersham, Braunschweig
Hybond N	Amersham, Braunschweig
HPTLC Aluminum folio	Merck, Darmstadt
Microcentrifuge tubes	Eppendorf, Hamburg

Petri dishes	Greiner, Nürtingen
Pipette tips	Eppendorf, Hamburg
RotiPlast paraffin	Roth, Karlsruhe
Superfrost slides	Superfrost slides
Transfection flasks	Lab-Tek/Nalge, Nunc, IL, USA
Whatman blotting paper	Schleicher and Schüll, Dassel
X-ray films	Amersham, Braunschweig

2.1.4 Sterilisation of solutions and equipments

All solutions that are not heat sensitive were sterilised at 121°C, 105 Pa for 60 min in an autoclave (Webeco, Bad Schwartau). Heat sensitive solutions were filtered through a disposable sterile filter (0.2 to 0.45 µm pore size). Plastic wares were autoclaved as above. Glasswares were sterilised overnight in an oven at 220°C.

2.1.5 Media, antibiotics and agar-plates

2.1.5.1 Media for bacteria

LB-Agar:
1% Bacto-Peptone
0.5% Yeast extracts
1% NaCl
1.5% Agar

LB Medium (pH 7.5):
1% Bacto-Peptone
0.5% Yeast extracts
1% NaCl

The LB medium was prepared with distilled water, autoclaved and stored at 4°C.

2.1.5.2 Media for cell and embryo culture

Embryonic stem (ES) cell medium:
DULBECCO´s Modified Eagles Media (DMEM)
1 mM Non essential amino acids
1 mM Sodium pyruvate
10 µM ß-Mercaptoethanol

	2 mM L-Glutamine 20% FCS 1000 U/ml Recombinant leukaemia inhibitory factor (LIF)
Fibroblast and NIH 3T3 cell medium:	DMEM supplemented with sodium pyruvate (1 mM) 10% fetal calf serum (FCS), heat inactivated 1% glutamine (200mM), 1% penicillin (50units/ml)/ streptomycin (50 µg/ml)
HepG2 cell medium:	RPMI-1674 basic medium 2 mM L-Glutamine 1 % Pen/Strp 10% FCS
HeLa cells medium:	DMEM supplemented with sodium pyruvate (1 mM) 10% FCS, heat inactivated 2% penicillin (50 units/ml)/ streptomycin (50 µg/ml)

For long time storage of the cells in liquid nitrogen, the following freezing medium was used:

Freezing medium:	20% FCS 10% DMSO in DMEM

2.1.5.3 Antibiotics

Antibiotic	Mastersolution	Solvent	Final concentration
Ampicillin	50 mg/ml	H2O	50 µg/ml
Kanamycin	50 mg/ml	H2O	50 µg/ml

2.1.6 Bacterial strain

***E. coli* DH5α** (Invitrogen, Karlsruhe)

2.1.7 Plasmids

pGEM-T Easy	(Promega, Wisconsin, USA)
pDsRed-Monomer-N1	Clontech, Saint-Germain-en-Laye France

2.1.8 Synthetic oligonucleotide primers

The synthetic oligonucleotide primers used in this study were obtained from OPERON and dissolved in dH2O (Ampuwa) to a final concentration of 100 pmol/µl.

EIIa-CreF	5’ CCAGGCTAAGTGCCTTCTCTACA 3’
EIIa-CreR	5’ AATGCTTCTGTCCGTTTGCCGGT 3’
Lox1f1	5’ GTGAGTGTCATGTTCTCCCAG3’
Lox1R1	5’ TGAGAACCTGAGAGGATCCAG 3’
Lox2f2	5’ AATCTGTCTGTCTAGCCATTC 3’
Lox2R2	5’ CATTTTGAAAAGGAAGCCCCG 3’
mHPRT-F	5`CGTCGTGATTAGCGATGATG 3`
mHPRT-R	5`TATGTCCCCCGTTGACTGAT 3`
NeoF1	5`GTAGGTGCATTCTATTCTGG 3`
PGKR3	5`TCTGAGCCCAGAAAGCGAAGG 3'
qp-HPRT-F	5’AGCCCCAAAATGGTTAAGGTTGC3’
qp-HPRT-R	5’TTGCAGATTCAACTTGCGCTCAT 3’
RosaCreER-F	5’ ACCAGCCAGCTATCAACTC 3’
RosaCreER-R	5’TATACGCGTGCTAGCGAAGATCTCCATCTTCCAGCAG 3’
SP6-pGEMT	5-TTAGGTGACACTATAGAATACTCAAGC-3’
SRY-F	5-AAGATAAGCTTACATAATCACATGGA -3’
SRY-R	5-CCTATGAAATCCTTTGCTGCACATGT -3’
SX-Cyto-F2	5-GCGTGGAAATATTCTTATTGGTAG-3’
SX-Cyto-R1	5-CAGTTTAAGATCAGAAAGACCTTC-3’
SX-Cyto-R2	5-AGAGTAACATTAGATCCAACAGTC-3’
SX-Dsredxho-F3	5-GGGCTCGAGTTGCATATGCAGCCAGCAGAC-3’
SX-Dsredbam-R3	5-CCCGGATCCGCTCAGGTTCCGGCTCAGGC-3’
SX-exon1b-F	5’GGCCAGAGGCATAGGTTGTA 3’
SX-exon1-F	5’GTTCAGGCAGCCTTCGGACT 3’
SX-exon2-F	5’CCATCCCAGACACTTTCGTG 3’
SX-exon3-F	5’CTACTCTGAAGGTGGACAGG 3’
SX-exon4-F	5’GCCCTTTTGTACCATCCAAG 3’
SX-exon4-R	5’AAGACAAGGAAATAGGATGG 3’
SX-exon5-F	5’CACGGCCACTGGAGTTTTAG 3’
SX-exon6-F	5’GTTCAGGCAGCCTTCGGACT 3’
SX-exon7-R	5’CGCCTTGCTCAGAGGCTCAA 3’
SX-Probe2F1	5-GGGAAATCTGGGTTGGTTCT-3
SX-Probe2R1	5-ATTGGCTCCTCCATTTCCTT-3
SX-sipip -F	5’GGAAGGTCTTTCTGATCTTA 3’
T7-pGEMT	5’AATACGACTCACTATAGGGCGAATTGG 3’
Vill-probe-F	5’GAGGTTCAAGGCAACGAGAG 3’
Vill-probe-R	5’AGCTTGAGTGCAGCCTTAGC 3’
Vsig1-ex1-ex2-R	5-TGAAAGCTTTTCCAGGGACT -3

Vsig1-ex1b-ex3-R 5-GTCAAGGAGGCCTTGGTTTT-3

2.1.9 Eukaryotic cell lines

HeLa	ATCC, Rockville, USA
HepG2	ATTCC, Rockville, USA
NIH 3T3	S.A. Aaronson, Bethesda, U.S.A.

2.1.10 Mouse strains

Mouse strains C57BL/6J, 129/Sv, and NMRI were initially ordered from Charles River Laboratories, Wilmington, USA, and further bred in Animal Facility of Institute of Human Genetics, Goettingen.

2.1.11 Antibodies

Primary Antibodies:	
Mouse anti mouse α-tubulin	Sigma, Deisenhofen, Germany
Mouse anti mouse γ-tubulin	Sigma, Deisenhofen, Germany
Mouse monoclonal anti-Cytokeratin5/6	Dako, Glostrup, Denmark
Mouse monoclonal anti-H^+/K^+ ATPase	Acris Antibodies, Hiddenhausen, Germany
Rabbit polyclonal anti-Vsig1	Institute of Human Genetics
Mouse monoclonal anti-Cyclin E	Santa Cruz Biotechnology, Heidelberg
Mouse monoclonal anti-HSP70	Santa Cruz Biotechnology, Heidelberg
Secondary Antibodies:	
Anti-Mouse IgG FITC conjugated	Sigma, Deisenhofen, Germany
Anti-Mouse IgG Peroxidase conjugated	Sigma, Deisenhofen, Germany
Anti-Rabbit IgG Peroxidase conjugated	Sigma, Deisenhofen, Germany
Anti-rabbit polyclonyl IgG Cy3 conjugated	Sigma, Deisenhofen, Germany
Anti-rabbit-IgG conjugated with alkaline phosphatase	Sigma, Deisenhofen, Germany

2.1.12 Enzymes

Immolase DNA Polymerase	Bioline, Luckenwalde
Proteinase K	Sigma, Deisenhofen
Platinum Taq polymerase	Invitrogen, Karlsruhe
Restriction enzymes (with supplied buffers)	Invitrogen, Karlsruhe
RNase inhibitor	Invitrogen, Karlsruhe
Superscript-II	Invitrogen, Karlsruhe
Taq polymerase	Invitrogen, Karlsruhe
T4 DNA ligase	Promega, Mannheim
Trypsin	Invitrogen, Karlsruhe

2.1.13 Kits

QIAquick Gel Extraction Kit	Qiagen, Hilden
Rediprime II DNA Labeling System	Rediprime II DNA Labeling System
PCR Purification Kit	PCR Purification Kit
RNAeasy Kit	Qiagen, Hilden
Midi Plasmid Kit	Invitrogen, Karlsruhe

2.1.14 Radioactive substances

α-32P-dCTP	Amersham, Braunschweig

2.1.15 Equipments

ABI PRISM 377 DNA Sequencer	Applied Biosystem, Darmstadt
Autoclave	Webeco, Bad Schwartau
Centrifuge 5415D	Eppendorf, Hamburg
Centrifuge 5417R	Eppendorf, Hamburg
Confocal microscope	Olympus, Planegg
Cryostat (Modell CM 1900-1-1)	Leica Microsysteme Vertrieb GmbH, Bensheim
DNA Sequencer MegaBACE 1000	Amersham, Freiburg
GeneAmp PCR System 9600	Perkin Elmer, Berlin
Histocentre 2 embedding machine	Shandon, Frankfurt a M.
Inverted mikroscop IX81	Olympus, München
Microscope BX60	Olympus, München
Semi-Dry-Blot Fast Blot	Biometra, Göttingen
Spectrophotometer Ultraspec 3000	Amersham, Freiburg
Thermomixer 5436	Eppendorf, Hamburg
Turboblotter™	Turboblotter™

UV StratalinkerTM1800	UV StratalinkerTM1800
X-Ray Automatic Processor Curix 60	X-Ray Automatic Processor Curix 60

2.2- Methods:

2.2.1 Isolation of nucleic acids

2.2.1.1 Isolation of plasmid DNA

2.2.1.1.1 Small-scale isolation of plasmid DNA

(Birnboim and Doly, 1979)

A single *E.coli* colony was inoculated in 5 ml of LB medium with the appropriate antibiotic and incubated for 16 hrs at 37°C with a shaking speed of 160 rpm. After the incubation, the saturated culture was centrifuged at 2000 x g for 10 min. The pellet was resuspended in 100 µl of solution P1. The bacterial cells were lysed with 200 µl of P2 solution and then neutralized with 150 µl of P3 solution. The precipitated solution was centrifuged at 10000 x g at RT. The supernatant was transferred into a new tube and centrifugation was done again. The supernatant was transferred into a new tube and 1 ml of 100% ethanol was added to precipitate the DNA. The solution was then stored on ice for 15 min, centrifuged at full speed for 20 min, and finally the pellet was washed with 70% ethanol and after air-drying was dissolved in 30-50 µl of Ampuwa.

P1: 50 mM Tris-HCl, pH 8.0; 10 mM EDTA; 100 µg/ ml RNase A.
P2: 200 mM NaOH; 1% SDS.
P3: 3.0 M Potassium acetate, pH 5.5.

2.2.1.1.2 Endotoxin free preparation of plasmid DNA

Endotoxins, also known as lipopolysaccharides or LPS, are cell membrane components of Gram-negative bacteria (e.g., *E. coli*). During lysis of bacterial cells, endotoxin molecules are released from the outer membrane into the lysate and strongly influence the transfection

efficiency of cultured cells like embryonic stem (ES) cells. Increased endotoxin levels lead to sharply reduced transfection efficiencies. Endofree plasmid preparation kit integrates endotoxin removal into standard plasmid preparation procedure. The neutralised bacterial lysate was filtered through a QIA filter cartridge (provided in kit) and incubated on ice with a specific Endotoxin Removal buffer (patented by Qiagen). The endotoxin removal buffer prevents LPS molecules from binding to the resin in the columns (QIAGEN-tips), thus allowing purification of DNA containing less than 0.1 IU endotoxin per µg plasmid DNA.

2.2.1.2 Isolation of genomic DNA from murine tail biopsies

(Laird *et al*., 1991)

To determine the genotype, 1 cm of the mouse tail was incubated in 700 µl of lysis buffer I containing 35 µl proteinase K (10 µg/µl) at 55°C overnight in Thermomixer 5436. The tissue lysate was centrifuged at 14000 x g for 15 min and the supernatant was transferred into a new E-cup. DNA was then precipitated by adding an equal volume of isopropanol, mixed by inverting several times and centrifuged at 14000 x g at RT for 15 min. Finally, DNA was washed with 1 ml of 70% ethanol, dissolved in 50-100 µl of dH2O and incubated at 60°C for 10 min.

2.2.1.3 Isolation of genomic DNA from cultured cells

Cells were washed with PBS and incubated overnight in 500 µl of lysis buffer II at 37^{o}C. Equal volume of isopropanol was added, mixed by inverting several times and incubated for 10 min at RT. Mixture was then centrifuged for 15 min at maximal speed. DNA pellet was washed with 70% ethanol and was dissolved in 80 µl of dH2O and incubated at 60 ^{o}C for 10 min.

2.2.1.4 Isolation of total RNA from tissue samples and cultured cells

The composition of RNA isolation reagent includes phenol and guanidine thiocyanate in a mono-phase solution. Tissue sample (100-200 mg) was homogenised in 1 ml of TRI Reagent by using an E-cup homogeniser. To isolate total RNA from cultured cells, 350 µl of reagent was added to the Petri dish (6 cm). Cells were homogenised with a rubber scraper and the lysate was transferred into a microcentrifuge tube, where it was incubated at 4°C for 5 min to permit the complete dissociation of nucleoprotein complexes. Then, 0.2 ml of chloroform was added, mixed vigorously, and stored at 4°C for 10 min. After centrifugation at 12000 xg for 15 min at 4°C, the upper aqueous phase was transferred into a new tube. The RNA was precipitated by adding 0.5 ml of isopropanol. Pellet was washed twice with 75% ethanol and dissolved in 30-80 µl of RNase free water (DEPC dH2O).

2.2.2 Determination of nucleic acid concentration

The concentration of nucleic acids was determined spectrophotometrically by measuring absorption of the samples at 260 nm. The quality of nucleic acids i.e. contamination with salt and protein was estimated by ratio of absorbance 260nm/280 nm. The correct value of the ratio is 1.8 for DNA and 2.0 for RNA.

2.2.3 Gel electrophoresis

2.2.3.1 Agarose gel electrophoresis of DNA

Agarose gels were used to run nucleic acid molecules. Usually, 1 g agarose was added to 100 ml of 0.5 x TBE buffer and boiled in the microwave to dissolve the agarose, and after cooling down to about 60°C 3 µl of ethidium bromide (10 mg/ml) was added. This 1% agarose gel was poured into a horizontal gel chamber.

2.2.3.2 Agarose gel electrophoresis of RNA

(Hodge, 1994)

RNA was pre-treated with formaldehyde and formamide in order to denature the secondary structure of RNA and it was run on an agarose gel containing formaldehyde. 1.25g of agarose was added to 10 ml of l0x MOPS Buffer and 74 ml DEPC treated H_20 and dissolved by heating in a microwave. After cooling of the agarose gel to about 60°C, 25 ml of formaldehyde (37%) was added, stirred and poured into a vertical gel chamber. RNA samples (10 – 30 µg) were mixed with double volume of sample buffer, then denatured at 65^oC for 10 min and chilled on ice. After the addition of loading buffer (equal volume to RNA sample), the gel was loaded and run at 70-80V at 4^oC for 4 – 5 hrs.

Sample buffer: 2 µl 10x E buffer; 3 µl 37% formaldehyde; 8 µl 40% formamide;

Loading buffer: 40 µl 1% ethidium bromide in 500 µl standard loading buffer.

2.2.3.3 SDS-PAGE gel for separation of proteins

(Laemmli, 1970)

NuPage 4-12% Bis-Tris gel is SDS-PAGE gel with 4-12% percentage gradient which allows more efficient separation of proteins. 20.5 µl of whole protein lysate was mixed with 7.5 µl 4 x NuPage sample buffer and 2 µl 1M DTT. Then, the samples were denatured at 95^oC for 10 min and chilled on ice. The gel electrophoresis was run in 1x MOPS buffer (Invitrogen). As a weight marker, a pre-stained molecular weight standard (See Blue Plus2, Invitrogen) was loaded. The gel was run at 100 V for 2 – 3 hrs at RT.

2.2.4 Purification of DNA fragments from agarose gel

2.2.4.1 QIAquick gel extraction method

The Qiagen gel extraction kit was used to extract the DNA fragment from the agarose gel. The principle of this method depends on selective binding of DNA to uniquely designed silica-

gel membrane. 3 volumes of QG buffer were added to an agarose gel piece and then incubated at 50°C for 10 min. After the gel slice was dissolved, the solution was applied to a QIAquick column and centrifuged for 1 min. The flow through was discarded and the column was washed with 0.75 ml of PE buffer. After drying, the column was placed into a fresh microcentrifuge tube. To elute DNA, 50 µl of dH2O was applied to the centre of the QIAquick membrane and the column was centrifuged for 1 min.

2.2.5 Enzymatic modifications of DNA

2.2.5.1 Restriction of DNA

Restriction enzyme digestions were performed by incubating double-stranded DNA with a restriction enzyme in amount of max. 1/10 reaction volume in a buffer recommended by the supplier and at the optimal temperature for the specific enzyme. Standard digestions included 2-10 U enzymes per 1 µg DNA. Usually incubation time was 1-3 hrs at 37°C. For genomic DNA digestion, the reaction solution was incubated overnight at 37°C.

2.2.5.2 Ligation of DNA fragments

The cloning of an insert DNA into a vector (digested with the same restriction enzyme) was carried out in the following ligation reaction mix in total volume of 10 µl:

• 30 ng vector DNA (digested)

• 50-100 ng insert DNA (1:3, vector: insert ratio)

• 1 µl ligation buffer (10x)

• 1 µl T4 DNA ligase (5 U/µl)

Ligations were carried out at RT for 2-4 hrs or 16°C overnight.

2.2.5.3TA-Cloning

(Clark, 1988; Hu, 1993)

Taq polymerase and other DNA polymerases have a terminal transferase activity that results in the non-template addition of a single nucleotide to the 3` ends of PCR products. In the presence of all 4 dNTPs, dATP is preferentially added. This terminal transferase activity is the basis of the TA- cloning strategy. For cloning of PCR products, the pGEM-T Easy vector system that has 5' T overhangs was used. The mixture was as follows:

50 µg pGEM-T Easy Vector

PCR product (1:3 vector to insert ratio)

1 µl of T4 DNA Ligase l0x buffer

1 µl of T4 DNA Ligase

in a total volume of 10 µl

The content was mixed by pipetting and the reaction was incubated overnight at 16°C. For transformation of the ligation reaction, DH5α competent cells were used (Invitrogen).

2.2.6 Transformation of competent *E.coli* bacteria

(Ausubel *et al.,* 1994)

Transformation of bacteria was done by gently mixing 50 µl-aliquot of competent bacteria (Invitrogen) with 10 µl of ligation reaction. After incubation for 30 min on ice, bacteria were heat-shocked for 45 sec at 37°C and cooled down for 2 min on ice. After adding 450-900 µl of S.O.C. medium, the mixture was incubated at 37°C, 400 rpm, for 1 hr to allow recovery of heat shocked bacteria which then were plated on LB-agar plates.

2.2.7 Polymerase Chain Reaction (PCR)

In general, the PCR reaction contained the following substances:

- 10 ng DNA
- 1 µl forward primer (10 pmol)
- 1 µl reverse primer (10 pmol)

- 1 µl 10 mM dNTPs
- 5 µl 10 x PCR buffer
- 1.5 µl 50 mM MgCl2
- 0.5 µl Taq DNA Polymerase (5 U/l)
- Up to 50 µl dH2O

The reaction mixture was placed in a 200 µl reaction tube and placed in a thermocycler. Thermal cycling was carried out for 35 cycles with denaturation at 95°C for 30 sec, annealing at 55-60°C for 30 sec and extension at 72°C for 30 sec -1 min (depending on the product size).

2.2.7.1 Genotyping PCRs

CreEIIa PCR

Ingredients:		program	
H2O	6,1 µl	94 ^{o}C-5 min	
Buffer	1 µl	94 ^{o}C-30 sec.	30x
MgCl2	0,3 µl	53 ^{o}C -45 sec.	
dNTPs	0,2µl	72 ^{o}C-2 min.	
EIIaCre-F	0,6µl	72 ^{o}C-10 min	
EIIaCre-R	0,6µl		
Taq Platinum	0,15µl		
DNA	0,5µl		

CreERT PCR

Ingredients:		Program:	
H2O	6,8 µl	94 ^{o}C-5 min	
Buffer	1 µl	94 ^{o}C-30 sec.	30x
MgCl2	0,4 µl	53 ^{o}C -30 sec.	
dNTPs	0,2µl	72 ^{o}C-50 sec.	
EIIaCre-F	0,5µl	72 ^{o}C-7 min	
EIIaCre-R	0,5µl		
Taq Platinum	0,15µl		
DNA	0,5µl		

Cyto-transgenic PCR		Program	
Ingredients:			
H2O	17,2 µl	95^{o}C-5 min	
Buffer	2,5 µl	94 ^{o}C-30 sec.	35x
MgCl2	0,8 µl	55 ^{o}C -40 sec.	
dNTPs	1µl	72 ^{o}C-50 sec.	

SX-cyto-F_1	0,5µl	72 ^{o}C-10 min
SX-cyto-R_1	0,5µl	
Taq Platinum	0,5µl	
DNA	1µl	

Vill-transgenic PCR		Program	
Ingredients:			
H2O	17,2 µl	95^{o}C-7 min	
Buffer	2,5 µl	94 ^{o}C-30 sec.	}
MgCl2	0,8 µl	58 ^{o}C- 30 sec.	} 35x
dNTPs	1µl	72 ^{o}C-45 sec.	}
SX-cyto-F_1	0,5µl	72 ^{o}C-10 min	
SX-cyto-R_1	0,5µl		
Taq Platinum	0,5µl		
DNA	1µl		

Genotyping PCR (1)			
Wild-type/Flox/Δ		Program	
Ingredients:			
H2O	19,3 µl	95^{o}C-7 min	
Buffer	2,5 µl	94 ^{o}C-30 sec.	}
MgCl2	0,5 µl	53 ^{o}C- 45 sec.	} 35x
dNTPs	0,5 µl	72 ^{o}C-2 min.	}
SX-cyto-F_1	0,5µl	72 ^{o}C-10 min	
SX-cyto-R_1	0,5µl		
Taq Immulase	0,2µl		
DNA	0,5µl		

Genotyping PCR (2)			
Wild-Type/Flox		Program	
Ingredients:			
H2O	19,3 µl	95^{o}C-7 min	
Buffer	2,5 µl	94 ^{o}C-30 sec.	}
MgCl2	0,5 µl	53 ^{o}C- 45 sec.	} 35x
dNTPs	0,5 µl	72 ^{o}C-2 min.	}
SX-cyto-F_1	0,5µl	72 ^{o}C-10 min	
SX-cyto-R_1	0,5µl		
Taq Immulase	0,2µl		
DNA	0,5µl		

2.2.7.2 Reverse transcription PCR (RT-PCR)

Reverse Transcription PCR (RT-PCR) is a technique, which generates cDNA fragments from RNA templates, and thereafter amplifies them by PCR. It is a very useful technique to

determine the expression of genes. 1-5 µg of total RNA was mixed with 1 µl of oligo (dT)18 primer (10 pmol/µl) in a total volume of 12 µl. For denaturation the mixture was heated to 70°C for 10 min and then quickly chilled on ice. After a brief centrifugation, the following substances were added to the mixture:

- 4 µl 5 x first strand buffer.
- 2 µl 0.1 M DTT.
- 1 µl 10 mM dNTPs.

The reaction was incubated at 42°C for 2 min. Then, 1 µl of reverse transcriptase enzyme (Superscript II, Invitrogen) was added and the mixture was incubated at 42°C for 50 min for the first strand cDNA synthesis. Next, the reaction was inactivated by heating at 70°C for 15 min 1 µl of the first strand reaction was used for the PCR reaction.

2.2.7.3 Quantitative Real-Time PCR

In contrast to regular PCR, Real-Time PCR or quantitative PCR (qPCR) allows accurate quantification of starting amounts of DNA targets. In Real-Time PCR using SYBR Green I, the increase of fluorescence as the dye binds to the increasing amount of DNA in the reaction tube is measured. SYBR Green I binds to all double-stranded DNA molecules, emitting a fluorescent signal of a defined wavelength on binding. The excitation and emission maxima of SYBR Green I are at 494 nm and 521 nm, respectively, and are compatible for use with any Real-Time cycler. Detection takes place in the extension step of Real-Time PCR. Signal intensity increases with increasing cycle number due to the accumulation of PCR product.

cDNA synthesis was done according to section 2.2.7.2 with preceding DNAse treatment. 5 µl 2x QuantiTect SYBR-Green PCR-Master-Mix, 1 µl Forward Primer (9µM), 1 µl Reverse Primer (9µM), 0.3µl MgCl2 (50mM) and 1µl of cDNA (in a 1/20 dilution) were mixed with RNase free water to a total volume of 10 µl. The following PCR program was used:

2 min 50°C

15 min 95°C

15 sec 95°C
30 sec 56°C } 40x
30 sec 72°C

15 sec 95°C
15 sec 60°C } melting curve
15 sec 95°C

Primer sequences are provided in section 2.1.8. qPCR for HPRT was used as endogenous reference. For standard curves, wild-type stomach cDNA was used, which has been selected according to preliminary experiments testing detection of expression of each gene by RT-PCR (2.2.7.2). Reliability of Real-time PCR data was also assessed in connection with the respective dissociation curves.

2.2.8 Protein methods

2.2.8.1 Isolation of total protein lysate

100 mg of tissue was homogenized in 500 µl of lysis buffer. To destroy the cell membrane, homogenate was sonicated with Branson ultra-Sonifier on ice 2 x 1 min and subsequently centrifuged at 8000 x g for 20 min at 4^{o}C. The supernatant was aliquoted in several microcentrifuge tubes and stored at -80^{o}C.

5 x 10^{6} cells/ml were washed with cold phosphate buffered saline (PBS) and resuspended in 50 - 200 µl of lysis buffer. The cells were left on ice for 30 min, treated with ultrasound on ice 2 x 30 sec and centrifuged at 24000 x g for 20 min at 4^{o}C. The supernatant with protein extract was either used immediately or stored at –80^{o}C.

2.2.8.2 Determination of protein concentration

(Bradford, 1976)

To determine the protein concentration, Bio-Radprotein assay was employed, which is a dye-binding assay based on the differential colour change of a dye in response to various concentrations of protein. The BSA stock solution of 1 mg/ml was diluted in order to obtain standard dilutions in range of 10 µg/ml to 100 µg/ml. The dye reagent concentrate (Bio-Rad Laboratories GmbH) was diluted 1:5 with H_2O and 2 µl sample were added. The absorption of the color reaction was measured at 595 nm in a spectrophotometer.

2.2.8.3 Fractionation of protein

(Andreeva *et.al.*, 2009)

To fractionate testis protein into membrane and cytosolic protein fractions, *Tunica albuginea* of fresh testis was removed by using fine two forceps in cold PBS. The seminefrous tubules were put in hypotonic buffer and passed through syringe 15-20 times. The lysate was centrifuged 5 min. 5000 xg at 4^{o}C. The supernatant (input) was then centrifuged 1hr. 45000 xg at at 4^{o}C. The supernatant is the membrane fraction of the protein, while the pellet is resuspended in equal amount of the supernatant as cytosolic fraction of protein.

For the fractionation of protein, which was extracted from NH1 3T3 embryonic fibrocytes cultured in 6-well plate, into nuclear and cytosolic fractions the following method has been followd. The cells in each well were incubated on ice in 100 µl lyses buffer. After that the cells have been scraped with cell scraper and again were incubated on ice for 30 min with inversion each 10 min. The lysate was sonicated with Branson ultra-Sonifier on ice 2 x 1 min and subsequently centrifuged at 13000 x g for 30 min at 4^{o}C. The pellet was resuspended in equal amount to the supernatant as nuclear fraction, while the supernatant was the cytosolic protein fraction.

2.2.9 Blotting techniques

2.2.9.1 Southern blotting of DNA to nitrocellulose filters

(Southern, 1975)

In Southern blotting, the transfer of denatured DNA from agarose gels to nitrocellulose membrane is achieved by capillary flow. After electrophoresis of DNA, the gel was treated for 20 – 30 min with 0.25 M HCl for depurination with denaturation solution for 30 min and neutralisation solution for 45 min. The transfer of the DNA to the nitrocellulose membrane was done in a Turbo-Blot apparatus (Schleicher & Schuell, Dassel). About 25-28 Whatman filter papers (GB 003) were layered on a Stack Tray, followed by 4 Whatman filter papers (GB 002) and 1 Whatman filter paper (GB 002) soaked with 20 x SSC. The equilibrated nitrocellulose filter, that was also soaked with 20 x SSC, was laid on the top. The agarose gel, treated as described above, was placed on the filter and was covered with 3 Whatman filter papers GB 002 soaked with 20 x SSC. The buffer tray was filled with 20 x SSC. Finally a wick, which was soaked with 20 x SSC, and the wick cover were put on top of the blot. The transfer was carried out for overnight. Finally, after disassembling of the blot, the DNA was fixed onto the filter by baking at 80°C for at least 2 hrs.

2.2.9.2 Northern blotting of RNA

The procedure performed for the transfer of RNA onto a nitrocellulose filter was the same as described above (2.2.9.1). However, the gel did not need to be denaturated, but was transferred directly onto the filter.

2.2.9.3 Western blotting of protein

(Gershoni and Palade, 1982)

After electrophoresis of proteins (2.2.3.3) the SDS PAGE gel and the PVDF membrane were moistened with transfer buffer. Three pieces of filter paper were soaked in transfer buffer and

placed on the semi dry transfer machine's lower plate. Then, the wet membrane and the gel were put, avoiding any air bubbles. Another three soaked Whatman papers were placed on the pile to complete the sandwich model. The upper plate was placed over this sandwich and the transfer was carried out at 3.5 mA/cm^2 for 1 hr. After blotting, the gel was stained with Comassie blue overnight at RT in order to check the amount of proteins which were not transferred.

2.2.10 "Random Prime" method for generation of 32P labeled DNA

(Denhardt, 1966; Feinberg and Vogelstein, 1984)

Rediprime™ II Random Prime Labeling System (Amersham Pharmacia) was used for labeling of DNA probes. Firstly, 25-50 ng of DNA were denatured in a total volume of 46 μl at boiling water for 10 min and quick chilled in ice for 5 min. After pipetting the denatured probe in Rediprime II Random Prime Labeling System cup containing dATP, dGTP, dTTP, Klenow fragment (4-8 U) and random oligodeoxy-ribonucleotides, 4 μl of [γ-^{32}P] dCTP (3000 Ci/mmol) was added to the reaction mixture. The labelling reaction was incubated at 37°C for 1 hr. The labelled probe was purified from unincorporated [γ-^{32}P] dCTP by using microspin columns (Amersham Pharmacia).

2.2.11 Non-radioactive dye terminator cycle sequencing

Non-radioactive sequencing was performed with the Dye Terminator Cycle Sequencing-Kit (ABI PRISM). The reaction products were analysed with automatic sequencing equipment, MegaBase DNA Sequencer. For the sequencing reaction, four different dye labelled dideoxy nucleotides were used (Sanger *et al.*, 1977), which, when exposed to an argon laser, emit fluorescent light that can be detected and interpreted. The reaction was carried out in a total volume of 10 μl containing 1 μg plasmid DNA or 100-200 ng purified PCR products, 10 pmol primer and 4 μl reaction mix (contained dNTPs, dideoxy dye terminators and Taq DNA polymerase). Elongation and chain termination took place during the following program in a

thermocycler: 4 min denaturation followed by 25 cycles at 95°C, 30 sec; 55°C, 15 sec, annealing; 60°C, 4 min, elongation. After the sequencing reaction, the DNA was precipitated with 1/10 volume 3 M sodium acetate and 2.5 volume 100% ethanol and washed in 70% ethanol. The pellet was dissolved in 4 µl of loading buffer, denaturated at 95°C for 3 min, and finally loaded on the sequence gel.

2.2.12 Hybridisation of nucleic acids

(Denhardt, 1966)

A membrane for hybridization was equilibrated in 2 x SSC and transferred to a hybridisation bottle. After adding 12 ml of Rapid-hyb buffer (GE Healthcare) and sheared denaturated salmon DNA, the membrane was incubated for 2 hrs in the hybridization oven at 65°C. Then, the labelled probe was denaturated at 95°C for 10 min, chilled on ice for 5 min, and added to the hybridisation solution. The hybridisation was performed overnight in the oven. The filter was washed for 10 min with 2 x SSC and with 2x SSC containing 0.2% SDS at 65°C for 10 – 20 min. Finally, the membrane was washed with 0.2 x SSC containing 0.1 % SDS at the hybridisation temperature. After drying the filter, it was sealed in Saran wrap and exposed to autoradiography overnight at -80°C. The film was developed in X-Ray Automatic Processor Curix 60.

2.2.13 Histological techniques

2.2.13.1 Tissue preparation for paraffin embedding

The freshly prepared tissues were fixed in Bouin's solution or 4% PFA for 24 hrs to prevent alterations in the cellular structure. The tissue to be embedded in paraffin should be free of water. The dehydration process was accomplished by passing the tissue through ascending series of alcohol. For this purpose, the tissue was incubated in 70%, 80%, 90%, 96% and 100% ethanol for at least 1 hr for each at RT. Tissue was then incubated in 1:1 mixture of xylol and

paraplast at 65°C overnight. Further, tissue was incubated in paraplast at 60°C overnight. Before embedding, paraplast was changed at least three times. Finally, the tissue was placed in embedding mould and melted paraffin was poured into the mould to form a block. The block was allowed to cool and was then ready for sectioning or was stored at 4°C or RT.

2.2.13.2 Sections of the paraffin blocks

Paraffin blocks were clamped into the microtome (Hn 40 Ing., Nut hole, Germany). The thickness of the section was 5-7 µm. The sections were floated on 40°C water to allow actual spread. Then, they were put onto slides. After complete drying at 37°C, slides were stored at 4°C for further analysis.

2.2.13.3 Tissue preparation for cryosectioning

The freshly prepared tissues were fixed in 4% PFA for 24 hrs to prevent alterations in the cellular structure. Then the tissues were treated with 30% and 60% succrose 3 hrs and overnight, respectively. The tissues were then embedded in freezing medium, and were put in dry ice to allow the media to become hard and ready for sectioning or stored in -80°C.

2.2.13.4 Cryosectioning

The cryostat (Leica Microsystems) was cooled down to approximately -20°C. The embedded tissues were cut into 5-6 µm thick slices and transferred to Superfrost slides. The slides were used immediately for immunohistochemistry.

2.2.13.5 Preparation of testicular suspension

Tunica albuginea of fresh testis was removed by using fine two forceps in cold PBS. The seminefrous tubules were cut into small pieces with fine scissors. One drop of cold PBS was put on a Superfrost slide, and approximately 10 µl of the suspension were added to the PBS drop and

then spread by using another slide. The slides were dried for 2 min and then fixed in methanol or in 4% paraformaldehyde at -20°C or 4°C respectively.

2.2.13.6 Hematoxylin-Eosin (H&E) staining of the histological sections

Slides with paraffin sections were first incubated three times in Xylol for 5 min each, followed by incubation in descending series of ethanol for 3 min each. Slides were then washed 1 min in dH_2O and stained for 5 min in hematoxylin. Staining was followed by washing in running tap water for 10 min. Thereafter slides were destained in acidic ethanol (70%) according to the staining intensity required, then stained with eosin (0.1% + 2% acetic acid) for 2-10 sec, then washed in dH_2O for 1 min and incubated in 50%, 70%, 80%, 90%, 96% and 100% ethanol for 3 min, each. Finally the slides were incubated in Xylol for 10 min and mounted with Eukitt-quick hardening mounting medium.

2.2.13.7 Immunofluorescence staining

For mouse tissues:

Tissue sections were deparafinized by incubation in xylene three times 10 min each (this step is skipped in case of using cryosections). Then, they were re-hydrated in a descending ethanol series (100%, 96%, 70% and 50%,) for 2 min each. For immunofluorescence staining, the sections were washed in PBS and then incubated with a blocking solution containing 10% of the appropriate serum in 0.2% Tween- 20 in PBS for 2 hrs at RT. Then, they were incubated with primary antibodies diluted with 1% serum in 0.2% Tween- 20 in PBS for overnight in a humidified chamber at 4°C. Subsequently, they were washed three times for 5 min in PBS and an appropriate secondary antibody was put for 1 hr. Finally, the slides were washed three times for 5 min in PBS and the nuclei were counterstained with DAPI. Immunostaining of the sections was examined using a fluorescence equipped microscope (BX60; Olympus).

For cells:

Cells, which have been cultured on microscopical chambers overnight, were rinsed in PBS fixed then in methanol at -20^{o}C or 4% paraformaldehyde in PBS at 4^{o}C for 15 min, rinsed in PBS and then permeabilized 10 min in 0,1% Triton 100 in PBS at RT. After that the procedure was the same like in case of immunostaining of tissue.

2.2.13.8 Phalloidin staining of cells

Cells were washed twice in PBS for 5 min, fixed for 15 min (4^{o}C) in 4% paraformaldehyde and washed 3 times in PBS. Then, they were incubated for 1 hr in phalloidin (diluted 1:1000) conjugated with Cy3 and washed 3 times in PBS. The slides were mounted with DAPI-containing medium.

2.2.14 Eukaryotic cell culture methods

2.2.14.1 Cell culture conditions

All cells were grown in their respective growth media (2.1.5.2). All the cells were cultured at 37°C in a humidified incubator with 5% CO_2 and grown to 80% confluence.

2.2.14.2 Trypsinization of eukaryotic cells

Cells were washed twice with sterile DPBS and incubated in a minimal amount of trypsin-EDTA (0.5 g/l trypsin, 0.2 g/l EDTA) (PAN) at 37°C until they had detached from the dish. The process was controlled under an inverted microscope. Trypsin activity was inhibited by addition of growth medium in which the cells were subsequently resuspended.

2.2.14.3 Transfection of monolayer eukaryotic cells with plasmid

The transfection involves the introduction of foreign DNA into mammalian cells for its expression. The reagent used in this method was “Lipofectamine 2000 TM” (Invitrogen, Karlsruhe, Germany). For transfection, approximately 4 x 10^5 NHI-3T3 cells were plated over

glass cover slip in 24-well plate with 1 ml of complete DMEM medium and incubated at 37^{o}C, 5% CO_2. 1µg of Lipofectamine 2000 TM reagent and 1µg of the DNA of interest were diluted each in a total volume of 50 µl, respectively, with OptiMEM I reduced serum medium (Invitrogen, Karlsruhe, Germany) and incubated at RT for 10 min. Subsequently, both of the diluted solutions were mixed together in a reaction tube and incubated for 25 min to allow DNA complex formation. The DMEM containing cells were washed twice with PBS and 500 µl of the same medium lacking FKS was added to the cells. After DNA complex formation, the mixture was added to the cells and incubated for 2-3 hrs at 37^{o}C, and after the FKS free medium has been replaced by complete medium, and the cells were incubated in 37^{o}C, 5% CO_2.

2.2.14.4 Cell spreading assay

Generally, cell spreading assay is used to test the ability of a specific type of cell or cell line to adhere to a specific adhesive substrate. A 96-well plate was coated with 0.1µg/ml fibronectine for 1-2 hrs at RT. After that, 1x 10^4 cells were plated, then ten microscopic fields were photographed after 30 min and 90 min, and unspread cells were counted.

2.2.14.5 Cell migration assay

Cell migration assay was performed based on the healing speed of scratched wound in stable transfected HepG2 monolayer cells. The cells were grown at 90-100% confluence to form a monolayer in 10 cm^2 culture dishes. By using a p200 pipet, a scratch of the cell monolayer was created in each clone. After drawing the scratch, the cells were washed two times with PBS and immediately photographed and then further incubated. Further images were photographed after 12 hrs, 24 hrs and 48 hrs. The images acquired for each sample were further analyzed quantitatively by using computing software "Soft Imaging System" software (Olympus).

2.2.14.6 Preparation of MEF feeder layers

A frozen vial of MEFs (Mouse Embryo Fibroblasts) was quickly thawed at 37°C and transferred to 10 ml MEF medium. After centrifugation at 1000 x g for 5 min, the cell pellet was gently resuspended in 10 ml MEFs medium and plated on a 50 ml culture flask. Cells were incubated at 37°C in 5% CO2. When the cells formed a confluent monolayer after three days, they were trypsinised, transferred to five 10 cm dishes and grown until they formed confluent monolayer, or directly treated with mitomycin C (1mg/ml) for 3 hrs. Then, the cells were washed twice with 10 ml PBS, resuspended with 10 ml medium and centrifuged. Next, they were resuspended in MEFs medium and plated onto dishes, which were pretreated with 0.1% gelatine for 30 min. The feeder cells were left to attach by incubation overnight at 37°C, 5% CO_2, or used after 2 hrs of incubation. Before adding ES cells on the feeder layer, the medium was changed to ES cell medium.

2.2.14.7 Growth of ES cells on feeder layer

One aliquot of frozen ES cells was quickly thawed at 37°C and cells were transferred to a 12 ml tube containing 6 ml ES cell medium. After centrifugation, the cell pellet was resuspended in 5 ml ES cell medium and plated on 6 cm dishes containing feeder layer. Next day the medium was changed. The second day, cells were washed with PBS, treated with 2 ml trypsin/EDTA at 37°C, 5% CO2 for 5 min, resuspended with 5 ml ES medium and centrifuged. The cell pellet was resuspended in 10 ml ES cell medium and distributed either to 5 or 6 dishes (6 cm) or to 2 dishes (10 cm) containing feeder layers.

2.2.14.8 Random differentiation of ES cells

After trypsinization, cells were transferred to sterile bacterial dish, where they were cultured in 10 ml ES medium without LIF for 10 days. Afterwards, EBs were either collected for analysis or trypsinised and plated on gelatin-coated 6-well plates in 2 ml medium without LIF.

2.2.15 Tamoxifen (TAM) treatment of cKO mice

The 15-day old mice were injected intraperitoneally with 0.2-0.3 mg per day for 5 days.

Preparation of tamoxifen

50 mg TAM were suspended in 500 µl 100% ethanol. Next, 4 ml of sunflower oil was added and it was mixed till powder was dissolved. An obtained solution (1mg/100 µl) was aliquoted and stored in -20^{o}C max. for 4 weeks.

2.2.16 Embryological techniques

To determine the age of the embryo vaginal plug date were checked, which equal to 0.5dpc of the embryo.

2.2.16.1 Isolation and Immunostaining of two-cell and blastocyst stages

(Lorthongpanich, 2008)

Mouse two-cell and blastocyst stage embryos were collected by flushing the oviducts or uterus of female mice at 1.5 dpc or 3.5 dpc, respectively, and were fixed in 4% paraformaldehyde in PBS for 15 min at 4^{o}C. Thereafter, the embryos were washed in PBS and then permeabilized 10 min in 0,1% Triton-X 100 in PBS at RT. Non-specific reactions were blocked by incubation in 10 % sheep serum in 0.2% TBS (tween-20 in PBS) for 2 hrs at RT. Vsig1 antibody was diluted in 1 % sheep serum in 0.2% TBS (tween-20 in PBS) and added to the embryos and incubated overnight at 4^{o}C. After extensive washing in PBS containing 0.1% Triton X-100, the samples were sequentially labeled with anti-rabbit indocarbocyanine (Cy3) secondary antibody. After samples were washed 4 times with PBS containing 0.1% Triton X-100, the nuclei were counterstained with DAPI. Immunostaining of the sections was examined using a confocal microscope (Olympus, Planegg).

2.2.16.2 Isolation of (E14.5, E 15.5 and E17.5) prenatal gonads

Pregnant female mice were scarified by cervical dislocation on desired days of pregnancy. The uterus was pulled out with one set of forceps. After opening the uterus the extraembryonic membranes were removed, and then the anterior half of the embryos were cut (exactly below the arm). The posterior part dissection was proceeded under the dissecting microscope, in which a cut along the ventral midline of the embryos´ posterior half was made and liver and intestine were scooped out. The female gonads, which are located beside the kidney, or the male gonads, which are located at the two sides of the urinary bladder, were isolated carefully and immediately frozen in liquid nitrogen.

2.2.17 Computer analysis

For the analysis of the nucleotide sequences, programs like BLAST, BLAST2, MEGABLAST and other programs from National Center for Biotechnology Information (NCBI) were used (www.ncbi.nlm.nih.gov). For protein studies ExPASy tools (www.expasy.ch) were used. Mouse genome sequence and other analysis on mouse genes, transcripts and putative proteins were done in Ensembl database (www.ensembl.org).

3-Results

3.1- Expression pattern of *Vsig1* splice variant

In previous studies, murine *Vsig1* expression was found to be restricted to stomach and testis (Oidovsambuu, 2009). A search in gene data bank (aceview ncbi) showed that *Vsig1* gene has two alternatively spliced mRNAs (*Vsig1A* and *Vsig1B*), which may be regulated by two different promoters (Fig. 3.1). *Vsig1A* represents the longer transcript (2708 bp) that contains the sequence of exon 1a and exon 2 to exon 7, and it encodes a protein with 407 amino acids (aa). *Vsig1B* transcript (1236 bp) contains the sequence of exon 1b and exon 3 to exon 7, and encodes the shorter protein (isoform 2) which consists of 300 aa (Fig. 3.1).

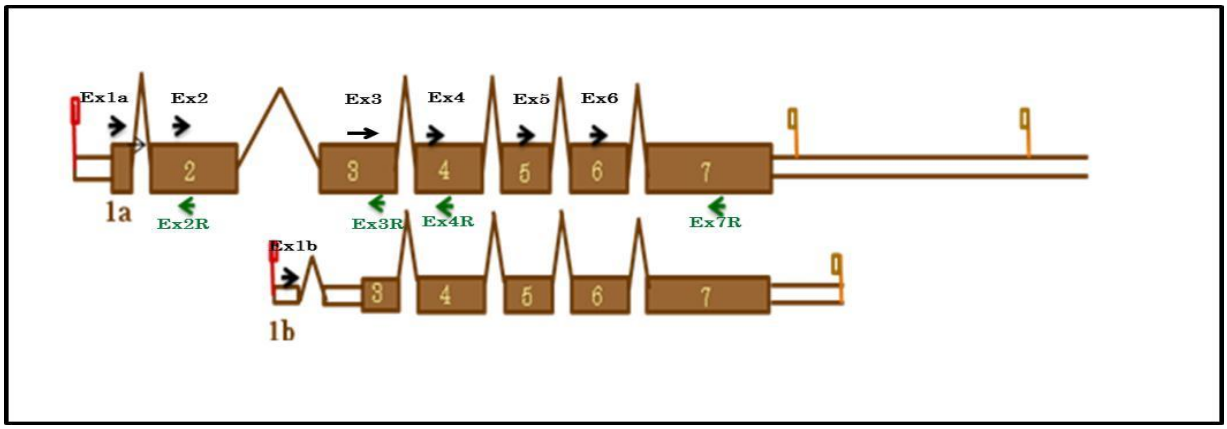

Figure 3.1: *Schematic diagram showing the position of the primers which have been designed for RT-PCR reactions. The primers are SX-exon1-F (Ex1a), SX-exon1b-F (Ex1b), SX-exon2-F (Ex2), SX-exon3-F (Ex3), SX-exon4-F (Ex4), SX-exon5-F (Ex5), SX-exon6-F (Ex6), SX-exon4-R (Ex4R), SX-exon7-R (Ex7R), Vsig1-ex1-ex2-R (Ex2R) and Vsig1-ex1b-ex3-R (Ex3R).*

Specific expression of *Vsig1A* and *Vsig1B* variants was analyzed by RT-PCR using six pairs of primers (Fig. 3.1 and 3.2). The first pair of primers Ex1a (SX-exon1-F) and Ex4R (SX-exon4-R) amplifies 1249-bp fragment of *Vsig1A* transcript. The second pair of primers Ex1b (SX-exon1b-F) and Ex7R (SX-exon7-R) amplifies 1117-bp fragment of Vsig1B transcript. The third pair of primers Ex2 (SX-exon2-F) and Ex4R (SX-exon4-R) amplifies 411-bp fragment of *Vsig1A* transcript. The other sets of primers amplify both of *Vsig1A* and *Vsig1B* spliced variants. The primers Ex3 (SX-exon3-F) and Ex7R (SX-exon7-R) amplify 909-bp fragment, Ex4 (SX-exon4-F) and Ex7R (SX-exon7-R) amplify

682-bp fragment and Ex5 (SX-exon5-R) and Ex7R (SX-exon7-R) amplify 555-bp fragment (Fig. 3.2). The results of RT-PCR revealed that *Vsig1A* is expressed in stomach and testis, while expression of *Vsig1B* is restricted to testis. Integrity of the RNA used for RT-PCR was proven by amplification of HPRT transcript.

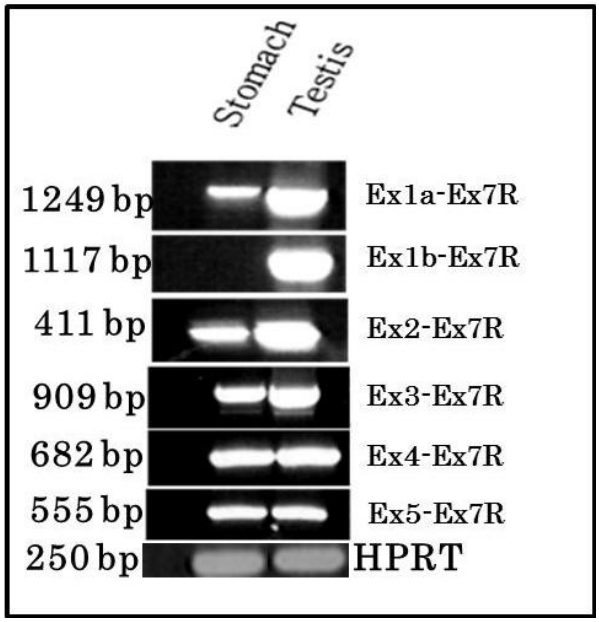

Figure 3.2: *Expression of Vsig1A and Vsig1B transcripts. Specific Vsig1A RT-PCR products were detected in stomach and testis while specific Vsig1B RT-PCR products were restricted to testis. Integrity of the RNA used for RT-PCR was proven by amplification of the HPRT transcript.*

3.2- Expression analysis of murine *Vsig*-1 gene

To determine the expression of *Vsig1* in different tissues, RT-PCR analysis was performed using two pairs of primers and total RNA, which was isolated from different adult mouse tissues including colon, cecum, stomach and testis (Fig. 3.1 & Fig. 3.3). The first pair Ex1a (SX-exon1-F) and Ex2R (Vsig1-ex1-ex2-R) amplifies 360-bp fragment of Vsig1A transcript, while the second pair Ex1b (SX-exon1b-F) and Ex3R (Vsig1-ex1b-ex3-R) amplifies 220-bp fragment of Vsig1B (Fig. 3.1). The results of RT-PCR analysis showed that *Vsig1A* is expressed in cecum, stomach and testis, while *Vsig1B* is only expressed in testis. Integrity of the RNA used for RT-PCR was proven by amplification of HPRT transcript (Fig. 3.3).

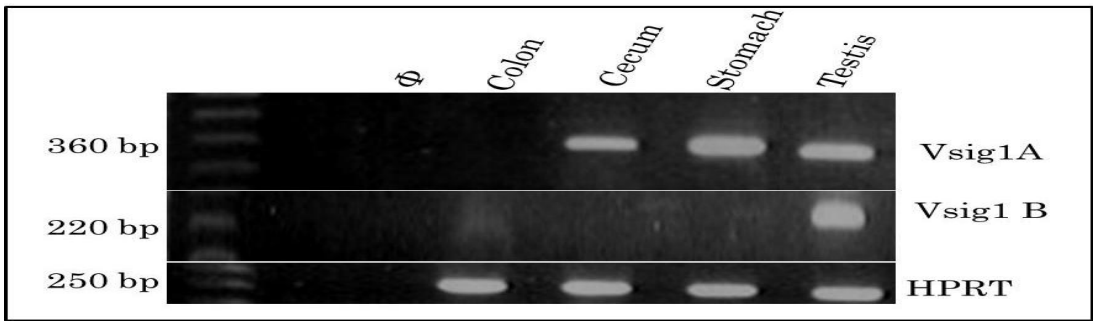

Figure 3.3: *RT-PCR analysis of Vsig1 expression in different adult mouse tissues. In control PCR reaction (φ) water was added instead of RT mix. The PCR was performed with two sets of primers. Each set is specific to amplify the 360bp and 220bp cDNA fragment of Vsig1A and Vsig1B, respectively. PCR products were analyzed on a 1 %-agarose gel. Integrity of the RNA used for RT-PCR was proven by amplification of the HPRT transcript.*

3.3- Expression of *Vsig1* in preimplantative stages of mouse development

Expression of *Vsig1* in preimplantative stages of embryonic development was studied by immunostaining of embryos at two-cell and blastocyst stages with rabbit anti-VSIG1 antibody. VSIG1 was found in cells of embryos at two-cell stage (Fig. 3.4A) as well as in inner cell mass and trophoblast of blastocyst (Fig. 3.4B). In control experiment using the diluted serum instead of anti-VSIG1 antibody, no specific immunostaining could be detected (Fig. 3.4C).

To determine the expression of *Vsig1* during prenatal embryonic stages 8.5, 9.5, 10.5, 12.5 and 14.5dpc, RT-PCR analysis was performed using two pairs of primers (Fig. 3.1 & Fig. 3.5). The first pair Ex1a (SX-exon1-F) and Ex2R (Vsig1-ex1-ex2-R) amplifies a 360-bp fragment of *Vsig1A*, while the second pair Ex1b (SX-exon1b-F) and Ex3R (Vsig1-ex1b-ex3-R) amplifies a 220-bp fragment of *Vsig1B*. *Vsig1A* transcript was detected in all studied prenatal stages, while no expression of *Vsig1B* could be detected in any of these embryonic stages. Integrity of the RNA used for RT-PCR was proven by amplification of HPRT transcript.

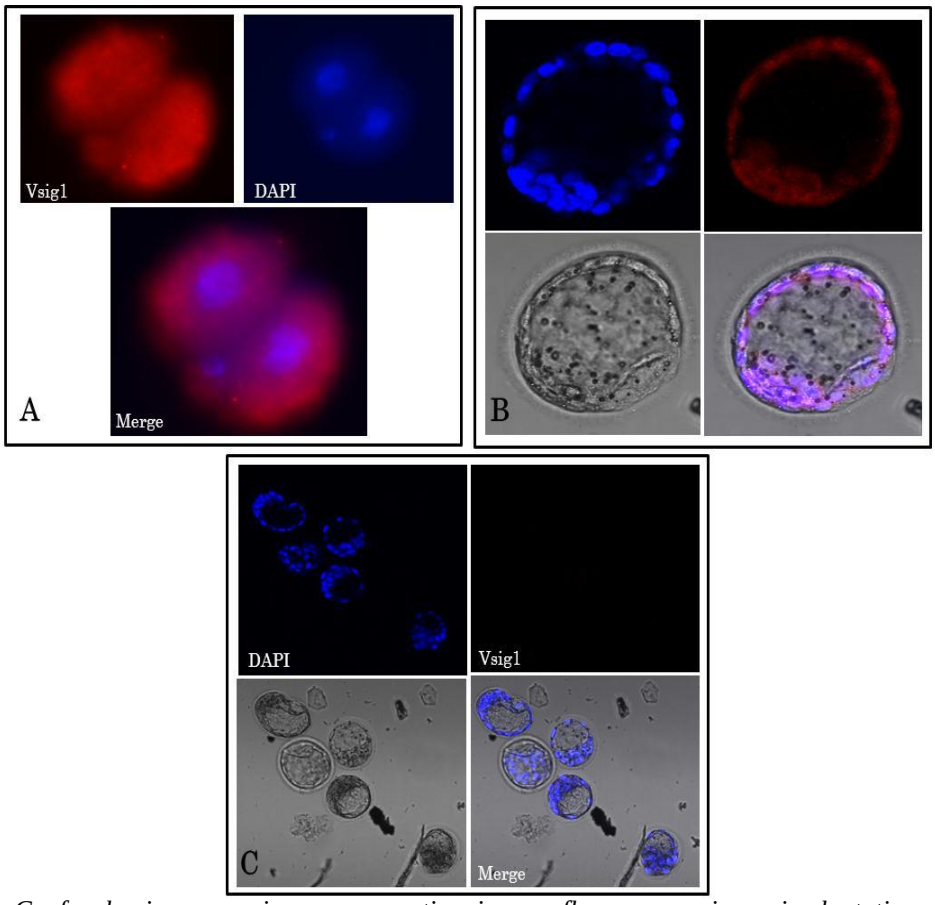

Figure 3.4: *Confocal microscopy images presenting immunofluorescence in preimplantation mouse embryos: Two-cell embryo (A), Blastocyst (B) were stained with anti-VSIG1 antibody. Immunofluorescet analysis shows the expression of VSIG1 protein in two cell stage as well as in the trophoblast and inner cell mass of blastocyst. DNA stained with DAPI (Vectashield). (C) Negative control without primary antibody incubation shows no immunofluorescent signal.*

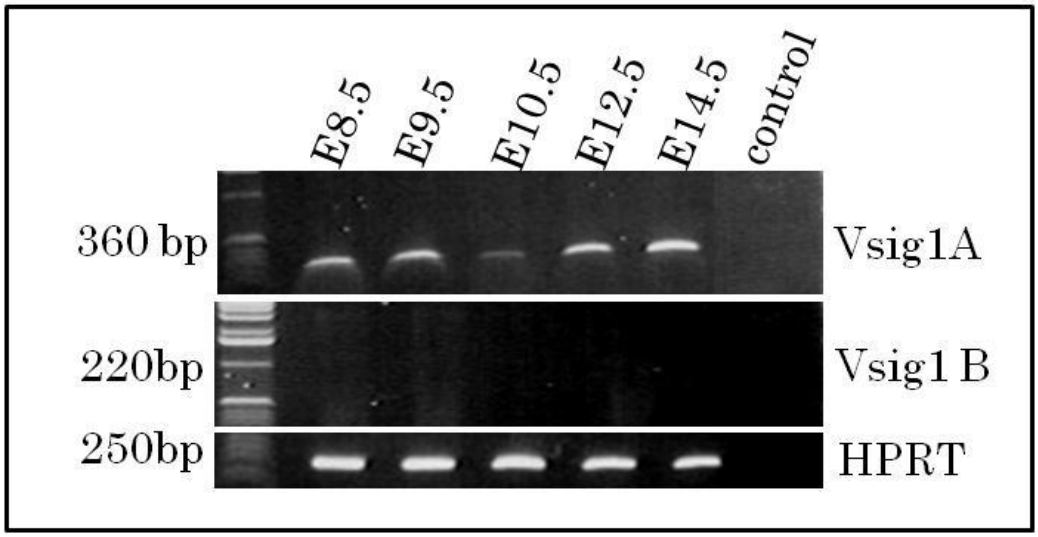

Figure 3.5: *RT-PCR analysis of Vsig1 expression in different mouse prenatal stages. The 360bp cDNA of Vsig1A transcript was amplified in RNA isolated from E8.5, E9.5, E10.5, E12.5 and E14.5. In contrast, the 220bp cDNA fragment of Vsig1B could not be amplified in RNA of these embryos. Integrity of the RNA used for RT-PCR was proven by amplification of the HPRT transcript.*

3.4- Expression analysis of murine *Vsig1* in testis

3.4.1- *Vsig1* expression in prenatal gonads

To determine the expression of *Vsig1* during prenatal development of testis and ovary, gonads were isolated from embryos at E13.5, E14.5, E15.5 and E17.5. Testes were recognized under dissecting microscope by the development of seminiferous tubules in the gonads. Total RNA was isolated from testes and ovaries. Expression of *Vsig1A* and *Vsig1B* variants in prenatal testis and ovary of E13.5, E14.5, E15.5 and E17.5 was analyzed by RT-PCR using primers that specifically amplify *Vsig1A* and *Vsig1B* (Fig. 3.1& Fig. 3.6). The first pair of primers Ex1a (SX-exon1-F) and Ex2R (Vsig1-ex1-ex2-R) amplifies 360-bp fragment of *Vsig1A*. The second pair Ex1b (SX-exon1b-F) and Ex3R (Vsig1-ex1b-ex3-R) amplifies the 220-bp fragment of *Vsig1B* (Fig. 3.1). The RT-PCR analysis revealed the early expression of *Vsig1A* variant in male and female gonads of all studied embryonic stages, while the *Vsig1B* variant was not expressed in testis and ovary of these embryonic stages (Fig. 3.6).

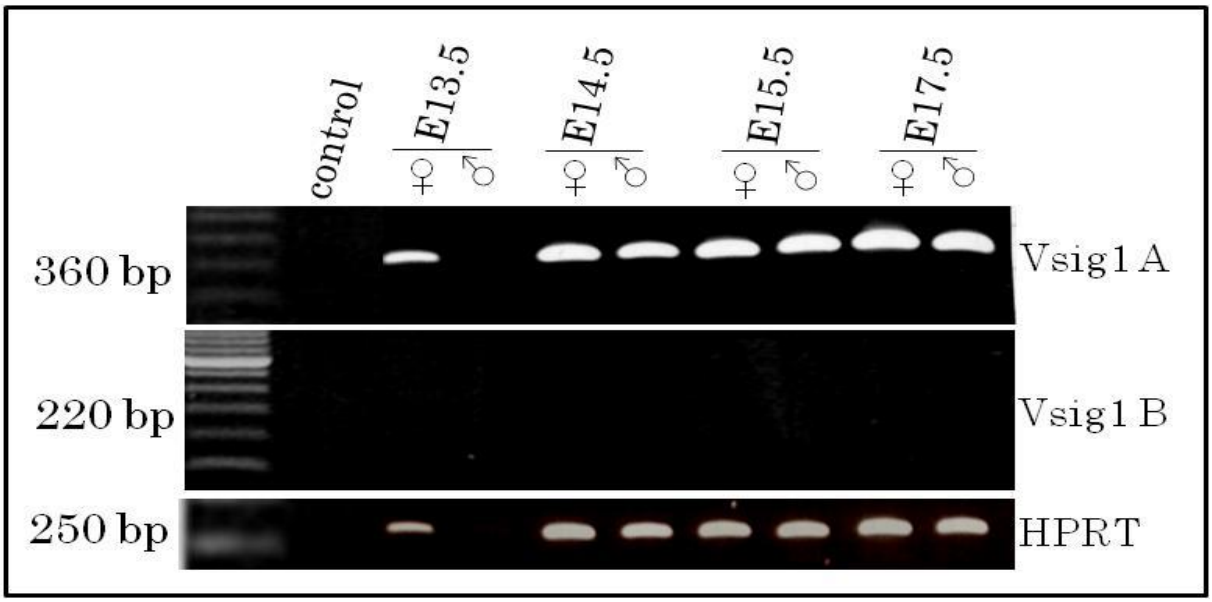

Figure 3.6: *RT-PCR analysis of Vsig1 expression in prenatal development of testis and ovary. Specific Vsig1A product was detected in male and female gonads of E13.5, E14.5, E15.5 and E17.5, while no specific Vsig1B band was detected. Integrity of the RNA used for RT-PCR was proven by amplification of the HPRT transcript.*

3.4.2- *Vsig1* expression in postnatal testes

Expression of Vsig1A and *Vsig1B* variants in different postnatal testes 5, 10, 15, 22, 25, 30 and 40 dpp was analyzed by Northern blotting and by RT-PCR (Fig. 3.7). A cDNA fragment located in the upstream sequence of the first poly-A signal was amplified with the primers (SX-Probe2F1 and SX-Probe2R1) and used as a probe in Northern blot hybridization. Northern blot hybridization showed that *Vsig1A* transcript is detected in all studied postnatal testicular stages 5, 10, 15, 22, 25, 30 and 40dpp, while the *Vsig1B* mRNA is firstly expressed in testis at 25 dpp (Fig. 3.7A). Expression of *Vsig1*during postnatal development of testis was detrmined by western blot analysis (Kim *et al.*, 2010).

The results of Northern blot were confirmed by RT-PCR using two sets of primers. The first pair Ex1a (SX-exon1-F) and Ex7R (SX-exon7-R) amplifies 1249-bp fragment of *Vsig1A*. The second pair Ex1b (SX-exon1b-F) and Ex7R (SX-exon7-R) amplifies 1117-bp fragment of Vsig1B (Fig. 3.1). Results of RT-PCR analysis showed that the *Vsig1A* variant was expressed in all studied postnatal testes, while the *Vsig1B* variant is firstly expressed at low levels in 20 dpp, which explains why it was not detected by Northern blot analysis, and then highly expressed in older stages (Fig. 3.7B).

To determine the cellular localization of VSIG1 in testis, immunohistological staining was performed with anti-VSIG1 antibody and testicular sections from mice at postnatal days 25, 27 and adult. As shown in figure 3.8, no specific immunostaining could be detected in Leydig cells. Specific VSIG1-immunostaining could be detected at plasma membrane of cells locating in seminiferous tubules.

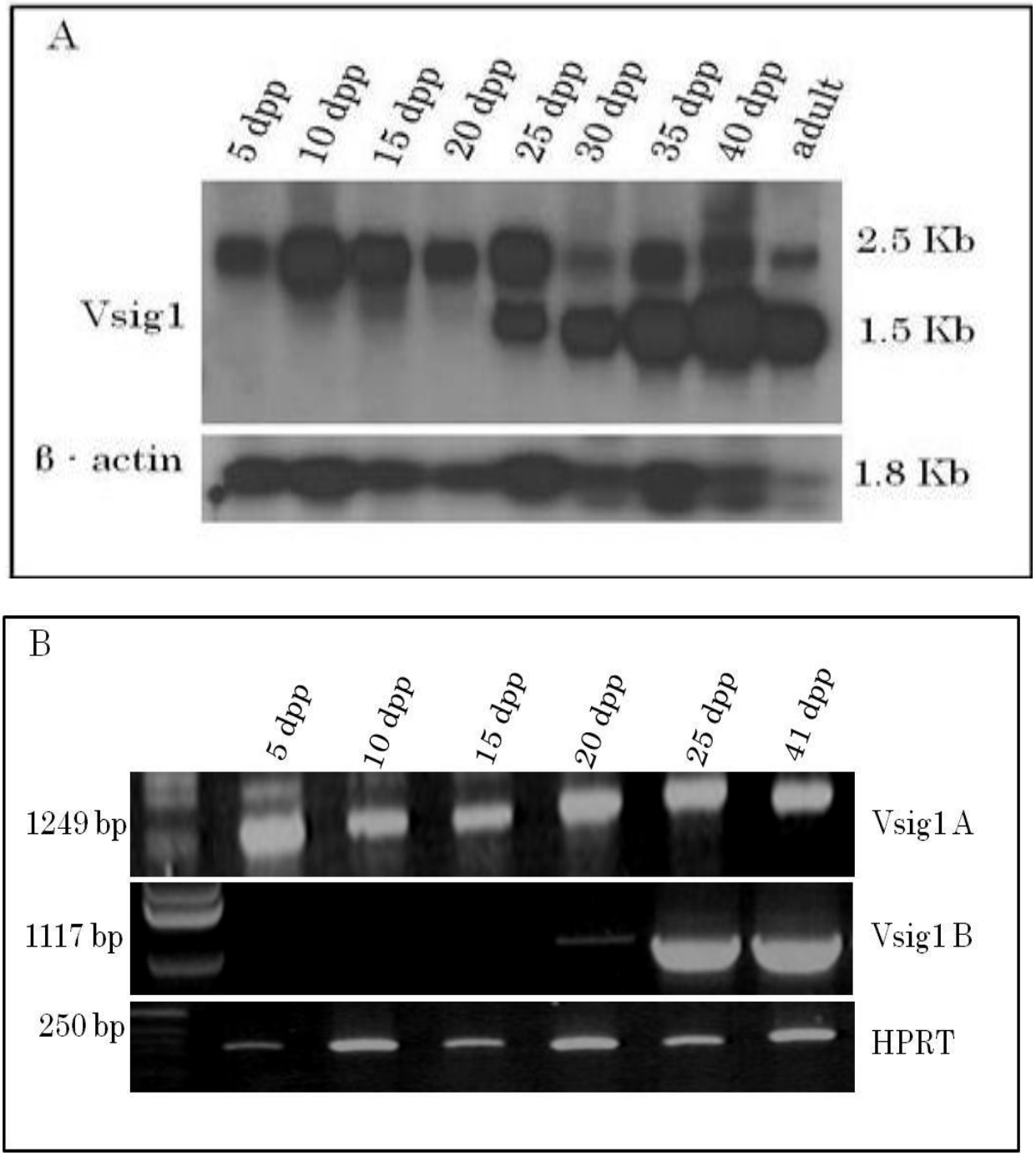

Figure 3.7 *(A) Northern blot analysis of Vsig1 expression in postnatal testes. Northern blot containing total RNA from 5-, 10-, 15-, 20-, 25- and 41-day-old testes was hybridized with cDNA fragment located in the upstream sequence of the first poly-A signal. The positions of the two Vsig1 transcripts are indicated. Integrity and variation of loaded RNA samples were checked by rehybridization with β-actin. (B) RT-PCR analysis of Vsig1 expression in postnatal testes. Specific Vsig1A product was detected in all studied stages, specific Vsig1B band was firstly detected 20 dpp and then in older stages. Integrity of the RNA used for RT-PCR was proven by amplification of the HPRT transcript.*

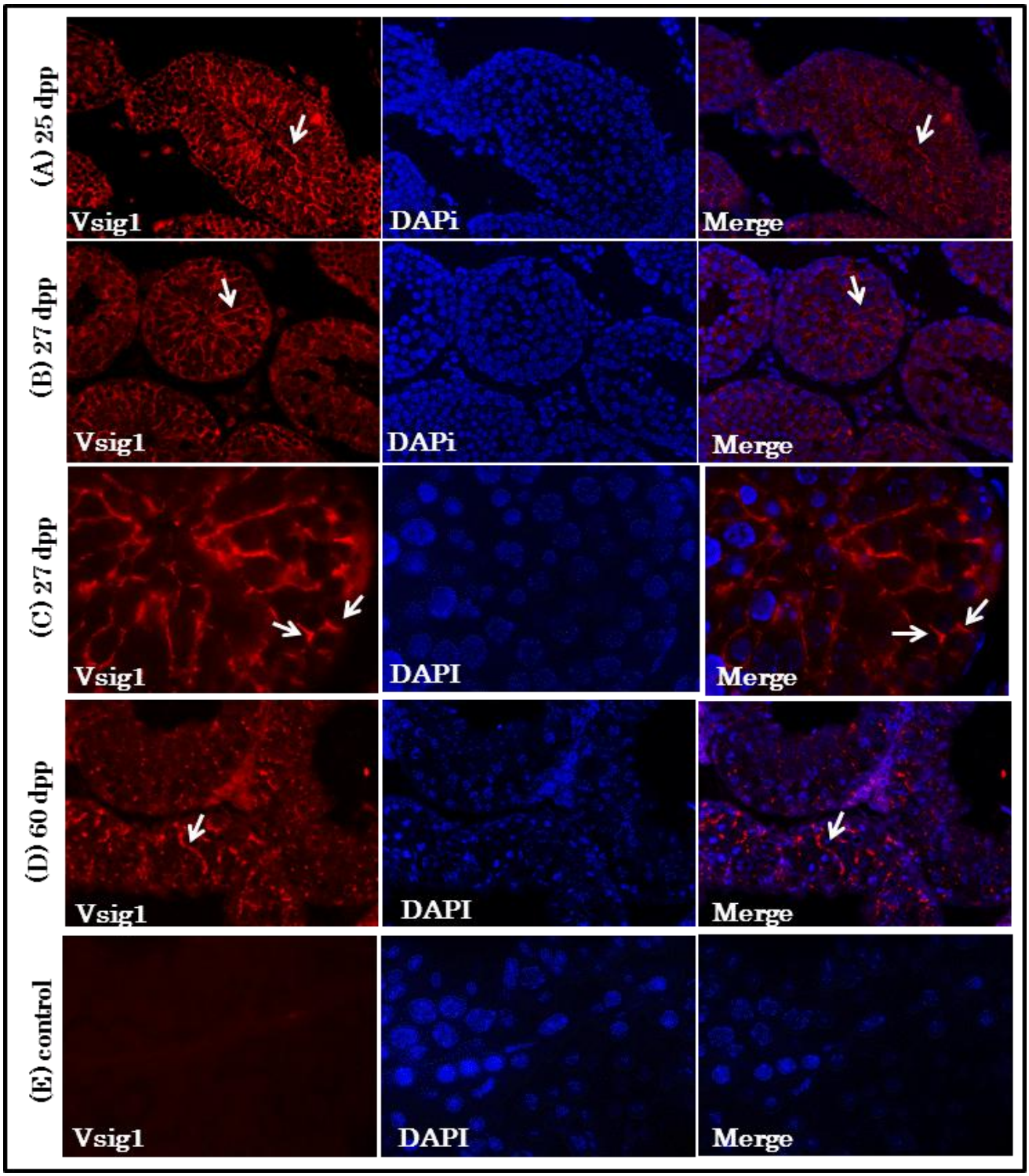

Figure 3.8: *Immunohistological analysis of histological sections from 25- (A), 27- (B and C), and 60-day-old (D) testes using anti-VSIG1 antibody. VSIG1 protein was detected at membrane of some cells in all of the studied postnatal testes and it might be localized at in cell-cell junction (arrows). The lower panel (E) shows the negative control. Optical magnifications: A, B and D 20X, C and E 60X.*

3.4.3- *Vsig1* expression in mutant testes

To determine the cell type-specificity of *Vsig1A* and *Vsig1B*, expression of *Vsig1A* and *Vsig1B* variants was analyzed in testis of W/W^v (which lack germ cells), *olt/olt* and *qk/qk* (in which spermatogenesis is arrested at spermatid stages) by Northern blotting and RT-PCR (Fig. 3.9). A cDNA fragment located in the upstream sequence of the first poly-A signal was amplified with the primers (SX-Probe2F1 and SX-Probe2R1) and used as a probe in Northern blot hybridization. Northern blot showed that *Vsig1A* RNA isoform is highly expressed in W/W^v testis and weakly detected in *olt/olt* and *qk/qk* testes, while the Vsig1B RNA isoform is expressed in *olt/olt* and *qk/qk* testes, but not expressed in W/W^v testis (Fig. 3.9A).

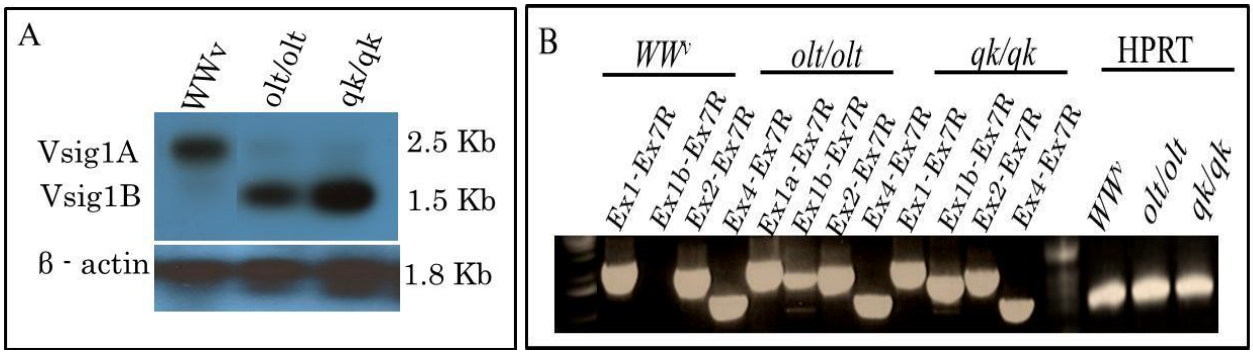

Figure 3.9: *(A) Northern blot analysis of Vsig1 gene expression in mutant testes. Blot with total RNA isolated from W/W^v, olt/olt and qk/qk testes was hybridized with cDNA fragment locating in the upstream sequence of the first poly-A signal as a probe. Integrity and variation of loaded RNA samples were checked by rehybridization with β-actin. (B) RT-PCR analysis of Vsig1 expression in mutant testes. Specific Vsig1A product was detected in all studied mutant testes, while specific Vsig1B band was detected in olt/olt and qk/qk, but not detected in W/W^v testes. Integrity of the RNA used for RT-PCR was proven by amplification of the HPRT transcript.*

The results of Northern blot were further confirmed by RT-PCR using four sets of primers. Two primer pairs Ex1a (SX-exon1-F) and Ex7R (SX-exon7-R), and Ex2 (SX-exon2-F) and Ex7R (SX-exon7-R) amplify 1249-bp and 1110-bp fragments of *Vsig1A* respectively. The third pair Ex1b (SX-exon1b-F) and Ex7R (SX-exon7-R) amplifies 1117-bp fragment of *Vsig1B*. The other pair Ex4 (SX-exon4-F) and Ex7R (SX-exon7-R) amplifies 682-bp fragment of *Vsig1A* and *Vsig1B*. The

results of RT-PCR analysis showed that the *Vsig1A* variant is expressed in all studied mutant testes. The *Vsig1B* variant is not expressed in W/W^v but is expressed in *olt/olt* and *qk/qk* testes (Fig. 3.9B).

3.4.4- Subcellular localization of *Vsig1* in testicular suspension

To determine the subcellular localization of VSIG1, germ cell suspension prepared from adult testis was stained with rabbit anti-VSIG1 and either anti-γ-tubulin (centrosome marker) or anti-Fej1 (acrosomal marker) (Fig. 3.12). In negative control, in which the sample was incubated with diluted serum instead of diluted primary antibody showed no specific immunostaining (Fig. 3.12 A). VSIG1 was localized in the centrosomes of spermatids, where the centrosome position is at the basal side opposite to the acrosomal side (Fig. 3.12B). The localization of VSIG1 in centrosome was partially colocalized with that of γ-tubulin, which is centrosomal marker (Fig. 3.12C). Germ cell at metaphase showed VSIG1 protein expression in the membrane and also in the centrosome (Fig. 3.12 D). No VSIG1 was detected in spermatozoa (Fig. 3.12 E).

To confirm the cytoplasmic location of VSIG1 protein, testis protein was fractionated into cytoplasmic and membrane fractions (Fig. 3.13). Purity of the fractions was assessed by presence and absence of Pan-cadherin, a membrane marker. Western blots containing membrane and cytoplasmic protein fractions from 25- and 90-day-old testes of wild-type mice were incubated with anti-Pan-cadherin and anti-VSIG1 antibodies. As expected, 110kDa pan-cadherin was only found in the membrane fraction. The 64kDa *Vsig1A* was present in the membrane and in the cytoplasmic fractions, while the 55kDa *Vsig1B* was exclusively present in the cytoplasmic fraction (Fig. 3.13). The expression level of 55kDa VSIG1B in cytoplasmic fraction of 90-day-old testis was markedly higher than that in 25-day-old testis, suggesting that the *Vsig1B* is highly expressed in postmeiotic germ cells.

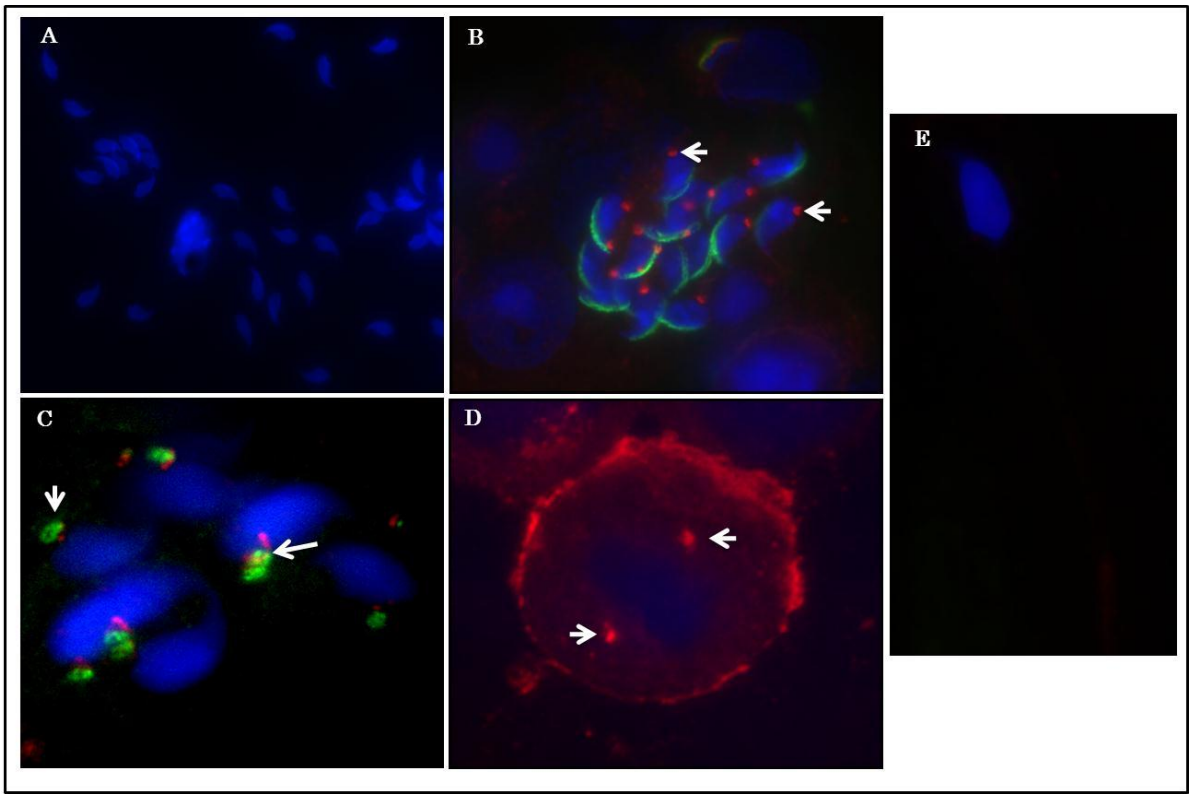

Figure 3.12: *Immunoflourescent analysis of germ cells of wild-type testis. (A) Negative control without primary antibody. (B) Double immunostaining using anti-VSIG1 (red) and anti-Fej1 (green) as acrosomal marker. (C) Double immunostaining using anti-VSIG1 (red) and anti Y-tubulin (green) as centrosomal marker. (D) Immunostaining of germ cell suspension in mitosis using anti-VSIG1 antibody. (E) Immunostaining of germ cell suspension in mitosis using anti-VSIG1 antibody. DNA stained with DAPI (Vectashield). Optical magnifications: (A) 10X, (B) 20X (C&D) 60X.*

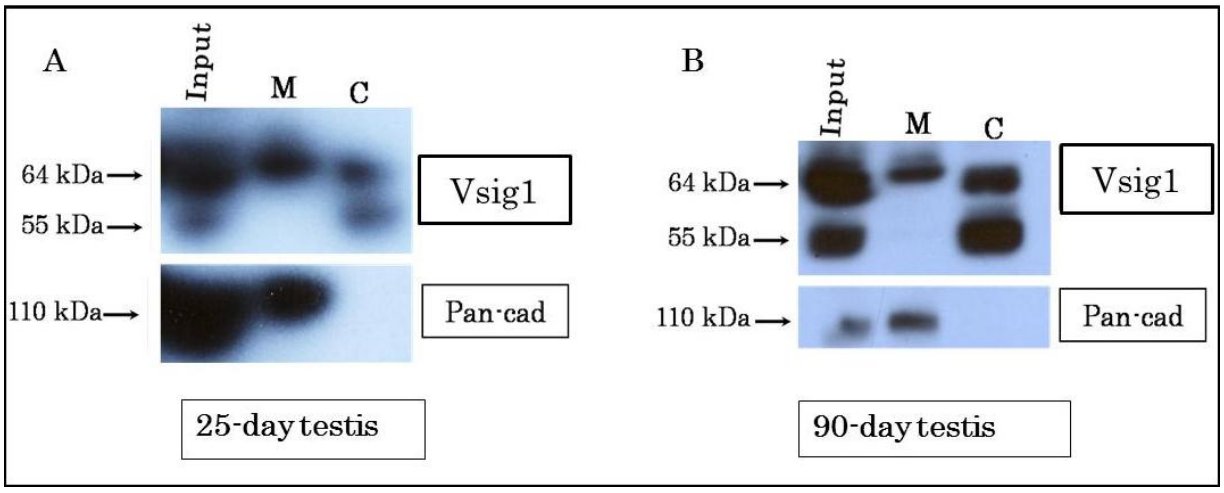

Figure 3.13: *Western blot showing the distribution of VSIG1 protein isoforms in membrane (M) and cytoplasmic (C) fractions. Blots with total testicular protein (input), membrane (M) and cytoplasmic (C) fractions isolated from 25- (A) and 90-day-old testes were probed with anti-VSIG1.*

3.5- *In vitro* study of *Vsig1* expression

3.5.1-Localization of VSIG1 in centrosome and nucleus of NIH 3T3 embryonic fibroblasts

To evaluate the subcellular localization of VSIG1 protein, double immunostaining of NIH 3T3 embryonic fibroblast cells was examined using confocal microscope (Fig. 3.14). Rabbit anti-VSIG1 antibody and either mouse anti-γ-tubulin antibody or mouse anti-α-tubulin antibody were used as primary antibodies. Immunostaining of methanol fixed cells with anti-VSIG1 and anti-γ-tubulin confirmed the localization of the VSIG1 protein in centrosome (Fig. 3.13A), while immunostaining of 4% paraformaldehyde-fixed cells with anti-VSIG1 and anti-α-tubulin showed the localization of the VSIG1 protein in nucleus (Fig. 3.14B). The discrepancy between the cellular localization of VSIG1 may be due to fixation procedure. It was reported that methanol fixation is optimal for centrosome preservation (Andreeva *et al*, 2009).

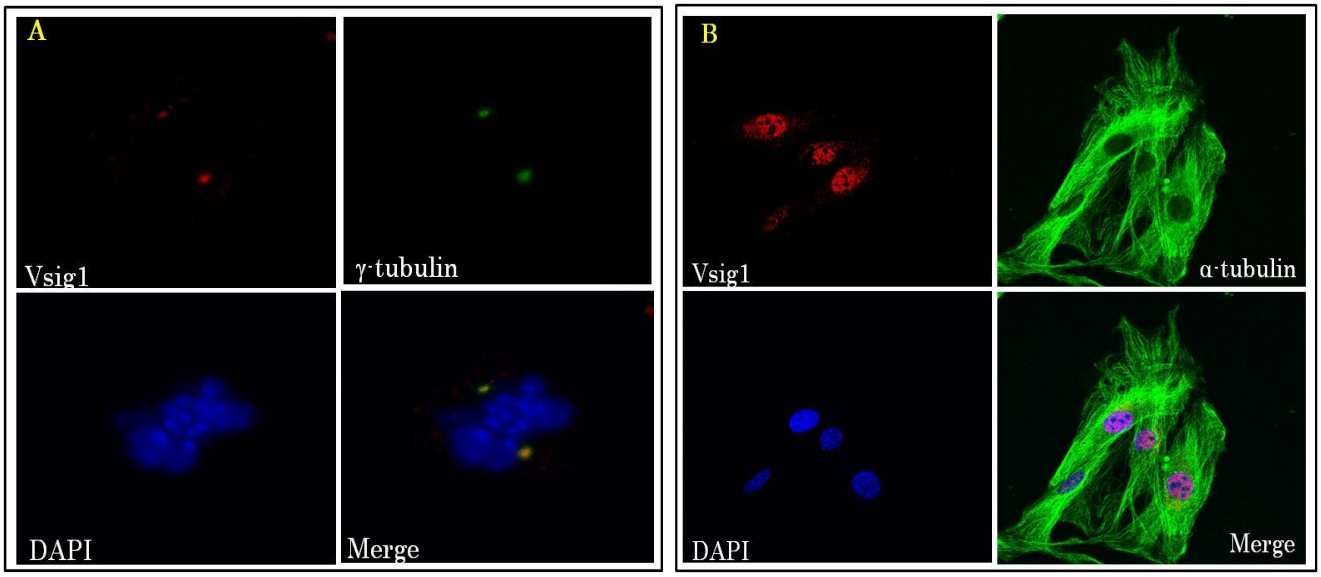

Figure 3.14: *VSIG1 is located in centrosome and nucleus of NIH 3T3 embryonic fibroblast cells. Cells were fixed either with methanol (A) or 4% paraformaldehyde (B) and immunostained with anti-VSIG1 and anti-γ-tubulin (A) or anti-α-tubulin (B). Nuclei were visualized with DAPI (blue). Optical magnifications: (A) and (B) 60X.*

To confirm the nuclear location of VSIG1, NIH 3T3 protein was fractionated into nuclear fraction and a fraction containing cellular compartments. (Fig. 3.15) Western blot containing

nuclear and cytoplasmic and membrane fractions was probed with anti-VSIG1 and cyclin-E (nuclear marker). Anti-VSIG1 antibody recognized a 55kDa protein at low level in nuclear fraction, that at higher level in a fraction containing cellular and membrane compartments. Anti-cyclin-E antibody recognized 57kDa protein only in the nuclear fraction.

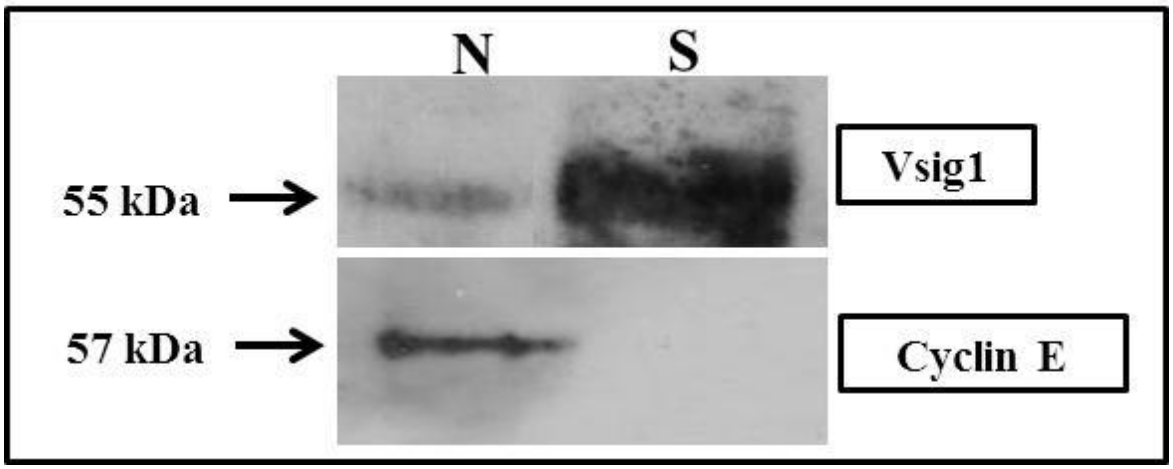

Figure 3.15: *Western blot containing nuclear fraction (N) and cytoplasmic and membrane fractions (S) were probed with anti-VSIG1 and anti-cyclin E antibodies.*

To confirm centrosomal localization of VSIG1, the location of VSIG1 protein during cell cycle was studied (Fig. 3.16). Double immunostaining of NIH 3T3 cells using rabbit anti-VSIG1 and mouse anti-γ-tubulin antibodies as primary antibodies was performed. This immunostaining showed VSIG1 protein localization in the typical centrosome positioning during the cell division. At interphase VSIG1 was located as two points in one side of the cell. VSIG1 protein was found as two points in one side of a cell at interphase, but as two points, one in each side of the chromosomes at metaphase while as one dot each in a pole of the dividing cells at anaphase.

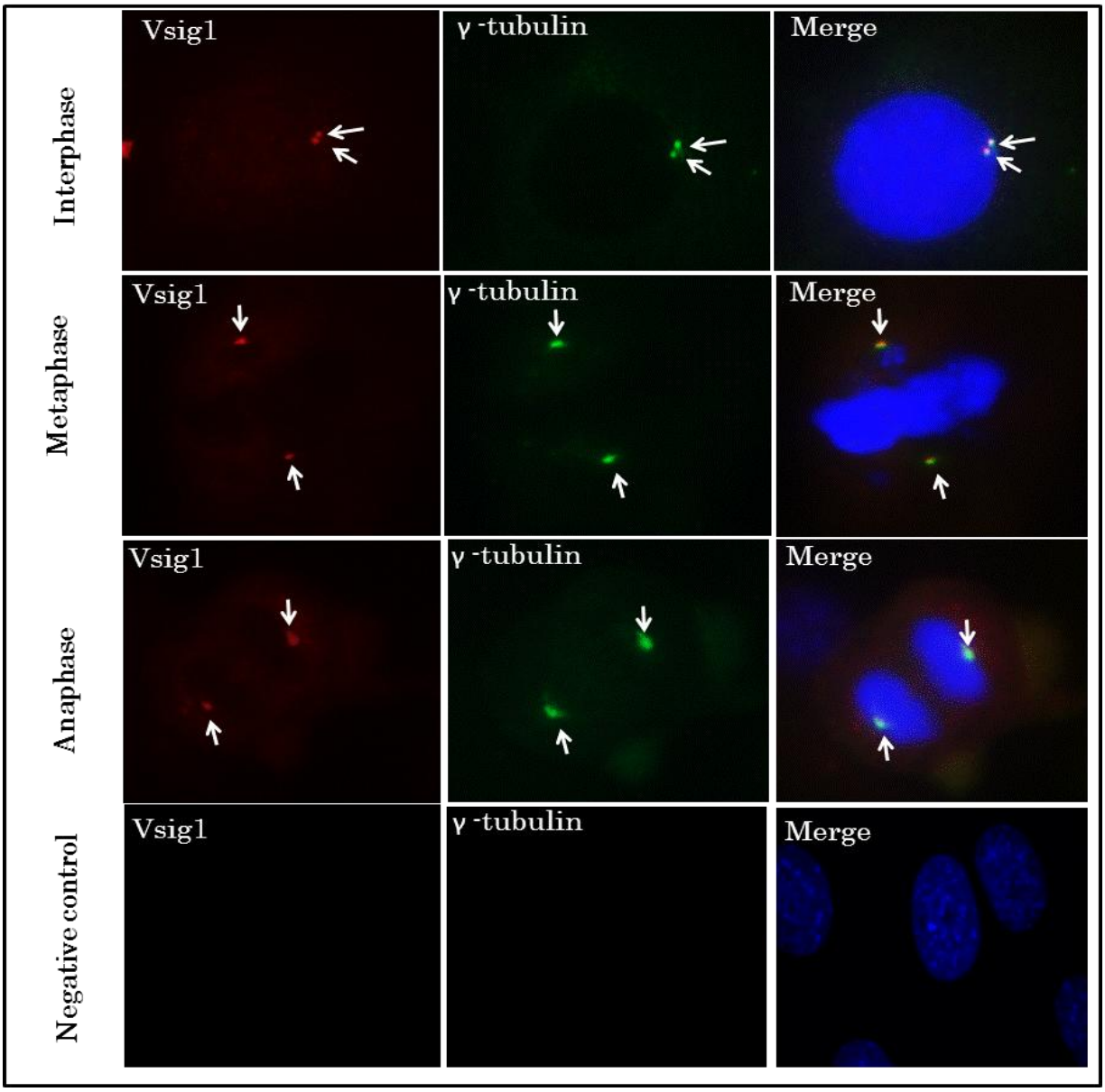

***Figure 3.16**: VSIG1 is located in centrosomes of NIH 3T3 embryonic fibroblast cells. Cells were fixed with methanol and co-immunostained with the rabbit anti-VSIG1 and mouse anti-γ-tubulin antibodies. Nuclei were visualized with DAPI (blue). The cell cycle phases are interphase, metaphase and anaphase. Centrosomes are indicated with arrows. Optical magnifications: 60X.*

3.5.2 -Subcellular localization of VSIG1 in different cell lines

To confirm the centrosomal localization of VSIG1, undifferentiated embryonic stem cells (Fig. 3.17A), mouse primary embryonic fibroblast (Fig. 3.17B) were fixed with methanol and immunostained with rabbit anti-VSIG1 and mouse anti-γ-tubulin antibodies as primary antibodies. The results showed partial colocalization of VSIG1 and γ-tubulin in the centrosome of all the studied cell lines, which confirms the localization of VSIG1 protein in centrosome.

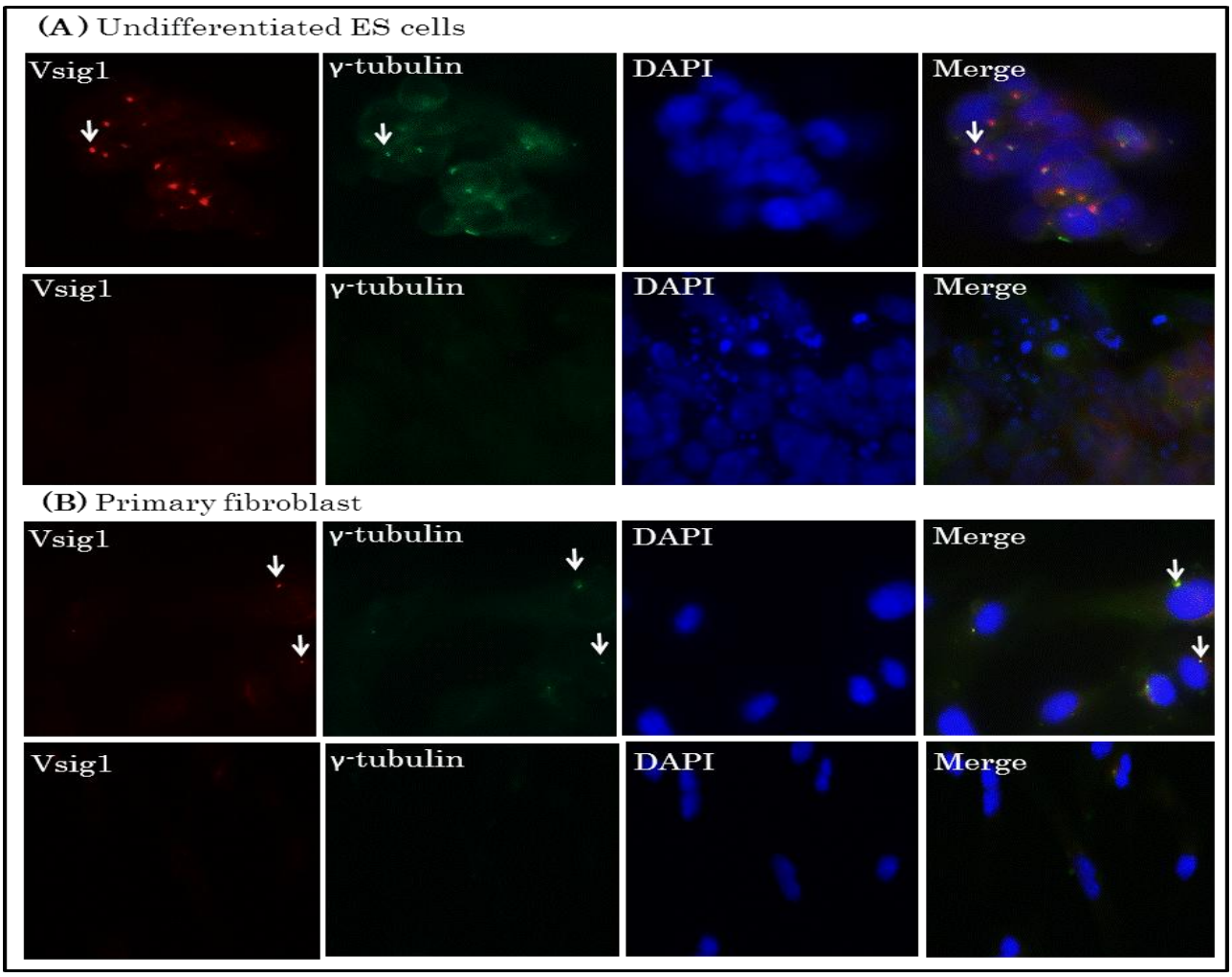

Figure 3.17*: VSIG1 is located in centrosomes of (A) undifferentiated ES cells (lower panel is the negative control) and (B) primary fibroblast cells (lower panel is the negative control). The cells were immunostained with the rabbit anti-VSIG1 and mouse anti-γ-tubuline antibodies. Nuclei were visualized with DAPI (blue). The arrows show the centrosome location. Nuclei were visualized with DAPI (blue). Optical magnifications 20X*

3.5.3- Subcellular localization of VSIG1B-DsRed fusion protein in transfected NIH 3T3 embryonic fibroblast cell line

To determine whether *Vsig1B* isoform is localized in centrosome, cDNA of *Vsig1B* was amplified, subcloned in pDsRed monomer N1 vector and the generated vector was used to transfect NIH 3T3 embryonic fibroblast cells. Strategy to subclone the *Vsig1B* cDNA in the pDsRed Monomer N1 vector is described in figure 3.18. The murine *Vsig1B* cDNA fragment was amplified using the primer SX-Dsredxho-F3, containing the sequence of the restriction site *XhoI* at the 3´end, and the primer SX-Dsredbam-R3 containing the sequence of the restriction site *BamHI* at the 5´end.

The 732-bp amplified fragment was digested with *XhoI* and *BamHI* enzymes and subcloned into XhoI/BamHI digested PGMT-easy vector, and sequenced. The *Vsig1B* fragment was subcloned into *XhoI*/*BamHI* digested pDsRed monomer N1 vector. NIH 3T3 cells grown to 80% confluence on glass cover slip in 24-well plate were transfected with 1µg of the Vsig1B-pDsRed plasmid. After 24 h of transfection, cells were fixed with 4% paraformaldehyde and immunostained only with anti VSIG1 (Fig. 3.19A) or fixed with methanol and immunostained with anti-γ-tubulin as centrosomal marker (Fig. 3.19B). VSIG1-immunofluorescent and DsRed were colocalized in nucleus (Fig. 3.19A). In the second experiment, DsRed and γ-tubulin-immunofluorescent were colocalized in centrosomes (Fig. 3.19B).

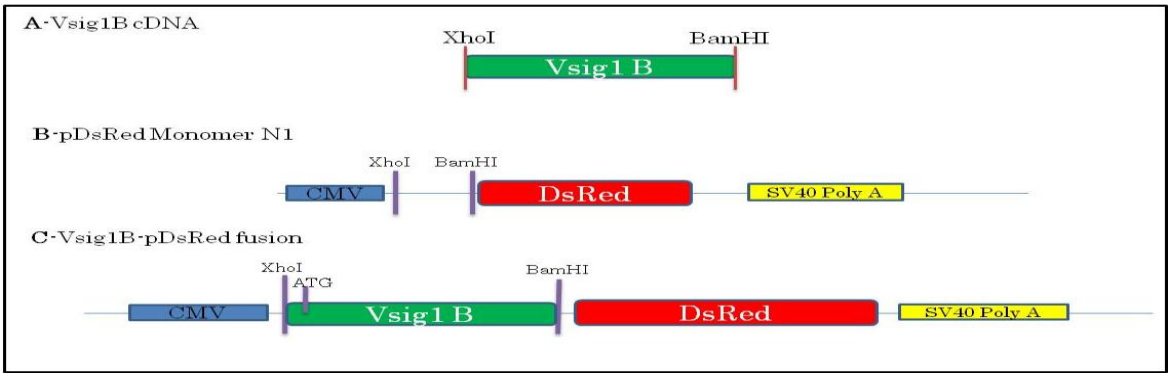

Figure 3.18: *Strategy to subclone the Vsig1B cDNA in the pDsRed Monomer N1 vector. (A) The murine Vsig1B cDNA fragment was amplified using the primer SX-Dsredxho-F3, which contains the sequence of the restriction site XhoI at the 3´end and the primer SX-Dsredbam-R3 containing the sequence of the restriction site BamHI at the 5´end. The 732-bp amplified product was digested with XhoI and BamHI enzymes and subcloned into XhoI/BamHI digested pDsRed monomer N1 vector. (B) Structure of the pDsRed monomer N1 vector. (C) Vsig1B –pDsRed fusion protein. ATG, start codon; CMV, Human cytomegalovirus promotor.*

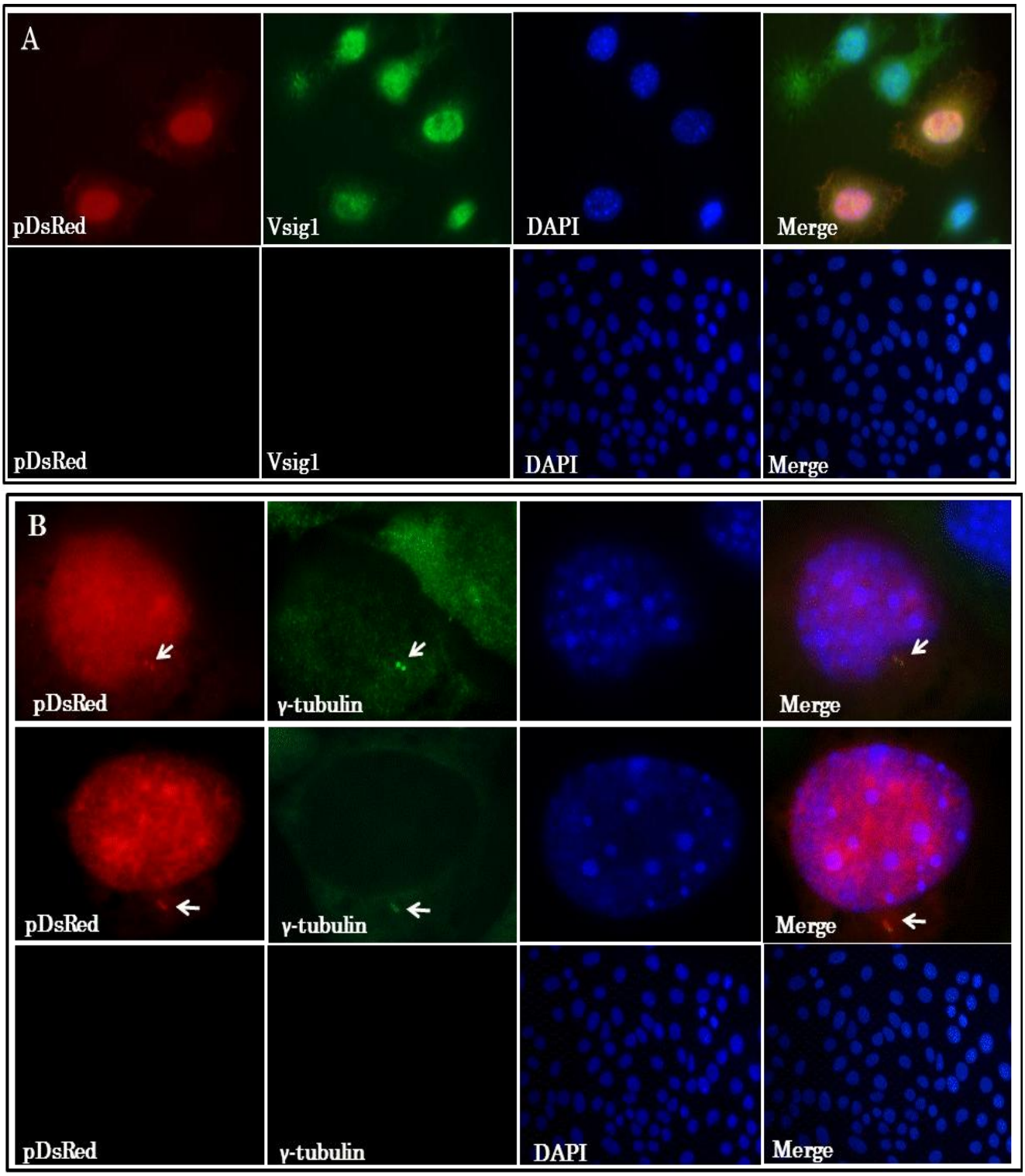

Figure 3.19: *Immunostaining of transfected NIH 3T3 embryonic fibroblast cells with Vsig1B-pDsRed-fusion construct. Transfected cells were fixed in 4% paraformaldehyde and immunostained with anti-VSIG1 (A) or fixed with methanol and immunostained with anti-γ-tubulin antibody (B) (Arrows indicates the position of centrosomes. Nuclei were visualized with DAPI (blue). Optical magnifications: (A) and (B) 60X.*

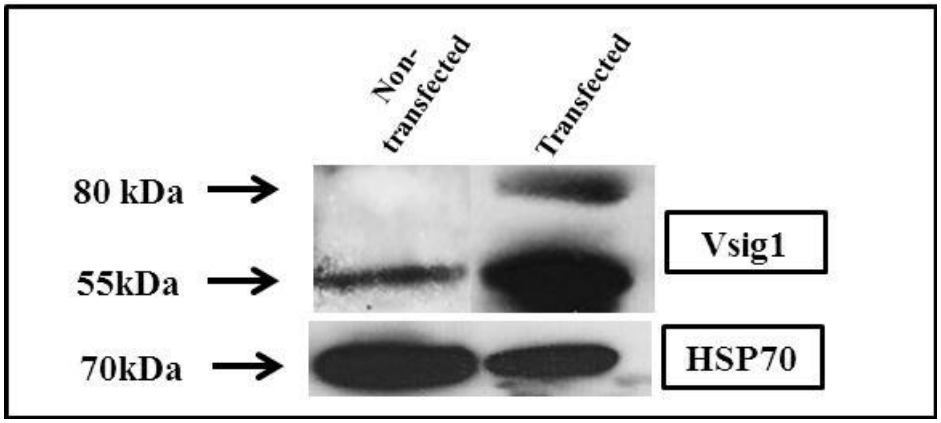

Figure 3.20: *Western blot showing the distribution of Vsig1 protein isoforms in transfected and non-transfected NIH 3T3 embryonic fibroblast cells. Rabbit anti-Vsig1 recognizes 55kDa protein in both of transfected and non-transfected cells proteins, while the DsRed-VSIG1 fusion protein is only recognized in the transfected cells protein. 70kDa HSP70 protein band is shown as control.*

To determine the expression of 80kDa DsRed-VSIG1 fusion protein in transfected cells, Western blot containing protein extracts from transfected and non-transfected NIH 3T3 embryonic fibroblast cells was subsequently probed with anti-VSIG1 and anti-Hsp70 (Fig. 3.20). In extract of non-transfected NIH 3T3 cells, anti-VSIG1 recognizes only the 55kDa VSIG1 protein. In extract of transfected cells, anti-VSIG1 antibody recognizes 55kDa VSIG1 and 80kDa DsRed-VSIG1 fusion protein. The 80kDa protein band represents the expected molecular weight of DsRed protein (26kDa) plus VSIG1B variant (55 kDa).

3.5.4-Analysis of migration properties of the HepG2 cell line overexpressing VSIG1

To determine the effect of *Vsig1*-overexpression on cell migration, migration assay was performed using mouse hepatocyte (HepG2) cell line, and VSIG1 overexpressing hepatocytes (HepG2) which contain pcDNA-VSIG1 construct (Fig. 3.21A). 2 x 10^6 cells were grown at 90-100% confluence to form a monolayer in 10 cm^2 culture dishes. By using a p200 pipet, a scratch of the cell monolayer was created in each cell culture. The wound healing assay showed that the VSIG1 overexpressing cells were able to migrate faster than that of control cells. This result

suggests that VSIG1 has a role in cell migration, and the overexpression of VSIG1 in HepG2 cells increases the cell migration property (Fig. 3.21 B).

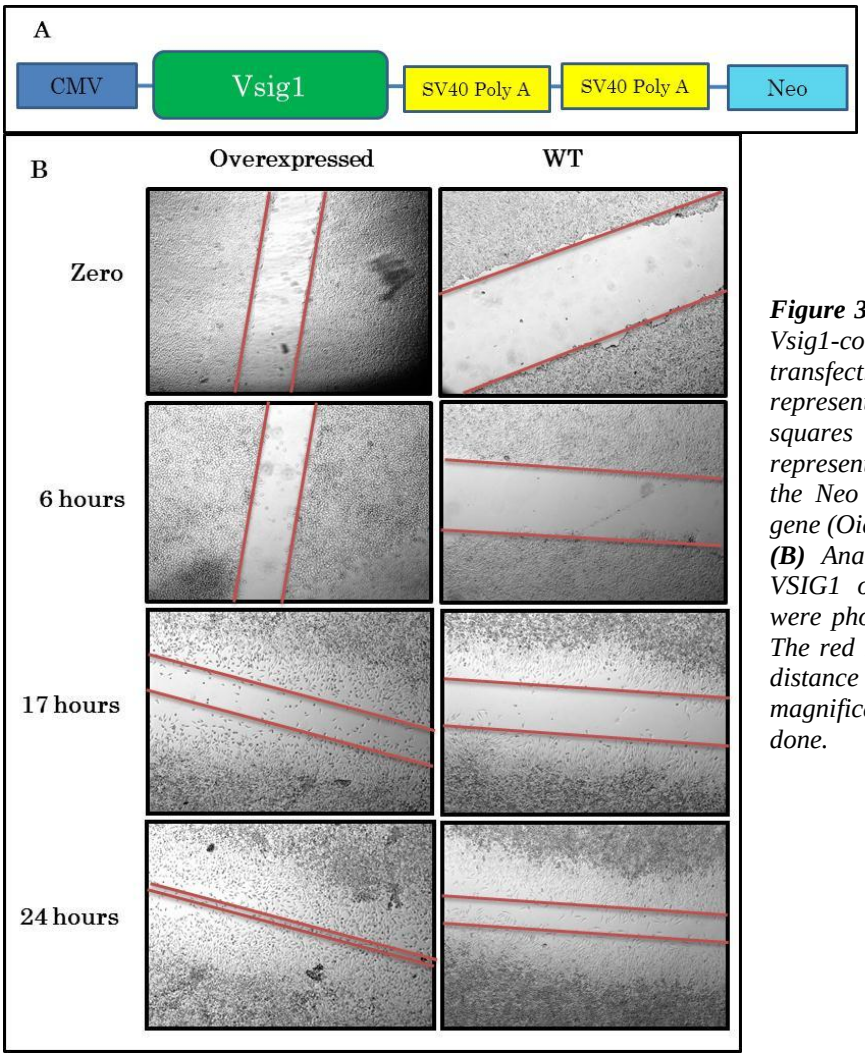

***Figure 3.21**: **(A)** Schematic diagram represents the Vsig1-construct which was used in stable transfection of Hepg2 cell line. Blue square represents cytomegalovirus (CMV) promotor, green squares represents Vsig1 cDNA, yellow squares represent the SV40 polyadenylation signal, while the Neo square represents the neomycin resistant gene (Oidovsambuu, 2009).*
***(B)** Analysis of cell migration of wild-type and VSIG1 overexpressing HepG2 cell lines. Images were photographed after 6 hrs, 17 hrs and 24 hrs. The red lines were drawn to show the approximate distance between the two edges of wounds. Optical magnifications 4X. Three biological replicates were done.*

3.5.5-Analysis of spreading properties of the HepG2 cell line overexpressing VSIG1

Spreading assay was done with wild-type mouse hepatocytes (HepG2) and VSIG1-overexpressing hepatocytes, which were transfected with pcDNA-*Vsig1* construct (Fig. 3.22 A). The adhesive property of the VSIG1 overexpressing cells and wild-type HepG-2 cells was evaluated by cell spreading assay (Fig. 3.22 B). 1x 10^4 cells were plated, then ten microscopic fields were photographed after 30 min and 90 min, and unspread cells were counted (Fig. 3.22 A At 30 min after spreading, the majority of VSIG1-overexpressing HepG2 and control cells had not spread

and exhibited a round morphology. At 90 min after spreading, ~80% of VSIG1-overexpressing HepG2 cells were spread compared with ~30% of control cells ($p < 0.001$) (Fig. 3.22 B). These results suggest that VSIG1 overexpression increases the cell adhesion.

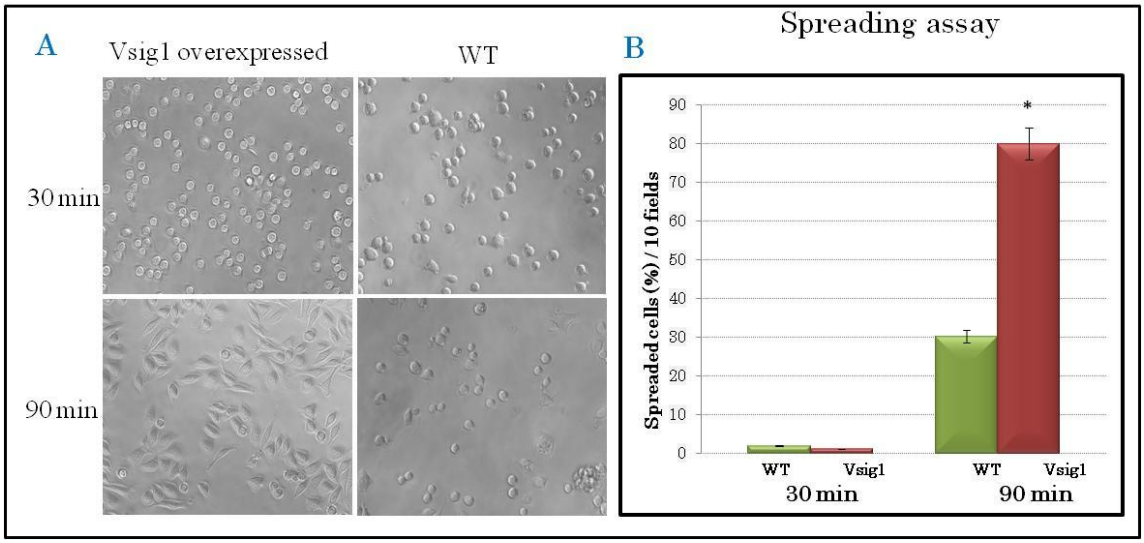

***Figure 3.22**: Cell spreading assay. (A) VSIG1-overexpressing HepG2 (left panels) and control HepG2 (right panels) cells were allowed to spread on fibronectin-coated plates for 30 min and 90 min. Optical magnifications 4X. (B) The percentage of spread cells on fibronectin ($p < 0.001$). Three biological replicates were done.*

3.6- Functional analysis of *Vsig1*

3.6.1- Analysis of conditional *Vsig1* knockout mice

Analysis of chimeric mice, which were generated by injection of conventional knockout ES cells (*Vsig1*$^{-/Y}$) to blastocysts revealed that chimeric mice with highly distributed *Vsig1*$^{-/Y}$ cells died during embryonic development (Oidovsambuu, 2009). To overcome the early lethality of *Vsig1*-deficient mice, a *Vsig1* conditional knockout mouse line (*Vsig1*-cKO) was generated in the Institute of Human Genetics, Göttingen. In the conditional knockout allele (*Vsig1*^{F}) exon 3 is flanked with two LoxP elements (Fig. 3.23). We expected that insertion of these elements in introns 2 and 3 would not disrupt the expression of floxed *Vsig1* allele (*Vsig1*^{F}) and thereby *Vsig1*$^{F/F}$ and *Vsig1*$^{F/Y}$ mice would develop normally. To recombine the floxed allele, we have generated two mouse lines

by introduction of two different transgenic *Cre* recombinase alleles in the genome of *Vsig1*$^{F/Y}$ and *Vsig1*$^{F/F}$ mice.

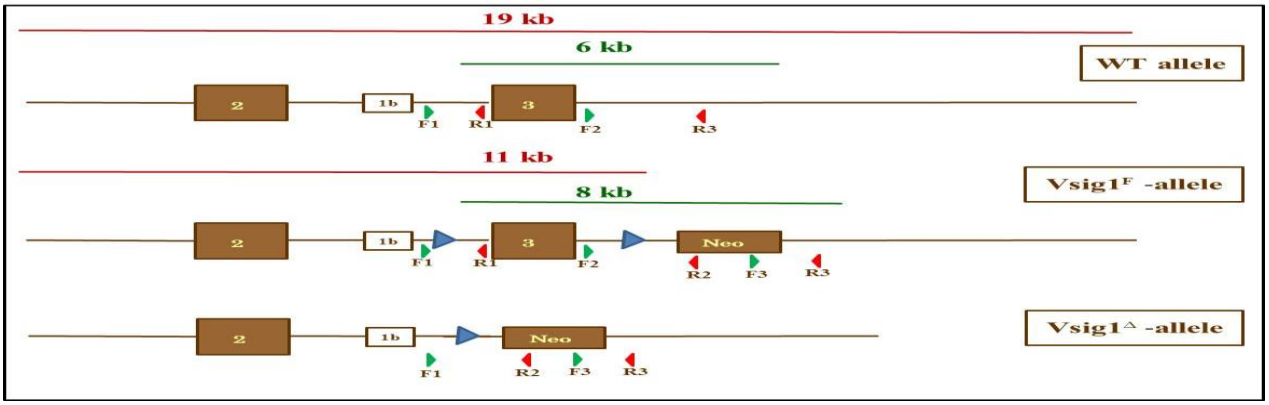

Figure 3.23*: Schematic representation of the different Vsig1 alleles. A restriction map of the wild-type allele, Vsig1*^{F} *allele, Vsig1*$^{\Delta}$ *allele is shown. 2 & 3 squares represent Vsig1 exons, whereas Neo one is a symbol of Neomycin cassette. Blue triangles stand for LoxP sites. Primers used in genotyping: Green triangles are the forward primers which are F1=Lox1F1, F2= Lox2F2, F3= NeoF1. Red triangles are the reverse primers which are R1=Lox1R1, R2= Lox2R2, R3= PGK3R.*

The *EIIaCre* recombinase allele is expressed under the control of adenovirus EIIa promoter (Lakso *et al*., 1996). EIIa promotor is activated in oocytes shortly after fertilization (Dooley *et al.*, 1989). Therefore, we expected that *Cre*-mediated recombination would occur at one-cell stage and effectively delete the LoxP-flanked *Vsig1* fragment.

To achieve temporal inactivation of floxed *Vsig1* allele in vivo, *Cre-ERT* fusion allele was introduced in the genome of *Vsig1* floxed mice. In this fusion allele, the *Cre* recombinase gene is fused with the mutated ligand binding domain of the human estrogen receptor (ERT). The fusion protein become active upon administration of the synthetic estrogen antagonist 4-hydroxytamoxifen (OHT), but not in the presence of the natural ligand 17β-estradiol (Feil *et al*., 1996). To avoid the random integration of the *CreERT* transgenic allele into the mouse genome which often results in mosaic gene expression (Garrick *et al.*, 1998; Henikoff, 1998), the *CreERT* fusion gene was inserted into the ubiquitously expressed *ROSA26* (R26) locus by gene targeting (Vooijs *et al*., 2001). The *R26CreERT* is expressed throughout mouse development and in adult

life, but *Cre* recombinase only become active after administration of the OHT or tamoxifen (TAM).

The wildtype allele for *Vsig1* is amplified by Lox2F2, NeoF1 and Lox2R2 primers in PCR1 assay resulting in a PCR product of about 150bp bp, while the *Vsig1* floxed allele generates a fragment of 200 bp. In the PCR2 assay Lox1F1, Lox2F2, PGK3R and Lox2R2 primers are used to amplify wild-type allele for *Vsig1* (200bp), floxed allele of *Vsig1* (234bp) and deleted allele (500-bp).

3.6.1.1-*Vsig1*-CreEIIa

To generate *Vsig1*$^{\Delta/y}$*EIICre* and *Vsig1*$^{\Delta/\Delta}$*CreEIIa*, heterozygous *Vsig1*$^{flox/+}$ females were bred with *Vsig1*$^{+/y}$*CreEIIa* transgenic males to obtain *Vsig1*$^{\Delta/y}$*CreEIIa* and *Vsig1*$^{\Delta/+}$*CreEIIa* (Fig. 3.24) which were bred together to obtain *Vsig1*$^{\Delta/\Delta}$*EIIaCre* and *Vsig1*$^{\Delta/Y}$*CreEIIa* in F_2 generation. Mice were genotyped by using two PCRs.

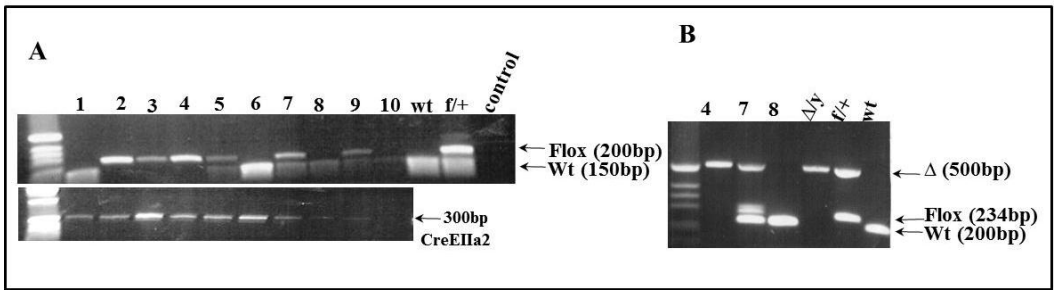

***Figure 3.24**: Genotyping PCRs for Vsig1-creEIIa mice. (A) Genotyping PCR amplifies wild-type and Flox alleles, and the lower showed the PCR amplifying creEIIa. (B) Genotyping PCR amplifies Δ, flox and wild-type alleles. The numbers (1-10) show the animals' numbers. PCR conditions are presented in chapter 2.2.7.1.*

The genotyping of the first litter (10 animals) derived from the breeding between *Vsig1*$^{F/+}$ female and *Vsig1*$^{+/y}$*CreEIIa* transgenic male using genotyping PCR (1) showed that three males were *Vsig1*$^{F/y}$ and three females were *Vsig1*$^{F/+}$, and all of these animals had Cre allele (Fig. 3.24A). Genotyping PCR (2) showed that one of the male animals was *Vsig1*$^{\Delta/y}$, while the females were chimeras with *Vsig1*$^{F/+}$ and *Vsig1*$^{\Delta/+}$ genotypes (Fig. 3.24 B).

To analyze *Vsig1* expression in stomach and testis of hemizygous *Vsig1*$^{\Delta/y}$ male, RT-PCR and quantitative RT-PCR analysis were performed (Fig. 3.25). Total RNA was isolated from testes of hemizygous and wild-type mice. RT-PCR analysis was performed using two primer pairs. The first primer pair, Ex1a (SX-exon1a-F) and Ex7R (SX-exon7-R), amplifies a 1249-bp fragment of *Vsig1A*. The second primer pair, Ex3 (SX-exon3-F) and Ex7R (SX-exon7-R), amplifies a 909-bp fragment of *Vsig1A* and Vsig1 B (Fig. 3.25 A). Real-Time RT-PCR was performed as described in 2.2.7.3, with HPRT as endogenous reference (Fig. 3.25 C).

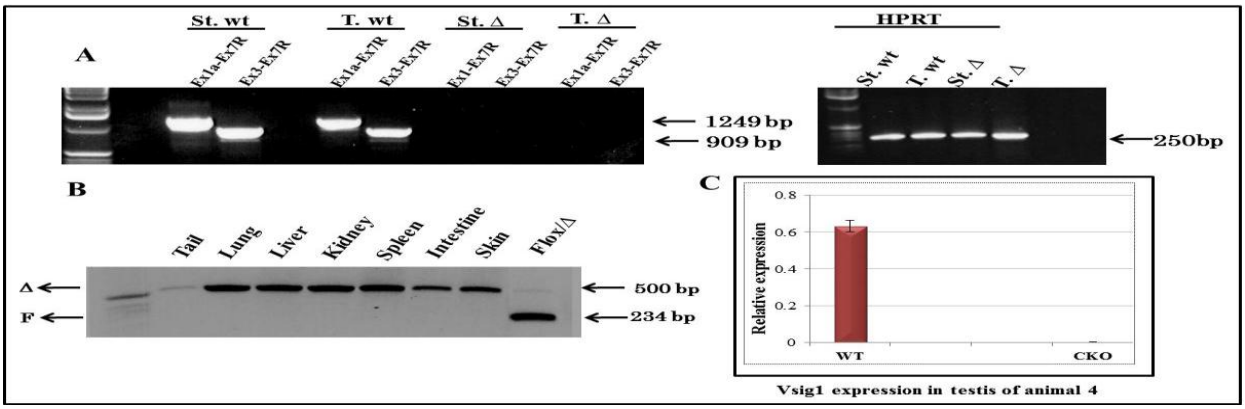

Figure 3.25*: (A) RT-PCR analysis of Vsig1 expression in stomach (St.) and testis (T.) of the hemizygous Vsig1*$^{F/y}$*EIICre animal. The RT-PCR was performed with two sets of primers. The first set (Ex1a-Ex7R) was used to detect the specific band of Vsig1A variant. The second set (Ex3-Ex7R) was used to detect specific band of Vsig1A and Vsig1B variants. (B)Genotyping PCR for different organs of the hemizygous animal. Genomic DNA was isolated by the same method as described (chapter 2.2.1.2) and it was genotyped with genotyping PCR 2. (C) Relative expression levels of Vsig1 detected by quantitative RT-RCR in testes of wild-type and hemizygous (Vsig1*$^{\Delta/y}$*) mice. Expression levels are normalized to the expression of endogenous control (HPRT). Two biological replicates were done.*

The results showed that stomach and testis of the hemizygous *Vsig1*$^{\Delta/y}$ male have no *Vsig1* expression (Fig. 3.25 A). Genotyping PCR of different tissues of this hemizygous animal showed that tail, lung, liver, kidney, spleen, intestine and skin have only the Δ allele (Fig. 3.25 B).

Stomach of conditional knockout mice were studied by immunostaining of stomach sections of hemizygous *Vsig1*$^{\Delta/y}$*EIICre* male and heterozygous *Vsig1*$^{\Delta/+}$*EIICre* female using anti-VSIG1 (Fig. 3.26) or mouse monoclonal anti-H^+/K^+ ATPase (parietal cell marker) antibodies (Fig. 3.27). The results showed the absence of VSIG1 protein in stomach of hemizygous *Vsig1*$^{\Delta/y}$*EIICre* male

(Fig. 3.26 B), while *Vsig1* expression in stomach of heterozygous *Vsig1*$^{\Delta/+}$*EIICre* female (Fig. 3.26 D) is in chimeric pattern. Cells of some gastric glands were VSIG1-positive, while cells of other gastric glands are not expressing *Vsig1* (Fig. 3.26 C). In wild type stomach, VSIG1 is restricted to plasma membrane of different cell types of glandular epithelium of stomach, while no VSIG1 could be detected in squamous epithelium of wild-type stomach (Fig. 3.26 A).

H^+/K^+ ATPase is only expressed in parietal cells of gastric gland (Fujii *et al*, 2009). Anti-H^+/K^+ ATPase antibody was used as parietal cell marker to show, if there is difference between wild-type and conditional knockout stomach in the number of parietal cells secreting hydrochloric acid to the gastric lumen (Fig. 3.27 A-D). The results showed that parietal cell number in wild-type stomach is significantly higher than in cKO stomach (Fig. 3.27 E).

To study the histological structure of the cKO stomach and testis, Haematoxyline and Eosine staining of wild-type and cKO stomach and testis were performed (Fig. 3.28 & Fig. 3.29). The results showed no difference in histological structure between hemizygous *Vsig1*$^{\Delta/y}$ stomach (Fig. 3.28 B) or heterozygous *Vsig1*$^{\Delta/+}$EIICre female stomach (Fig. 3.28 D) and wild-type stomach (Fig.3.28 A&C). There are also no structural differences between hemizygous 5dpp cKO testis (*Vsig1*$^{\Delta/y}$) and 5dpp wild-type testis (Fig. 3.29).

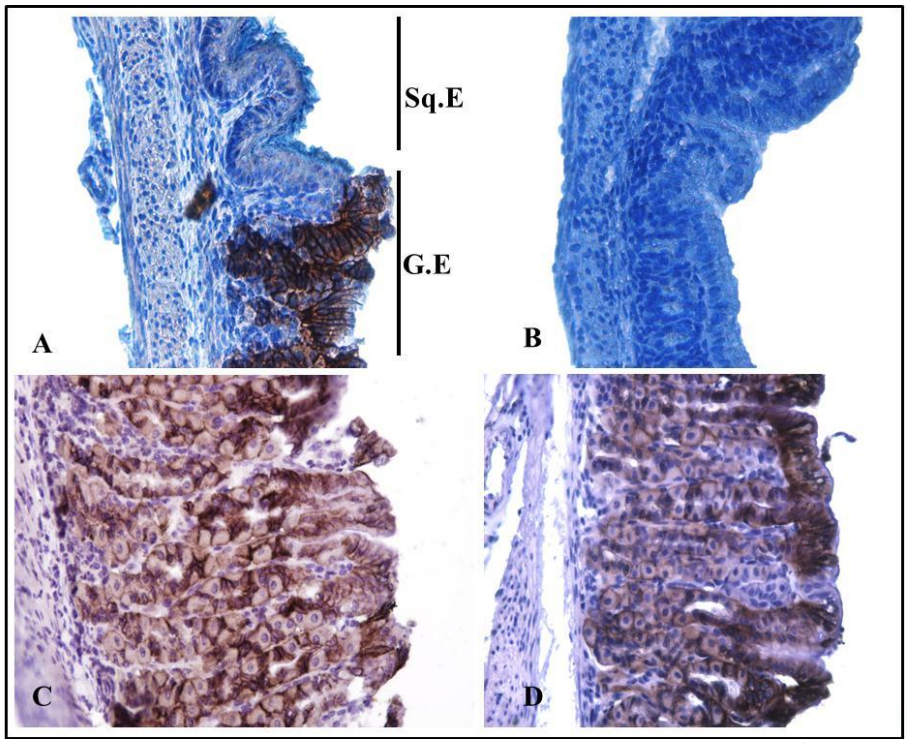

***Figure 3.26**: Immunohistological analysis of wild-type (A&C), hemizygous Vsig1$^{\Delta/Y}$ (B) and heterozygous Vsig1$^{\Delta/F}$ (D) conditional knockout stomach using anti-VSIG1 antibody. (A&C) The VSIG1 protein is distributed in all cells of gastric units (G.E), no VSIG1 expression could be detected in squamous epithelium (Sq.E). (B) No VSIG1 protein was detected in heterozygous stomach. (C) The VSIG1 protein is distributed in some gastric glands of the heterozygous stomach. Original magnification: (A&B) 10X and (C&D) 20X.*

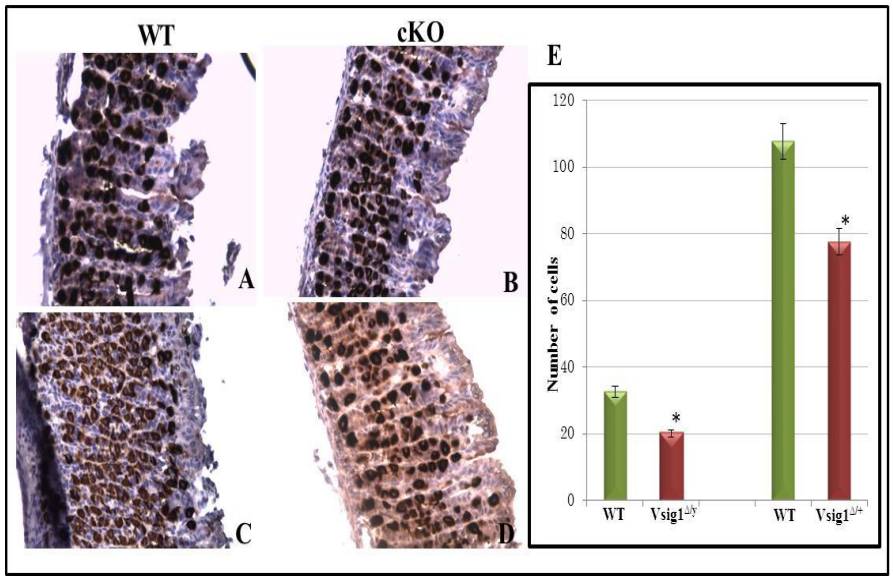

***Figure 3.27**: Immunohistochemical staining of wild-type (A and C), hemizygous Vsig1$^{\Delta/Y}$ (B) and heterozygous Vsig1$^{\Delta/F}$ (D) stomach with anti-H^+/K^+ ATPase. Original magnification: 20X. (E). Mean number of positive cells per microscopical field ($p < 0.01$).*

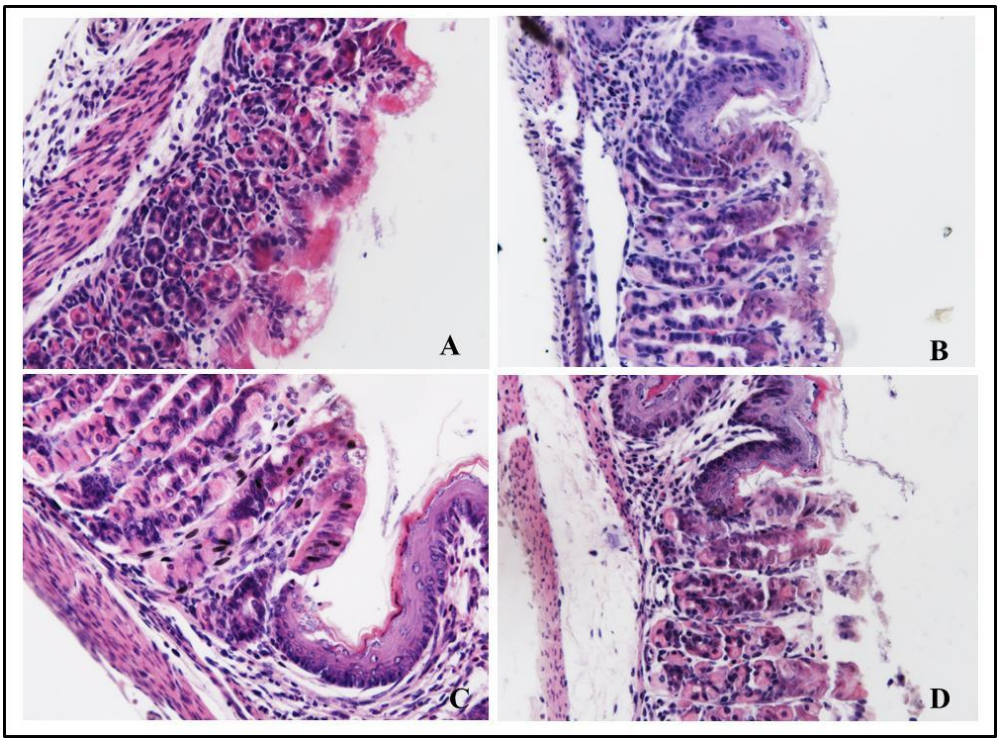

***Figure 3.28**: H&E staining of stomach sections of wild-type and cKO mice. Sections showed no difference in structure of the gastric units between wild-type (A&C) and hemizygous Vsig1$^{\Delta/Y}$ (B) or heterozygous Vsig1$^{\Delta/F}$ (D). Original magnification: 20X.*

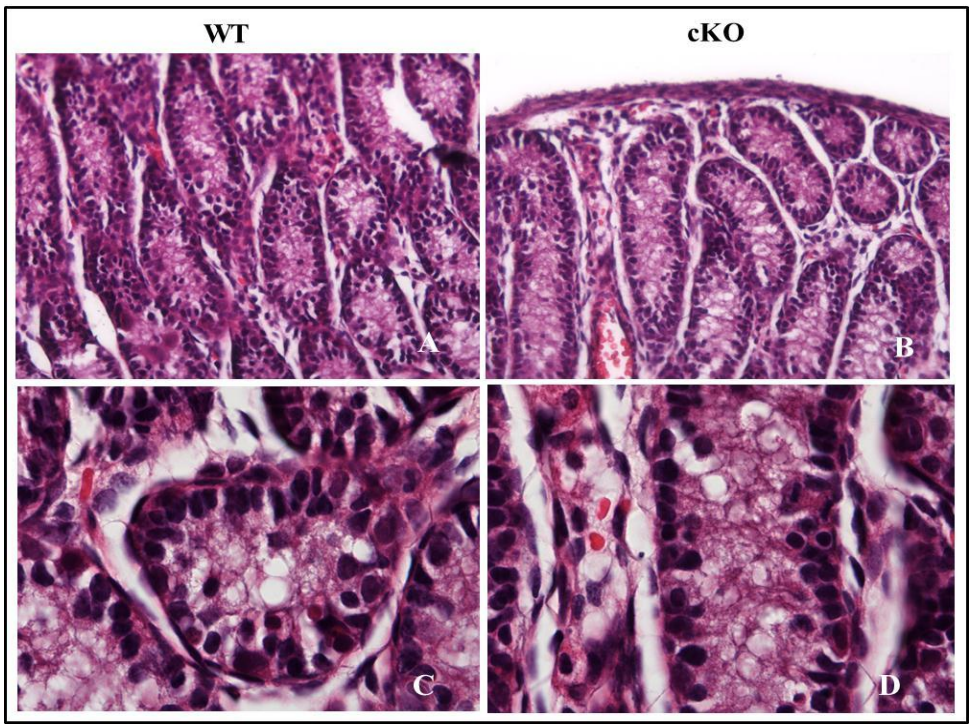

***Figure 3.29**: H&E staining of testis sections of wild-type (A, C) and hemizygous Vsig1$^{\Delta/Y}$ cKO (B-D) mice. Sections showed no structural differences between wild-type and hemizygous Vsig1$^{\Delta/Y}$ animals. Original magnification: (A&B) 20X and (C&D) 20X.*

3.6.1.2-*Vsig1*-cre *ERT*:

To study the effects of Vsig1 disruption on development of stomach and testis, *Vsig1-CreERT* mouse line was created by breeding the mice containing *Vsig1*-floxed allele with *Rosa26-CreERT*, which contains the inducible Cre allele (available in the Institute of Human Genetics).

Before TAM-treatment, mice were genotyped for *Vsig1* locus and to determine the presence of transgenic *CreERT* allele (Fig. 3.30 A). Ten 15-day-old animals were interaperitoneally injected with 0.2 mgTAM/day for 5 days, and then killed 10 and 20 days after last day of TAM application. The mice were genotyped again using genotyping PCR 2 assay, which amplifies the recombined $Vsig1^{\Delta}$ (500bp), $Vsig1^{F}$ (234 bp) and wild-type allele (200 bp) (Fig. 3.30 B,C).

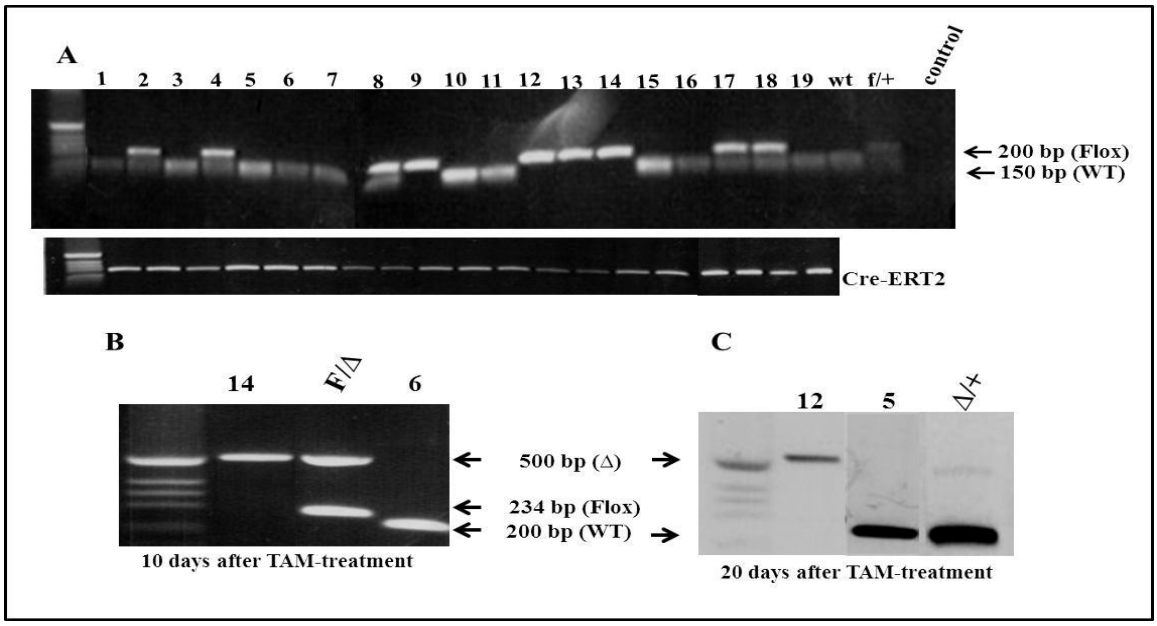

***Figure 3.30**: (A) PCR1 assay, which was used to amplify the 150bp fragment of wild-type and 200bp fragment of $Vsig1^{F}$ allele. DNA of same animals was genotyped to determine the presence of CreERT allele (lower panel). (B, C) PCR2 assay which was used to amplify the 200bp, 234bp and 500bp fragments of wild-type, $Vsig1^{F}$ and $Vsig1^{\Delta}$ alleles, respectively.*

To analyze the histological structure of the cKO stomach, H&E staining was performed (Fig. 3.31). The results showed no differences in histological structure between $Vsig1^{+/Y}$ and $Vsig1^{\Delta/Y}$ stomachs after 10 or 20 days of TAM treatment. Immunohistochemical analysis using Anti-H^{+}/K^{+} ATPase antibody which is staining parietal cell showed no significant difference

between TAM-treated *Vsig1*$^{\Delta/Y}$ and *Vsig1*$^{+/Y}$ mice (Fig. 3.32). Histological and immunohistological analysis of testes 10 days after TAM treatment showed that the number of round spermatids was lower in *Vsig1*$^{\Delta/Y}$ testis as comparing to treated control at the same age. These results were confirmed by immunostaining using anti-Apg1 antibody as meiotic and postmeiotic cell marker (Fig. 3.33 C&D).

Analysis of mutant and wild-type testes 20 days after TAM treatment showed that spermatogenesis is arrested at round spermatids comparing with treated control at the same age (Fig. 3.34 A&B). These results were confirmed by immunostaining using anti-Apg2 antibody as post meiotic cell marker (Fig. 3.34 C&D).

3.6.2- Analysis of ectopic expression of *Vsig1*:

The conventional *Vsig1* knockout results suggest that the *Vsig1*-deficiency leads to the transdifferentiation of the gastric glandular epithelium (monolayer epithelium) to the stratified squamous epithelium (multilayer epithelium) (Oidovsambuu, 2009). The epithelium of skin, oesophagus and forestomach is a multilayered squamous epithelium, while most gastrointestinal tract is lined by monolayer epithelium. It was interesting to study the effect of ectopic expression of VSIG1 in the stratified squamous or simple squamous epithelia which are not endogenously expressing it. Two mouse lines have been generated by Dr. O. Oidovsambuu in which *Vsig1* cDNA was ectopically expressed under control of cytokeratin 5 promoter (Institute of Human Genetics, Göttingen).

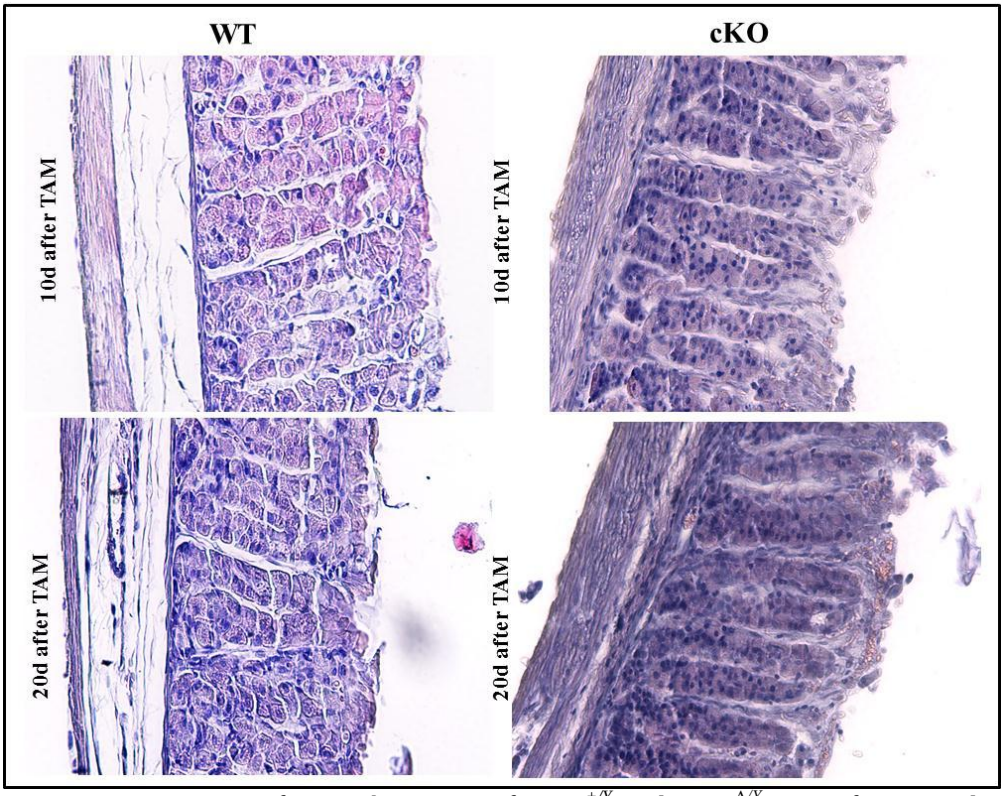

***Figure 3.31**: H&E staining of stomach sections of Vsig1$^{+/Y}$ and Vsig1$^{\Delta/Y}$ mice after 10 and 20 days of TAM treatment. Sections showed no difference in structure of the gastric units between Vsig1$^{+/Y}$ and Vsig1$^{\Delta/Y}$. Original magnification: 20X.*

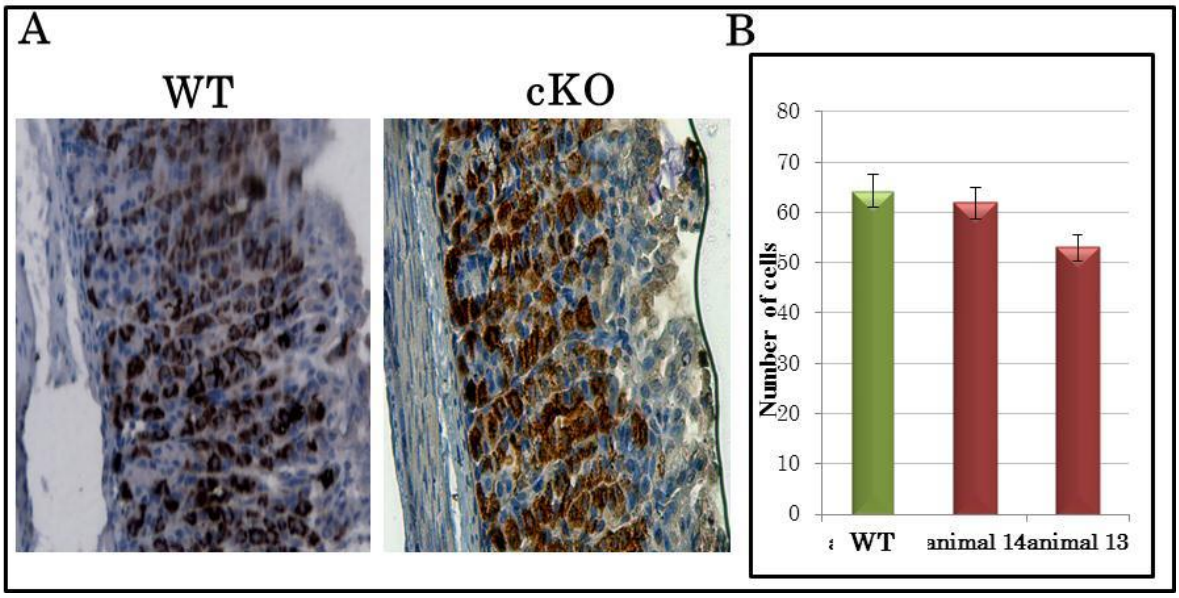

***Figure 3.32**: (A) Immunohistologyical analysis of Vsig1$^{+/Y}$ and Vsig1$^{\Delta/Y}$ stomach sections using Anti-H+/K+ ATPase antibody as parital cell marker. Original magnification: 20X. (B) Mean number of H^+/K^+ ATPase positive cells per microscopical field of wild-type stomach and Vsig1$^{F/+}$ stomach (animal 13 and 14).*

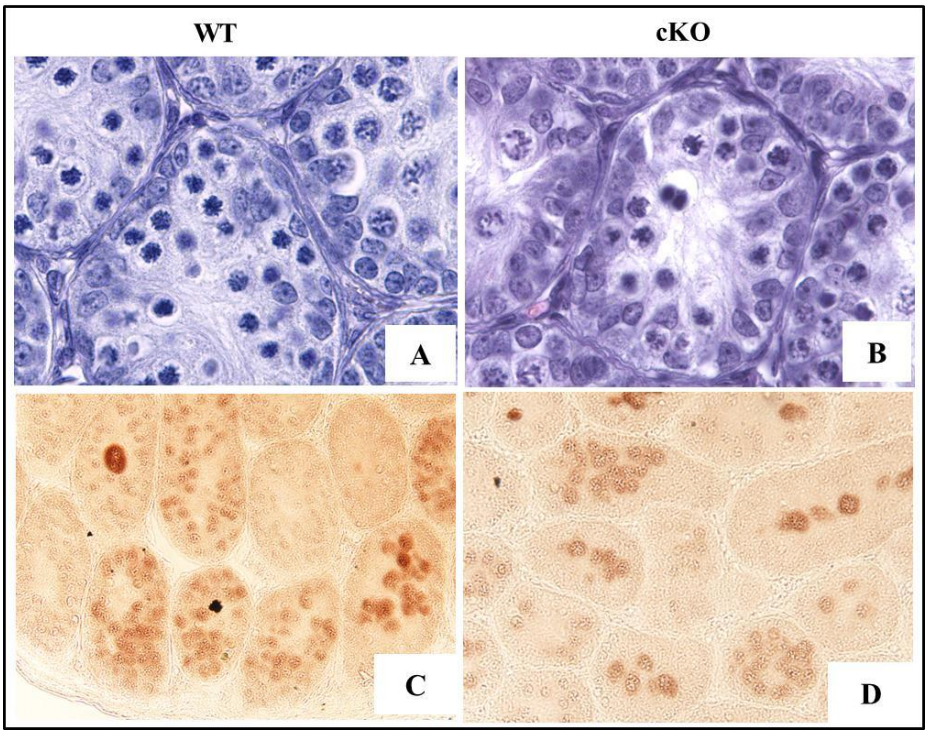

***Figure 3.33**: (A&B) H&E staining of testis sections of wild-type and cKO mice after 10 day of TAM-treatment. (C&D) Immunostaining of testis sections of wild-type and KO mice after 10 days of TAM-treatment using anti-Apg1 antibody. Original magnification: (A&B) 60X (C&D) 10X.*

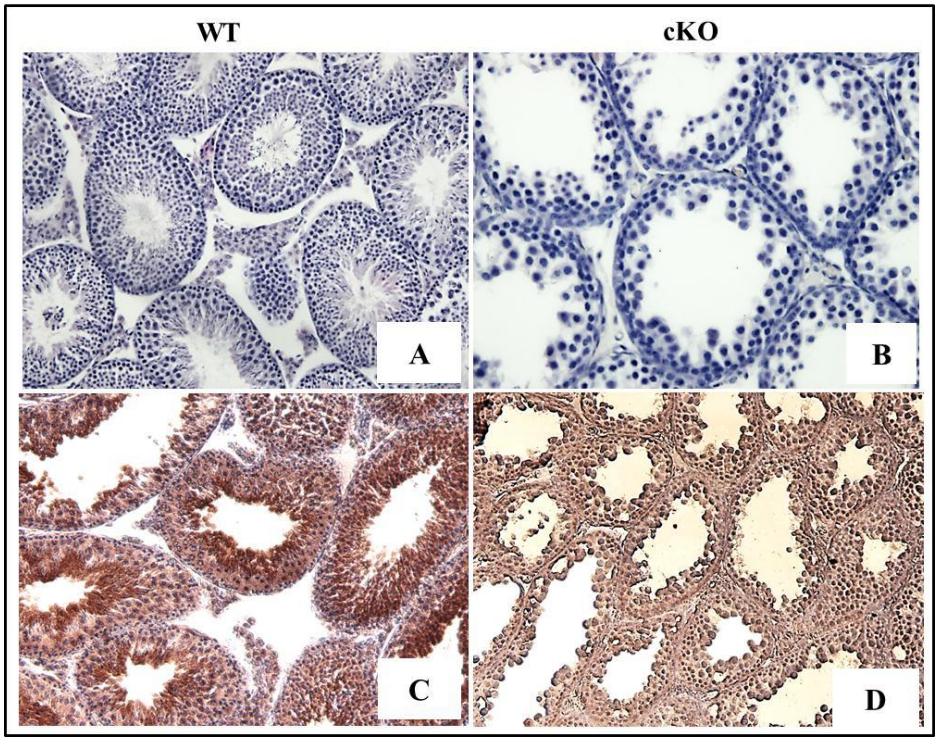

***Figure 3.34**: (A&B) H&E staining of testis sections of wild-type and cKO mice after 20 day of TAM-treatment. (C&D) Immunostaining of testis sections of wild-type and cKO mice after 20 day TAM-treatment using anti-Apg2 antibody. Original magnification: 20X.*

3.6.2.1- Cytokeratin 5 -*Vsig1* overexpressing mouse line:

Keratin filaments constitute a group of 8-nm fibers that form an integral and unique part of the cytoskeleton of almost all higher eukaryotic epithelial cells (Lersch and Fuchs, 1988). Cytokeratin 5 is specifically expressed in the basal layer of the stratified epithelium (Lersch and Fuchs, 1988). *Vsig1* gene was overexpressed under the control of cytokeratin-5 promoter (cyto5-*Vsig1*) to study the effect of VSIG1 overexpression in multilayer epithelia (Fig. 3.35).

Figure 3.35: *Schematic diagram showing the cyto5-Vsig1 construct. In transgenic construct, the Vsig1 cDNA is under the control of cytokeratin 5 promoter.*

To evaluate *Vsig1* expression at the protein level, Western blot was performed using rabbit anti-VSIG1 antibody (Fig. 3.36). Total protein lysates from six different wild-type and transgenic tissues (testis, stomach, skin, esophagus, kidney and lung) were extracted following the method mentioned above (2.2.8.1). The 55-kDa VSIG1 protein of transgenic allele was found in lysates of skin, esophagus and lung of transgenic mice, while 64-kDa VSIG1 protein of endogenous allele was detected in stomach from wild-type and transgenic animals. Both of VSIG1 protein isoforms were detected in wild-type and transgenic testes, while the 64-kDa VSIG1 protein of endogenous allele expression was not detected in skin, esophagus and lung of wild-type animals. Kidney lysate was used as negative control. These results revealed the ectopic expression of transgenic VSIG1 in skin, esophagus and lung.

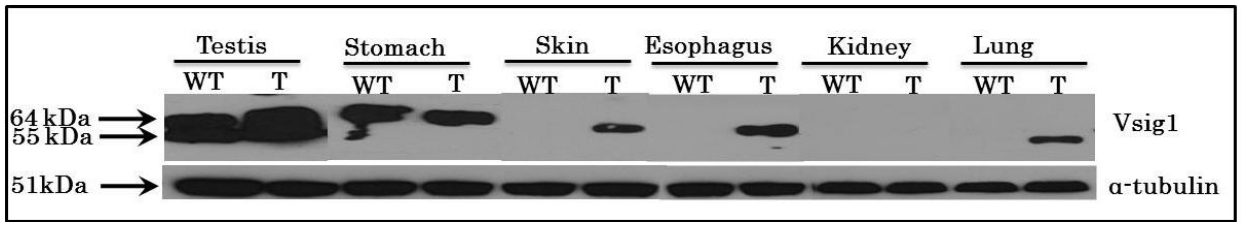

Figure 3.36*: Western blot analysis of VSIG1 expression in testis, stomach, skin, esophagus, kidney and lung of adult transgenic and wild type mice. Rabbit anti-VSIG1 recognizes the 64 kDa endogenous VSIG1 in testis and stomach, ectopically expressed 55 kDa VSIG1 in transgenic skin, esophagus and lung. The 51-kDa α-tubulin protein band is shown as a control.*

To evaluate the expression of VSIG1 and cytokeratin 5/6 in squamous epithelium, histological sections of wild-type and transgenic stomach were immunostained with rabbit anti-VSIG1 (Fig. 3.37 A) and mouse anti-cytokeratin 5/6 antibodies (Fig. 3.37 B). The results showed that VSIG1 protein is not expressed in the wild-type stratified squamous epithelium (Fig. 3.37 A), while the cytokeratin 5/6 was strongly expressed in the basal and keratinized layers of the wild-type stratified squamous epithelium (Fig. 3.37 B).

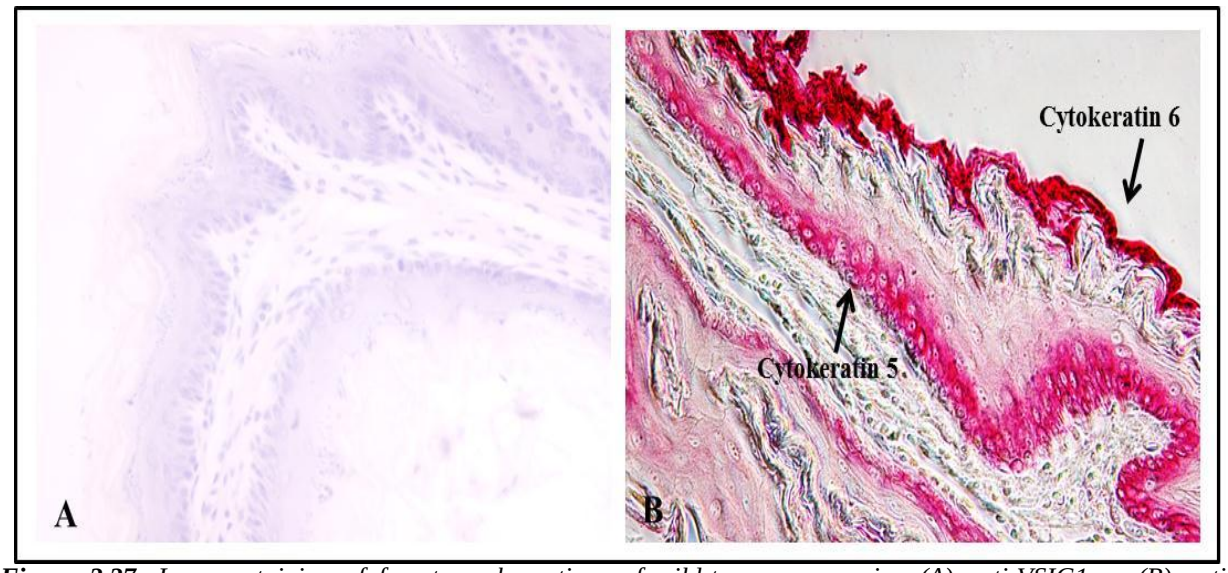

***Figure 3.37**: Immunostaining of forestomach sections of wild-type mouse using (A) anti-VSIG1 or (B) anti-cytokeratin 5/6 antibodies. VSIG1 protein is not expressed in wild-type stratified squamous epithelium, while the Cytokeratin5/6 proteins are expressed in the basal and keratinized layers of the stratified squamous epithelium. Original magnification: 20X.*

In cyto-*Vsig1* transgenic forestomach, VSIG1 is expressed in basal layer of squamous epithelium (Fig. 3.38 A). Further immunohistological analysis revealed the ectopic expression of VSIG1 in squamous epithelium of esophagus and skin (Fig. 3.38 B and C).

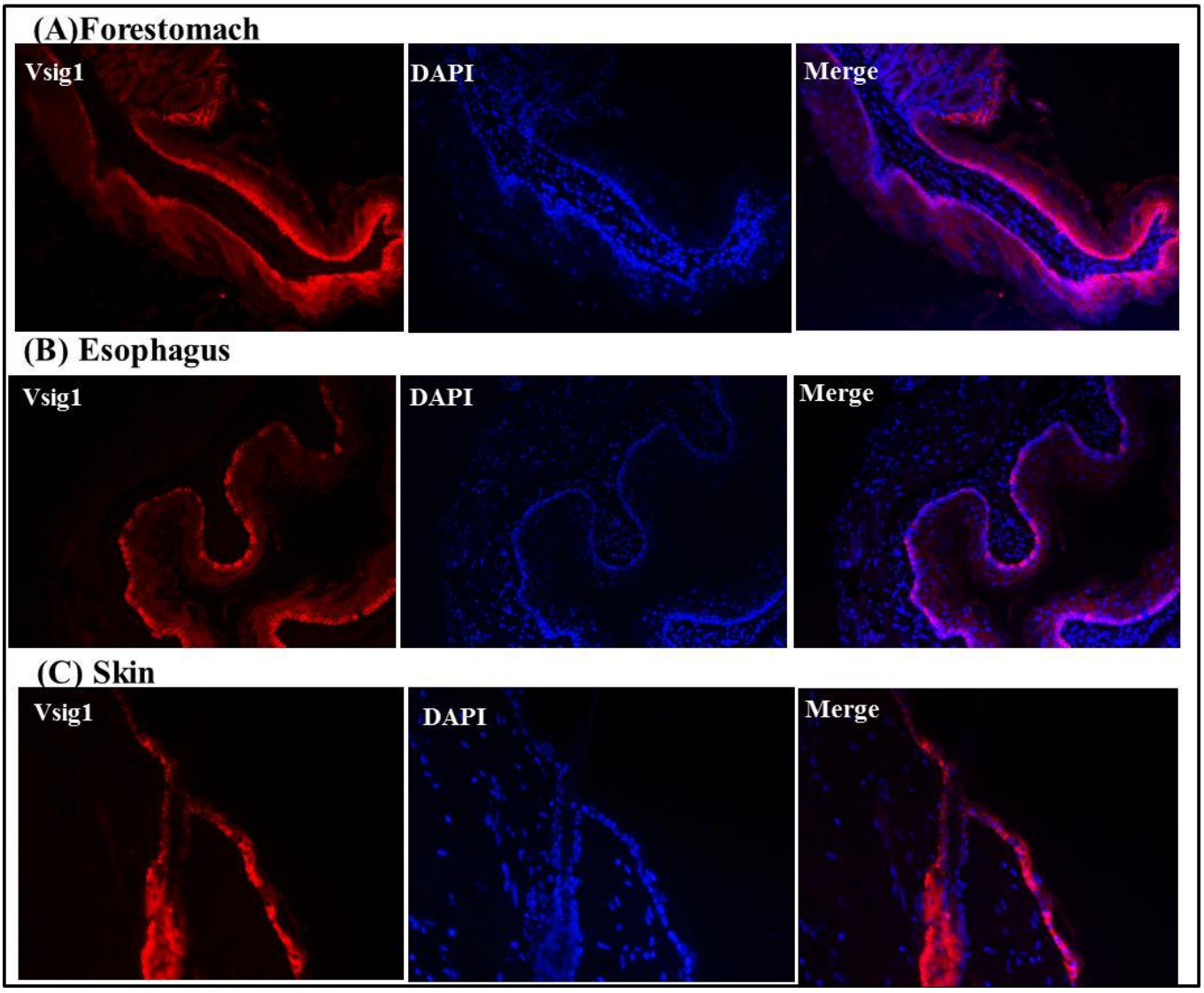

***Figure 3.38**: Immunohistologyical analysis of skin, forestomach and esophagus from cyto-Vsig1 transgenic mice using anti-VSIG1 antibody showing the location of VSIG1 (red) in the basal layer of the stratified squamous epithelium. Nuclei were visualized with DAPI (blue). Original magnification: 20X.*

To determine the effect of ectopic expression of VSIG1 on the squamous epithelium of skin, forestomach and esophagus, H&E staining was performed (Fig. 3.39). The results showed no structural difference between wild-type and transgenic tissues in histological structure of squamous epithelium, but it was found that the squamous epithelium in transgenic esophagus and forestomach is thinner than in wild-type, while no difference is noticed in skin between wild-type and transgenic mice.

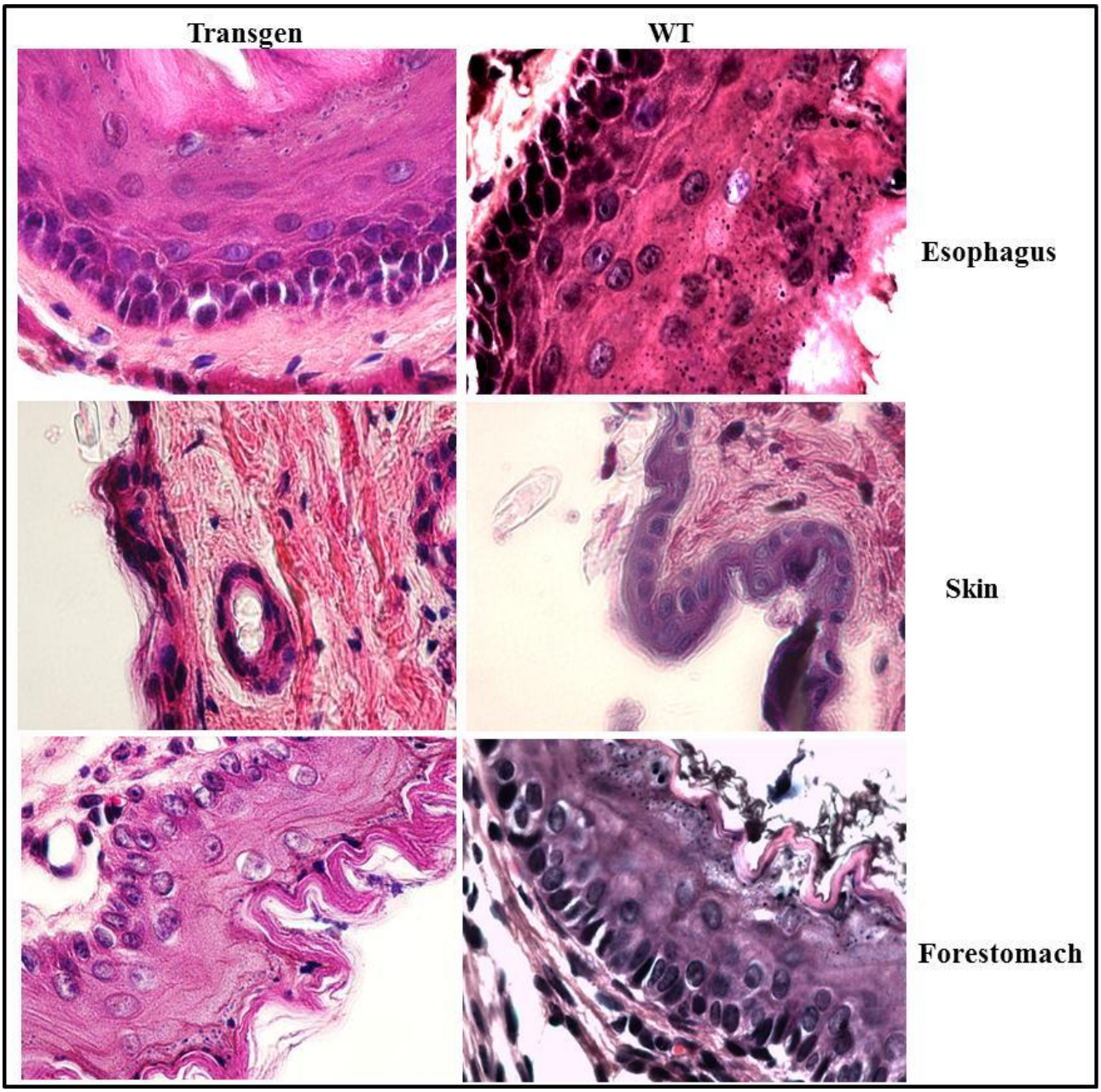

***Figure 3.39**: H&E staining of esophagus, skin and forestomach from wild-type and Vsig1-transgenic mice. Sections of different tissues showed no difference in histological structure between wild-type and vsig1-transgenes. Original magnification: 60X.*

To confirm these results, the thickness of the stratified squamous epithelium layer was measured by using computer software and the results were statistically analyzed (Fig. 3.40). The esophagus, forestomach and skin of six animals were sectioned and stained with H&E. The thickness of squamous epithelium was measured in five microscopical fields of five slides for each animal. The results were statistically analyzed and showed that the ectopic expression of *Vsig1*

significantly decreases the thickness of squamous epithelium layers of transgenic forestomach and esophagus.

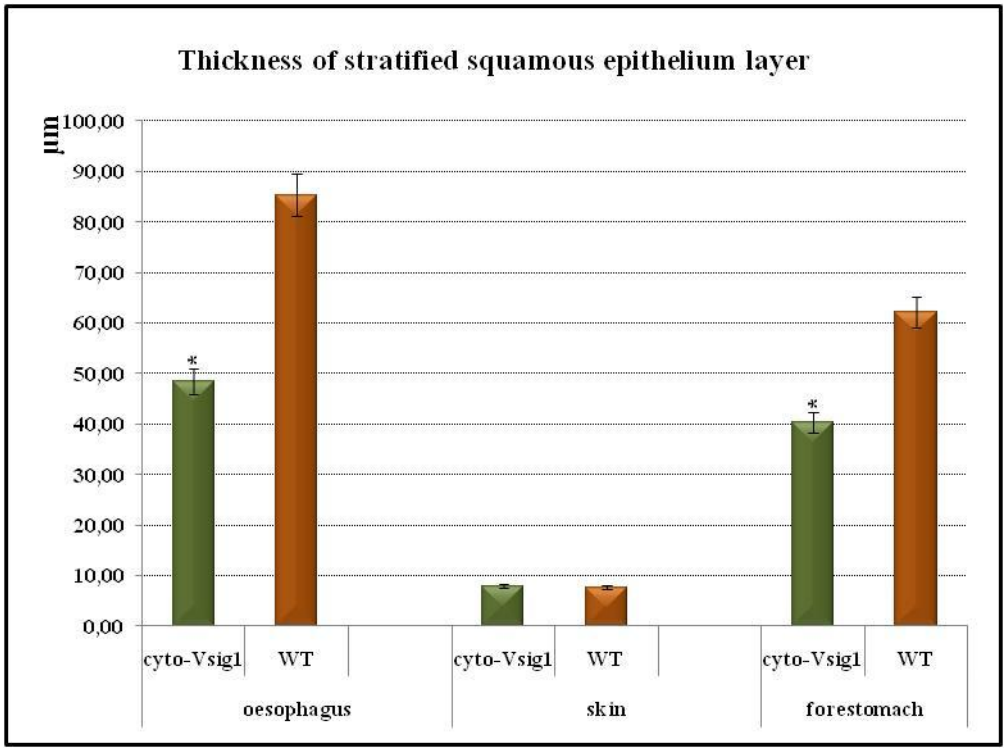

***Figure 3.40**: Thickness of stratified squamous epithelium in esophagus, skin and forestomach from wild-type and cytokeratin-transgenic mice. ($p < 0.01$).*

Breeding of hemizygous transgenic males with wild-type females revealed that six animals of transgenic males out of 13 were infertile. H&E staining was performed on testes of infertile males as well as wild-type testes. The results showed the extensive degeneration of germ cells in seminiferous tubules of transgenic testes comparing to wild-type (Fig. 3.41). Although transgenic testes exhibit early germ cells as well as Sertoli and Leydig cells, the number of late meiotic (i.e. late pachytene and diplotene spermatocytes) and postmeiotic (i.e. spermatids and spermatozoa) germ cells was markedly reduced. The reduction of late meiotic and postmeiotic germ cell was also observed in testis of 25 day old males (Fig. 3.41 C).

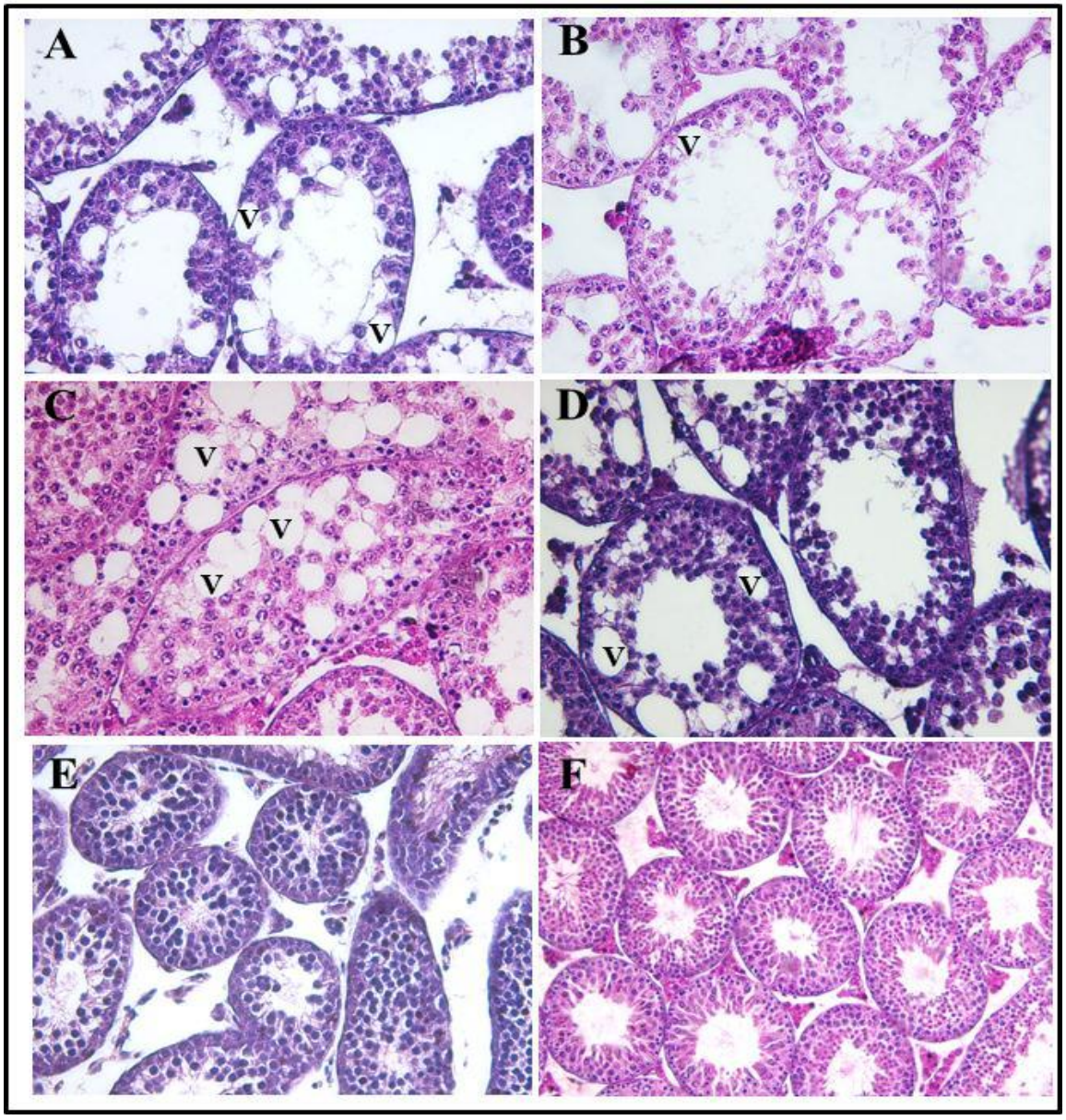

***Figure 3.41**: H&E staining of testis sections of 25 d old and adult wild-type and Cyto-Vsig1 cytokeratin-transgenic mice. Sections through testes of adult (A, B and D) and 25 d old (C) transgenic mice revealed extensive degeneration of a large fraction of seminiferous tubulesas compared to testis sections of wild-type adult (F) and 25 d old (E) mice. V= vacuole. Original magnifications 20X.*

The ectopic expression of VSIG1 in Cyto-*Vsig1* transgenic lung led us to determine the cellular localization of VSIG1 in lung (Fig. 3.42). Cellular localization of VSIG1 protein in transgenic lung was detected by immunostaining of histological sections of transgenic and wild-type lung using rabbit anti-VSIG1 antibody (Fig. 3.42). The results showed the ectopic expression

of VSIG1 protein in alveolar cells of transgenic lung, while there was no expression in wild-type lung.

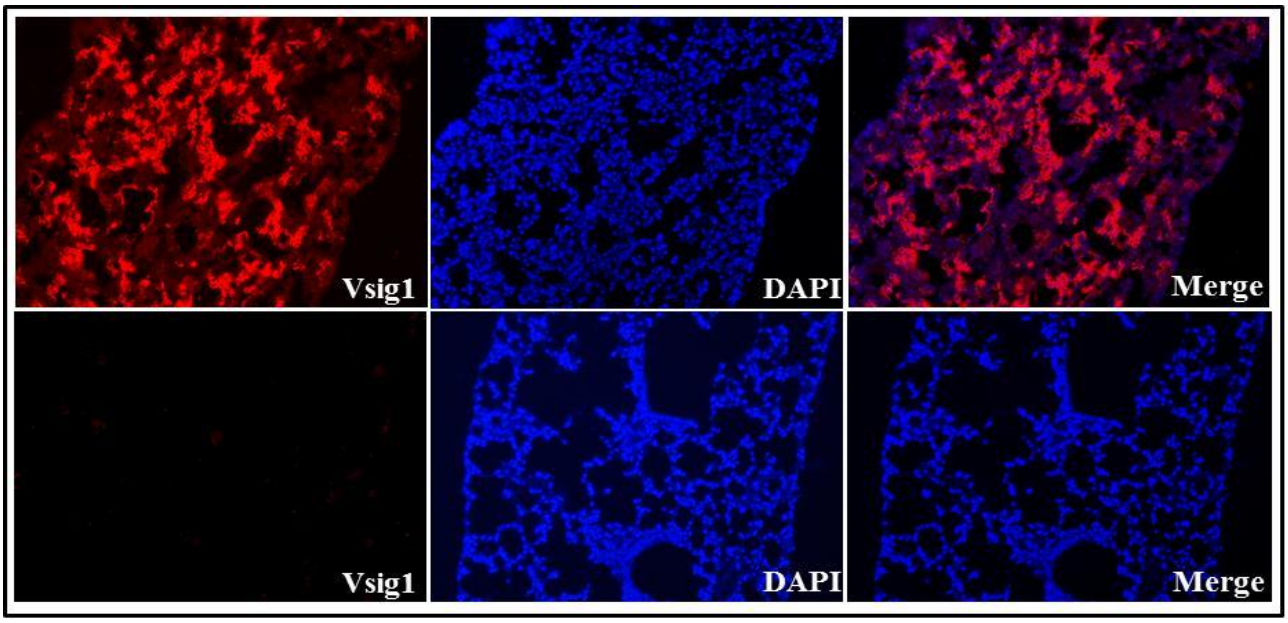

***Figure 3.42**: Immunohistological analysis of lung from Cyto-Vsig1 transgenic (upper panel) and wild-type (lower panel) mice showing the cellular localization of VSIG1 (red) in transgenic but not in wild-type lung epithelium. Nuclei were visualized with DAPI (blue). Original magnification: 20X.*

To determine the difference in histological structure of Cyto5-*Vsig1* transgenic lung comparing to wild-type lung, H&E staining was performed (Fig. 3.43). The results showed that the alveoli in transgenic lung are narrower than in wild-type lung due to the multilayer alveolar septa in transgenic lung. The epithelium of alveolar septa in transgenic lung is stratified in multilayer, while that of wild-type is monolayer (Fig. 3.43).

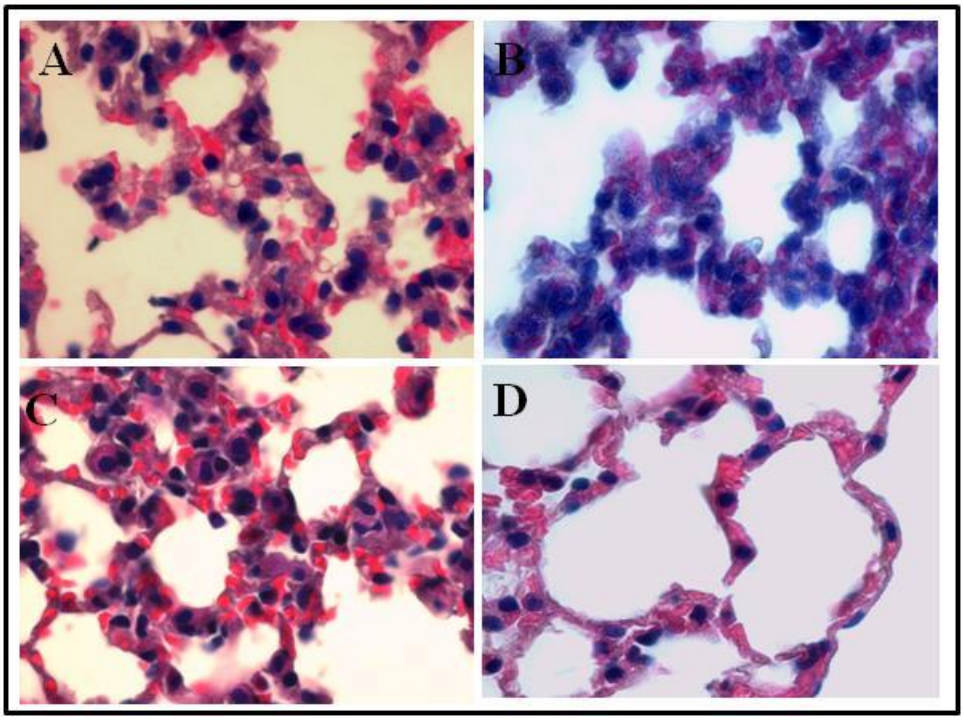

Figure 3.43*: H&E staining of lung sections of wild-type and cytokeratin-transgenic mice. Sections through transgenic lung (A, B and C) showed that the alveolar septa are multilayer and the alveoli are narrower comparing to wild-type (D). Original magnifications 60X.*

3.6.2.2-Ectopic expression of *Vsig1* in intestine:

To determine the consequence of ectopic expression of *Vsig1* in intestine, transgenic line (Villin-*Vsig1*) expressing *Vsig1* in intestine have been generated in Institute of Human Genetics. The transgenic allele (Villin-*Vsig1*) contains the *Vsig1* cDNA under the control of villin promoter (Fig. 3.44). The villin promoter is highly transactivated in intestine, colon and rectum (Maunoury *et al.*, 1992).

Figure 3.44: *Simplified diagram showing the Vill-Vsig1 construct used in ectopic expression of Vsig1 in intestine. The Vsig1 cDNA is under the control of villin promotor.*

To confirm the ectopic expression of *Vsig1*, Northern blot containing RNA from stomach, testis, intestine and rectum of wild-type and villin-*Vsig1* transgenic mice was hybridized with *Vsig1* cDNA fragment, which is located in the upstream sequence of the first poly-A signal. The blot was rehybridized then with villin and β-actin cDNA probes. The Vsig1 probe has been amplified with the primers (SX-Probe2F1 and SX-Probe2R1). Villin probe was amplified using (Vill-probe-F and Vill-probe-R) primers (Fig. 3.45). As shown in Figure 3.45, Vsig1 probe detected the 1.5 kb *Vsig1B* isoform in testis of wild-type and transgenic mice and 2.5 kb *Vsig1A* isoform in wild-type and transgenic mice. In contrast, *Vsig1* detected the 2.2 kb transgenic transcript only in RNA of transgenic intestine and rectum. Villin expression was detected in stomach, intestine and rectum of wild-type and transgene and very weak in wild-type testis.

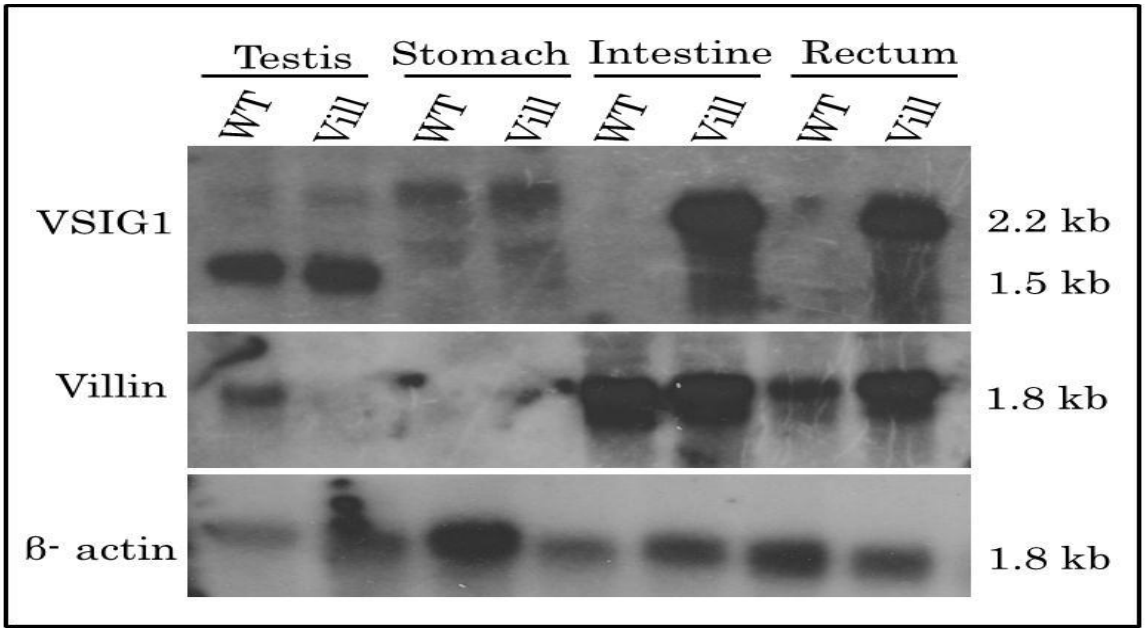

***Figure 3.45**: Northern blot analysis of VSIG1 and villin expression in wild-type and transgenic testis, stomach, intestine and rectum. Integrity and variation of loaded RNA samples were checked by rehybridization with β-actin.*

To detect the cellular localization of VSIG1 protein in transgenic intestine, immunostaining was performed in sections from wild-type and transgenic mice using rabbit anti-VSIG1 antibody (Fig. 3.46). VSIG1 was detected in epithelium of villin-transgenic intestine, while there was no

expression of VSIG1 protein in wild-type intestine. To evaluate the histology of the transgenic intestine, H&E staining was performed (Fig. 3.47). The results showed no structural difference in intestinal epithelium between wild-type and transgenic mice.

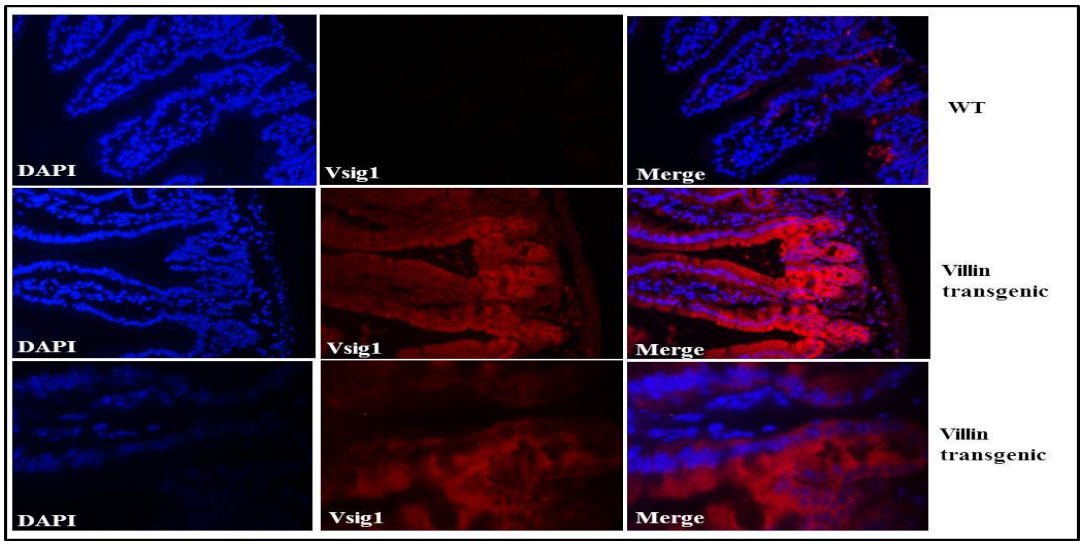

***Figure 3.46**: Immunohistological analysis of intestine from transgenic (middle panel) and wild-type (upper panel) mice showing the cellular localization of VSIG1 (red) in transgenic epithelium but not in that of wild-type. The higher magnification showed the localization of VSIG1 protein in the membrane of the columnar epithelium in transgenic intestine (lower panel). Nuclei were visualized with DAPI (blue). Original magnification: upper and middle panels) 20X, lower panel 60X.*

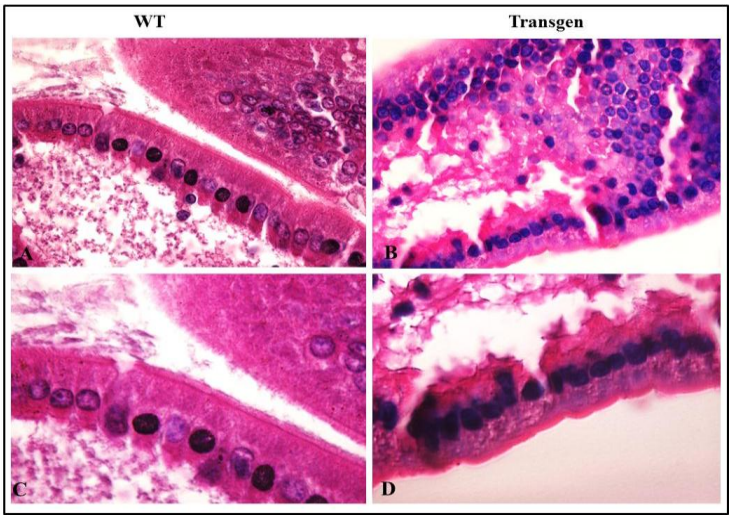

***Figure 3.47**: H&E staining of intestinal sections of wild-type and transgenic mice. Sections through transgenic (A, B and C) and wild-type (D) show no structural difference between transgenic and wild-type intestinal epithelium. Original magnifications (A&B) 20X and (C&D) 60X.*

4-Discussion

4.1-Brief overview of the results

Expression of murine *Vsig1* was found to be restricted to stomach and testis (Oidovsambuu, 2009). A search in data bank (aceview ncbi) showed that *Vsig1* gene is expressed as two alternatively spliced mRNAs variants, namely 2.4-kb *Vsig1A* and 1.6-kb *Vsig1B*. RT-PCR analysis revealed that *Vsig1A* is expressed in stomach and testis, while expression of *Vsig1B* is restricted to testis. Expression analysis of *Vsig1* during preimplantative stages of mouse development showed that VSIG1 is expressed as early as in blastomeres of two-cell stage and blastocysts.

RT-PCR analysis revealed that *Vsig1A* transcript is expressed in embryos of 8.5, 9.5, 10.5, 12.5 and 14.5dpc, while no expression of *Vsig1B* could be detected in any of these embryonic stages. Further analysis showed that *Vsig1A* variant is expressed during pre- and postnatal development of male and female gonads. Expression of *Vsig1B* isoform was first detectable in testis of postnatal day 20. No expression of *Vsig1B* could be detected in ovary of pre- and postnatal development. These results suggest that the expression of *Vsig1B* is restricted to haploid spermatids. Immunohistological analysis of testis sections using anti-VSIG1 antibody revealed that VSIG1 is localized at adhesion junction between cells locating in seminiferous tubules, while no VSIG1 was found in Leydig cells. Further Northern blot and RT-PCR analysis revealed that the *Vsig1A* isoform is expressed in testes of W/W^v mutant mice (which lack germ cells), of *olt/olt* and *qk/qk* mutant mice (in which spermatogenesis is arrested at spermatid stages). The *Vsig1B* variant is not expressed in W/W^v mutant testes, but is expressed in *olt/olt* and *qk/qk* testes. These results suggest that *Vsig1A* is expressed in Sertoli cells, while the expression of *Vsig1B* is restricted to germ cells.

Immunofluorescent analysis of germ cell suspension with anti-VSIG1 antibody revealed that the VSIG1 is localized in centrosomes of dividing germ cells and in spermatids. However, centrosomal localization of VSIG1 could not be detected in mature spermatozoa.

To confirm the subcellular localization, Western blots with cytoplasmic and membrane protein fractions isolated from testes of 25- and 90-day-old mice were probed with anti-VSIG1 antibody. Results of these experiments revealed that the 64-kDa VSIG1A isoform was present in the membrane and in the cytoplasmic fractions, while the 55kDa VSIG1B was exclusively present in the cytoplasmic fraction. The expression level of 55kDa VSIG1B in cytoplasmic fraction of 90-day-old testis was markedly higher than that in 25-day-old testis suggesting that the VSIG1B is a cytplasmic protein and is expressed in postmeiotic germ cells.

The centrosomal localization of VSIG1 was also confirmed by immunofluorescent staining of VSIG1 in NIH3T3 fibroblasts and mouse embryonic stem cells (ESC). The VSIG1 was colocalized with γ-tubulin, a marker of the centrosome, in centrosomes of all stages of mitotic division. Fluorescent microscopy of NIH 3T3 fibroblasts, which was transiently transfected with DsRed-*Vsig1B* fusion construct, revealed that the DsRed-fluorescent signals were localized in centrosome and nucleus. The nuclear localization of VSIG1 was also shown by immunofluoresence staining of NIH 3T3 fibroblasts with anti-VSIG1. Western blot analysis showed the presence of VSIG1 protein in nuclear fraction of NIH 3T3 protein extract.

To study the role of VSIG1 in cell-cell adhesion and migration, stable transfected HepG2 cells, which are overexpressing VSIG1, has been generated. Results of migration and spreading assays revealed that overexpression of VSIG1 increases the migration and adhesion properties of cells.

To investigate the function of *Vsig1* gene, conditional knockout mouse line (*Vsig1*-cKO) was created in the Institute of Human Genetics, Göttingen. In the conditional knockout allele ($Vsig1^{F}$), exon 3 is flanked with two LoxP elements. To recombine the floxed allele, we have generated two mouse lines by introduction of two different transgenic Cre recombinase alleles (*CreEIIa* and *CreERT*) in the genome of $Vsig1^{F/y}$ and $Vsig1^{F/F}$ mice.

RT-PCR and quantitative RT-PCR analysis revealed that *Vsig1* expression was not detected neither in stomach nor in testis of the hemizygous $Vsig1^{\Delta/y}$CreEIIa male. Immunostaining of stomach-sections showed the absence of VSIG1 protein in stomach of hemizygous $Vsig1^{\Delta/y}$ male. In stomach of heterozygous $Vsig1^{\Delta/f}$ female, *Vsig1* expression stomach was in chimeric pattern. Histological analysis of stomach from neonatal and adult $Vsig1^{\Delta/y}$ showed no overt abnormalities in comparison to that of wild-type mice. Immunostaining using anti-H^+/K^+ ATPase antibody, which is a marker of parietal cells of gastric gland, revealed that the number of parietal cells in wild-type stomach is significantly higher than in cKO stomach.

Histological analysis of stomach sections from TAM-treated $Vsig1^{F/Y}$*CreERT* and wild-type mice did not show differences in structure of gastric unit or in the number of parietal cells in gastric units between wild-type and cKO stomachs. Analysis of $Vsig1^{\Delta/y}$*CreERT* testes 10 and 20 days after TAM treatment showed that the number of round spermatids was markedly lower than that of treated control. These results suggest that *Vsig1*-deficiency leads to arrest the spermatogenesis at round spermatid stage.

Analysis of $Vsig1^{+/y} \leftrightarrow Vsig1^{-/y}$ chimeric stomach revealed that the *Vsig1*-deficiency leads to the transdifferentiation of the glandular epithelium (monolayer epithelium) to the stratified squamous epithelium (multilayer epithelium) in the $Vsig1^{-/y}$ regions of chimeric stomach (Oidovsambuu, 2009). Therefore, it was interesting to study the effect of ectopic expression of

VSIG1 in the stratified squamous epithelium, such as epithelium of skin, esophagus and forestomach. Transgenic mice, in which the *Vsig1* cDNA is under control of cytokeratin 5 promoter, were generated and characterized to determine the effect of VSIG1 overexpression in multilayer epithelia. Western blot analysis showed that a transgenic 55-kDa VSIG1 protein was expressed in skin, esophagus and lung of transgenic mice, while an endogenous 64-kDa VSIG1 protein was detected in stomach of wild-type and transgenic animals. Immunohistological analysis showed that VSIG1 protein was not expressed in the stratified squamous epithelium of wild-type stomach, while the cytokeratin 5/6 was strongly expressed in the basal and keratinized layers of the stratified squamous epithelium of wild-type stomach. In cyto-*Vsig1* transgenic mice, VSIG1 is expressed in basal layer of squamous epithelium of forestomach, esophagus and skin. Despite the ectopic expression of *Vsig1* in squamous epithelium, there was no structural difference between wild-type and transgenic tissues. However, it was found that the squamous epithelium in transgenic esophagus and forestomach were thinner than that in wild-type. Interestingly, some of Cyto-*Vsig1* transgenic males (6 of 15 mice) were infertile. Histological analysis of testes from infertile cyto-*Vsig1* males showed the extensive degeneration of germ cells in seminiferous tubules comparing to wild-type. Ectopic expression of VSIG1 in Cyto-*Vsig1* transgenic lung led us to determine the cellular localization of VSIG1 in lung. Immunostaining of lung sections with rabbit anti-VSIG1 antibody showed the ectopic expression of VSIG1 protein in alveolar cells of transgenic lung, while there was no expression of VSIG1 in lungs of wild-type animals. Histological analysis showed that the epithelium of alveolar septa in transgenic lung was stratified in multilayer, while that of wild-type lung was monolayer.

It was also interesting to study the effect of *Vsig1* overexpression in intestinal epithelium. Therefore, transgenic Villin-*Vsig1* transgenic mice have been generated. The transgenic allele

contains the *Vsig1* cDNA under the control of Villin-promoter, which is specifically transactivated in intestinal epithelium. RNA analysis revealed the expression of VSIG1 in transgenic intestine and rectum. Immunostaining with anti-VSIG1 antibody showed that VSIG1 was localized at baso-lateral membrane of villin-*Vsig1* transgenic intestine, while there was no expression of VSIG1 protein in intestine of wild-type mice. However, no overt histological differences were found between wild-type and transgenic intestine.

4.2-*Vsig1* transcribes two mRNA spliced variants

Alternative splicing is a process by which the sequence of exons in pre-mRNA is reconnected in multiple ways during RNA splicing. The resulting different mRNAs may be translated into different protein isoforms (Black, 2003). There are four different modes of alternative splicing, in which one or more exons are spliced out of the pre-mRNAs or retained (Fig. 4.1) (Zahler, 2005). There are two other mechanisms by which different mRNAs may be generated from the same gene by usage multiple promoters or multiple polyadenylation sites. The presence of multiple promoters transcribes different RNA isoforms, which may be differentially regulated. Multiple polyadenylation sites provide different 3' untranslated regions for the transcript. Both of these mechanisms are found in combination with alternative splicing and provide additional variety in mRNAs derived from a gene (Matlin *et al.,* 2005). In humans, up to 70% of genes are alternatively spliced (Modrek and Lee 2002; Johnson *et al*., 2003), which greatly increases the diversity of proteins that can be encoded by the low number of human genes. The resulting changes in amino acid sequence could potentially lead to the alteration of function of proteins, their intracellular localization, or their stability and posttranslation modifications (Resch *et al*., 2004; Sorek *et al.*, 2004).

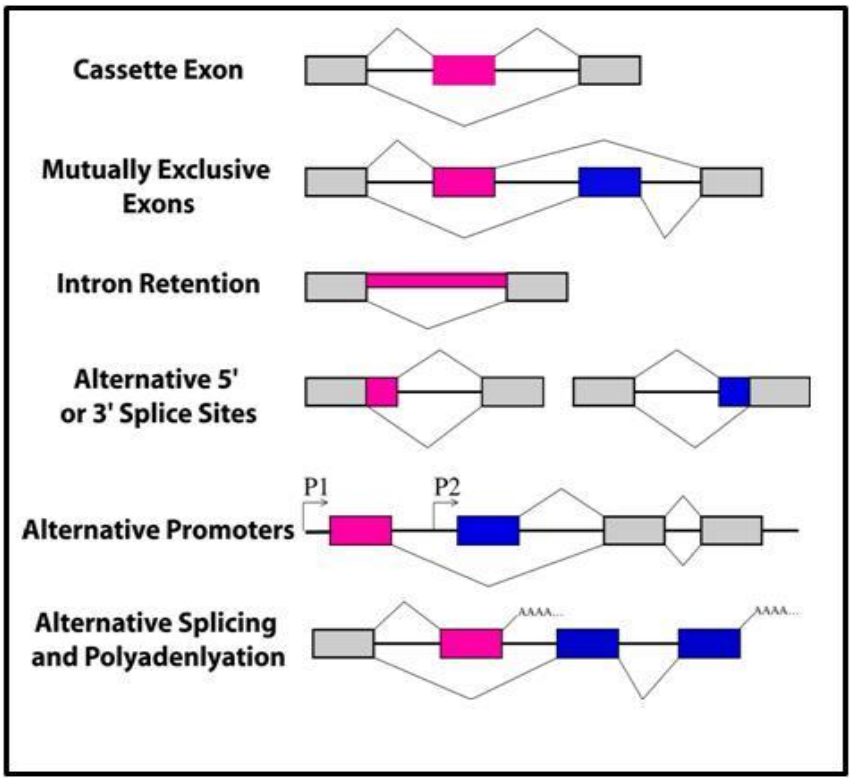

Figure 4.1: *Types of alternative splicing. In these graphics, exons are represented by boxes and introns by lines. Exon regions included in the messages by alternative splicing are colored while constitutive exons are shown in gray. Promoters are indicated with arrows and polyadenylation sites with AAAA (Zahler, 2005).*

Alternative usage of two promoters and their own first exons leads to production of stomach and testis-specific *Vsig1* mRNA isoforms. The *Vsig1A* transcript is regulated by sequences locating in 5´flanking region of exon 1a. Results of expression studies revealed that the *Vsig1A* is specifically expressed in stomach epithelium and in somatic cells of testis. Immunohistological analysis of stomach sections revealed the localization of the VSIG1 to basolateral membrane of glandular epithelium. The shorter transcript *Vsig1B* is presumably directed by sequences locating in the 5´flanking region of exon1b and is exclusively expressed in postmeiotic spermatid. Analysis of transgenic Vsig1- EGFP mice, in which the *EGFP* reporter gene is under the control of 4.5-kb sequence located in 5´flanking region of exon 1a of *Vsig1* gene, revealed that this promoter region directs the expression of EGFP in the glandular epithelium of stomach and in Sertoli cells of testis. No expression of EGFP could be detected in post-meiotic spermatids (Oidovsambuu, 2009).

Because the predicted amino acid sequence of the *Vsig1B* is lacking the sequence of signal peptide and the first Ig-like domain, it is likely that the spermatid-specific *Vsig1B* isoform is not a component of plasma membrane. To confirm the cytoplasmic localizations of VSIG1B protein, we probed Western blot containing membrane and cytoplasmic protein fractions extracted from 25- and 90-day-old wild-type testes with anti-VSIG1 antibody. As expected, the shorter 55-kDa VSIG1B protein was exclusively present in the cytoplasmic fraction, while the 65-kDa VSIG1A was found in membrane and cytoplasmic fraction. The expression level of VSIG1B in the cytoplasmic fraction extracted from 90-day-old testis was markedly higher than that in 25-day-old testis suggesting that the cytoplasmic VSIG1B is specifically expressed in the postmeiotic germ cells. Immunohistological analysis of germ cell suspension revealed the subcellular localization of VSIG1 to the centrosome of elongated spermatids. The centrosomal localization of VSIG1 is absent in mature spermatozoa. Analysis of VSIG1 expression during postnatal development showed that VSIG1 begins to be xpressed at postnatal day 15 (Kim *et al*., 2010).

Many proteins which belong to immunoglobulin superfamily are transcribed from different spliced mRNA variants (Becker *et al*, 1993; Lucka *et al*, 1995; Takai *et al*, 2003; Wegmann *et al*, 2006; Andreeva *et al*, 2009). Table 4.1 represents some members of IgSF, which transcribe different spliced mRNA variants.

Table 4.1: Members of IgSF, which transcribe different alternatively spliced mRNAs.

Name	Spliced variants	function	Reference(s)
Ceacam1a	Either two or four.	Cell adhesion molecule. Angiogenic factor. Tumor suppressor.	(Beauchemin *et al*, 1999; Hemmila *et al*, 2004)
Neurofascin	fifty	Promotes axon outgrowth.	(Volkmer *et al*, 1998)
C-CAM/gp110	Three	Involved in intercellular adhesion processes.	(Becker *et al*, 1993 ; Lucka *et al*, 1995)
T-cadherin	Nine	Mainly as signaling molecule	(Andreeva *et al*, 2009)
JAM-A	(murine) five, (human) four	Facilitate tight junction (TJ) assembly.	(Bazzoni and Dejana, 2001; Bazzoni, 2003)
ESAM	(murine) six (human) eleven	Play a rule in tight junction and participates in the migration of neutrophils through vessel wall.	Bazzoni, 2003; Wegmann *et al*, 2006)
A33	(murine) four (human) three	currently unknown	(Hemmila et al, 2004)
Nectin-3	(murine) nine (human) therteen	Play a role in Sertoli-spermatid interactions.	(Takai *et al*, 2003; Inagaki *et al*, 2006)
Nectin-2	(murine) four (human) six	Essential for the formation and maintenance of Sertoli-spermatid junction.	(Takai *et al*, 2003; Inagaki et al, 2006)

4.3-VSIG1 is located in centrosome and nucleus

In most cells, the centrosome consists of two morphologically distinct centrioles and of pericentriolar material (PCM), from which the aster and spindle fibers are generated (Palermo *et al*., 1997). The two centrioles are not identical and can be designated as mother and daughter centrioles based on their age and morphology (Conduit and Raff, 2010). The centrioles display the classic 9+0 pattern of nine triplet microtubules and they undergo a semiconservative duplication. Each daughter cell retains one of the mother's centrioles and a newly formed daughter centriole (Kochanski and Borisy, 1990). The functions of centrosomes are nucleation of microtubules and mitotic spindle formation (Bornens *et al*., 1990; Schatten, 1994). The core centrosomal components, the centrioles, have another distinct function as basal bodies that seed the growth of cilia and flagella, which have crucial roles in physiology, development and disease (Nigg, 2002; Badano *et al*., 2005; Praetorus and Spring, 2005). The centrosome is duplicated only once per cell cycle during the S phase. During the prophase stage, the centrosomes migrate to opposite poles of the cell. The mitotic spindle then forms between the two centrosomes. After division, each daughter cell receives one centrosome (Rieder *et al*., 2001).

During male germ cell development, mouse spermatocytes possess the major centrosomal proteins such as centrin and γ-tubulin (Manandhar *et al.*,1999*;* 2000a). In postmeiotic cells the round spermatids have apparently intact centrosomes comprising centrioles and centrosomal proteins. In elongated spermatids, the centrosome is located in the neck region and consists of a pair of centriols. Spermatid centrosomes cease to nucleate microtubules at the early stages of spermatogenesis before displaying without any signs of physical degeneration (Fig. 4.2 A) (Manandhar *et al.,* 1999). The spermatid centrosomes are gradually inactivated and fully degenerated. This phenomenon is termed the centrosome reduction (Manandhar *et al.*, 2000b). The γ -Tubulin has been found to be discarded in the residual bodies during the spermiation stage (Fig.

4.2 B) (Manandhar *et al.,* 1998; 1999). Centriolar reduction begins in the testis and continues through the epididymis. Mouse spermatozoa completely lose γ -tubulin, centrin, and centrioles (Fig. 4.2 C) (Manandhar *et al.,* 1998; 1999). Complete centriolar degeneration has also been reported in rat spermatozoa (Woolley and Fawcett, 1973; Manandhar *et al.,* 1999).

In an attempt to prove subcellular localization of VSIG1, methanol-fixed testis sections were probed with anti-VSIG1 antibody. In this experiment, we found that anti-VSIG1 labeled two dots in the neck region of elongated spermatids. The colocalization of VSIG1 with that of γ –tubulin suggested that VSIG1 is localized in the centrosome. No specific VSIG1 signal could be detected in epididymal spermatozoa. The subcellular localization of VSIG1 in centrosome could be confirmed by probed paraformaldhyde-fixed testis sections with anti-VSIG1 antibody. In paraformaldhyde-fixed testis sections, VSIG1 was localized at plasma membrane of adhesion junction between cells. The observed discrepancy in subcellular localization of VSIG1 could be due to fixation methods. Methanol fixation was found to optimize centrosome preservation (Andreeva *et al*., 2009). Immunohistological staining of methanol fixed germ cell suspension with VSIG1-antibody showed the association of VSIG1 to centrosome of dividing cells. In elongated spermatids, VSIG1 was also colocalized with γ –tubulin in centrosome located in the neck region. To further support the centrosomal localization of VSIG1, we probed three different cell lines (ESC, NIH3T3 and primary fibroblasts) with VSIG1 antibody. In all examined cell lines, VSIG1 was associated with the centrosome.

These results suggest that cytoplasmic truncated isoform of VSIG1B is associated with the centrosome in the somatic and male germ cells. Centrosomal localization was already found for some members of IgSF. For example, T-cadherin is located in centrosome and nucleus (Andreeva *et al*., 2009). Overexpression of T-cadherin results in an increase in the number of multinuclear cells,

whereas its downregulation leads to an increased number of cells with multiple centrosomes (Andreeva *et al*., 2009). These findings indicate that T-cadherin is a nuclear and centrosomal protein and that its deregulation may interfere with the cell cycle via disturbance in cytokinesis or centrosomal replication (Andreeva *et al*., 2009).

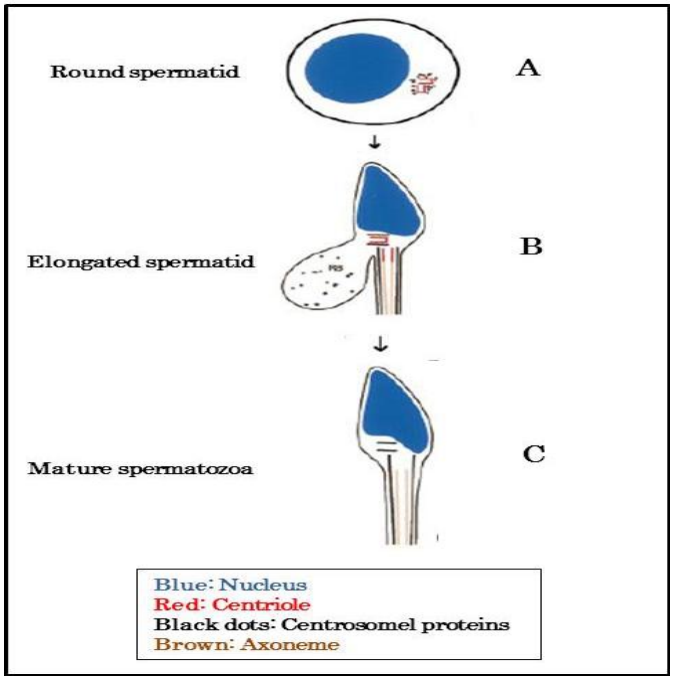

Figure 4.2: *Centrosome reduction during spermatogenesis. The male germ cells possess intact centrosomes containing centrioles and centrosomal proteins until the round spermatid stage (A). The microtubules of the distal centriole extend as axoneme of the spermatid tail (B). During spermiation, γ-tubulin and possibly other centrosomal proteins are disjuncted from the centrioles and discarded with the residual bodies (B). The centrioles are degenerated to various extents in spermatozoa of different species. Rodent and snail spermatozoa lose both centrioles completely (C). Modified of Manandhar et al., 2005.*

4.4-The role of Vsig1 in stomach development

The gastrointestinal tract (G1) develops from the primitive gut tube, which comprises the endodermal epithelium and surrounding mesoderm. The crosstalk between the two cell layers progressively undertakes the endoderm to organize into different classes of epithelia along the anterior-posterior (AP) regions of developing gastrointestinal tract (Wells and Melton, 1999). The endoderm of foregut give rise to the epithelia of esophagus, stomach and duodenum, while that of mid and hindgut differentiates to epithelial layer of intestine and colon, respectively. In mouse, the pseudostratified epithelium of foregut develops at embryonic days E10.5-E12.5 into stratified squamous epithelium in esophagus and forestomach, but into columnar glandular epithelium in distal stomach. The squamous epithelium of murine embryos is not keratinized and composed of

multilayer with basal layer containing precursor cells, and becomes keratinized around 4 weeks after birth. The final differentiation of glandular epithelium initiates from embryonic day 14.5 and continues to early postnatal development, where the monolayer epithelium investigates into the neighboring mesoderm and form a primordial of gastric units. Subsequent cytodifferentiation leads to epithelial differentiation to different cell lineages in the gastric glands (Van den Brink, 2007).

Expression analysis of *Vsig1* during stomach development revealed that the expression of *Vsig1* started in early stages of stomach development around embryonic day 13.5. The expression of *Vsig1* is restricted to glandular epithelium of corpus and antrum regions of stomach and is absent in squamous epithelium of forestomach (Oidovsambuu, 2009). Expression pattern of *Vsig1* during epithelial differentiation of glandular epithelium of stomach suggests that *Vsig1* is involved in differentiation of glandular epithelium of stomach.

Analysis of subcellular localization of *Vsig1* revealed a characteristic pattern of adhesion molecules. In nonpolarized cells located in gastric units such as partial and chief cells, *Vsig1* is accumulated at the cell-cell contact sites. In polarized cells in pit region of glandular epithelium, *Vsig1* localizes at basolateral membrane, but not at apical membrane. It is known that epithelial cell differentiation requires a complex sequence of molecular events to establish polarized domains with specialized functions. Therefore, we expected that depletion of *Vsig1* might disrupt the cell polarization of glandular epithelium. In an effort to determine the role of *Vsig1*in development of stomach epithelium, the X-linked *Vsig1* gene was inactivated in embryonic stem cells (ESC). Although the $Vsig1^{-/Y}$ conventional knockout ESC were only able to generate low coat chimeric mice, all chimeras did not transmit the targeted allele to their progeny suggesting that a high contribution of *Vsig1*-deficient cells lead to the lethality of chimeric embryos. Histological and immunological analysis of $Vsig1^{-/Y} \leftrightarrow Vsig1^{+/Y}$ chimeric stomachs revealed that some lesions of

glandular epithelium in corpus region of stomach contain *Vsig1*-defecient cells. Epithelium of these lesions has a typical morphology of the cornified epithelium, which is normally localized in the forestomach (Oidovsambuu, 2009). These results suggest that the *Vsig1*-deficiency lead to trandifferentiation of glandular epithelium to squamous epithelium.

Several signaling molecules and transcription factors controlling epithelial differentiation during stomach development have been identified including Indian and Sonic Hedgehog (Ihh and Shh), homeobox genes (Barx1), Fgf10 and Gata4 (Ramalho-Santos *et al,* 2000; Van Den Brink *et al.*, 2001; Van den Brink, 2007; Kim *et al.,* 2007). Mutations in a number of genes result in alteration of sharp boundary between the epithelia of squamous multilayer and glandular monolayer. Mice with tissue-specific loss of nuclear hormone receptor *Coup-TFII*, with hypomorphic allele of *Sox2, shh* and with mutation in *Sfrp2* show expansion of glandular epithelium into region of forestomach (Ramalho-Santos *et al*., 2000;Takamoto *et al*., 2005; Que *et al*., 2007; Matsuyama *et al.,* 2009). In contrast, stomach of embryos with mutations in *activin receptors type II* displays the development of multilayered squamous epithelium in corpus region of stomach (Kim *et al.,* 2007). The differentiation of $Vsig1^{-/Y}$ cells to squamous epithelium in corpus region of chimeric $Vsig1^{+/Y} \leftrightarrow Vsig1^{\Delta/Y}$ stomach is similar to that of chimeric $Gata4^{+/+} \leftrightarrow Gata4^{-/-}$ stomach (Jacobsen *et al.,* 2002).

To overcome the early embryonic lethality of chimeric mice with high contribution of *Vsig1*-deficient cells and to determine the function of *Vsig1* in stomach development, we used the Cre/loxP system to generate conditional knockout mice. Using the recombinant $Vsig1^{flox/Y}$ cells, several high chimeric male mice have been successfully generated in Institute of Human Genetics, Göttingen. I bred these chimeric males with C57Bl/J6 females to generate heterozygous $Vsig1^{flox/+}$ and hemizygous $Vsig1^{flox/Y}$ animals. To recombine the floxed *Vsig1* allele, we bred the $Vsig1^{flox/+}$

females with transgenic *CreEIIa* and *CreERT* males, and identified *Vsig1*$^{flox/Y}$*CreEIIa*, *Vsig1*$^{F/+}$*CreEIIa* and *Vsig1*$^{F/Y}$*CreERT* and *Vsig1*$^{F/+}$*CreERT* double transgenic mice in F_1 offspring of these mattings. In *CreEIIa* allele the Cre recominase gene is under the control of the adenovirus EIIa promoter. The expression of the *CreEIIa* is restricted to oocytes and early preimplantive stages of embryos (Lucka *et al.,* 1995). Therefore, we expected that Cre-mediated recombination of *Vsig1*^{F}allele will occur in one-cell or two-cell stages of embryos. Genotype analysis of F_1 generation revealed the recombination of flox-allele in all tissues of hemizygous *Vsig1*$^{\Delta/Y}$*CreEIIa* males. These results suggest that deletion of *Vsig1* gene did not disrupt the embryonic development. Immunohistological staining of stomach-sections with anti-VSIG1 antibody revealed the absence of VSIG1 protein in glandular epithelium of *Vsig1*$^{\Delta/Y}$*CreEIIa* stomach. According to X-inactivation, all cells of individual gastric unit in stomach of heterozygous *Vsig1*$^{\Delta/+}$*CreEIIa* female were either expressed VSIG1 protein or not. These results confirm the clonal origin of gastric unit. It has been shown that all cells in gastric unit are derived from one stem cell located in isthmus region (Brittan and Wright, 2002).

Histological analysis of *Vsig1*$^{\Delta/+}$*CreEIIa* did not display the expected phenotype namely the transdifferentiation of glandular epithelium to squamous epithelium, which has been shown in *Vsig1*$^{\Delta/Y}$↔*Vsig1*$^{+/Y}$ chimeric mice. The transdifferentiation of the glandular to squamous epithelium might not occur in the whole *Vsig1* mutant stomach, but only restricted to the corpus region locating beside the squamous epithelium of forestomach. Such transdifferentiation leads to extension of squamous epithelium in part of corpus region of stomach. The transdifferentiation of stomach epithelium and extension of squamous epithelium in part of corpus region, which normally contains glandular epithelium, was found in stomach of sonic hedgehog-deficient mice (Ramalho-Santos *et al*., 2000). The inability to detect, in our study, the expected transdifferentiation of glandular

epithelium and extension of squamous epithelium into corpus region of *Vsig1*$^{\Delta/+}$*CreEIIa* stomach may be due that the fact we have only investigated the stomach of adult mice, in which it is difficult to detect the extension of squamous epithelium.

To determine the consequences of temporal inactivation of *Vsig1*, *Vsig1*$^{F/Y}$*CreERT* male mice were studied. In the *CreERT* allele, the Cre recombinase gene is fused with the mutated ligand binding domain of the human estrogen receptor (ERT). The fusion protein becomes active upon administration of the synthetic estrogen Tamoxifin (TAM). I have only analyzed *Vsig1*$^{F/Y}$*CreERT* after 10 and 20 days of TAM-injection. Genotype analysis revealed the presence of *Vsig1*^{F} and *Vsig1*$^{\Delta}$ allele in all tissues of TAM-treated *Vsig1*$^{F/Y}$*CreERT* mice suggesting that the Cre-mediated recombination of *Vsig1*^{F} has not occurred in all cells of TAM-treated animals. Histological analysis of stomach of TAM-treated animals did not show any overt histological abnormalities. These results may be due to partial deletion of *Vsig1*^{F} allele in TAM-treated animals.

Epithelial cell differentiation requires a complex sequence of molecular events to establish polarized domains with specialized functions. Establishment of epithelial cell polarity is initially directed by cell adhesion molecules, followed by organization of cytoskeleton and sorting of different polarized proteins to basolateral and apical membranes, which strength the cell-cell adhesion and establishes the epithelial cell polarization (Gumbiner, 2000). These cell adhesion proteins and peripheral membrane proteins have been shown to control spindle orientation during mitotic division. The difference between multilayered epithelium of forestomach and monolayered epithelium of glandular stomach may reflect planar difference of spindle orientation in squamous epithelium from apical axis to planar-oriented spindle (David, 2004). As consequence of change in spindle orientation we expected the transdifferentiation of multilayered epithelium into monolayered in *Vsig1*-transgenic mice. To address this question, we generated cyto-*Vsig1* mice. In

cyto-*Vsig1* allele, the *Vsig1* cDNA is under the control of cytokeratin 5 promoter. This promoter is transactivated in basal layer of squamous epithelium. Analysis of cyto-*Vsig1* transgenic mice revealed overexpression of *Vsig1* in basal layers of squamous epithelium of esophagus and forestomach. However, histological analysis of transgenic forestomach and esophagus did not show overt structural changes in squamous epithelium.

It has been shown that ectopic expression of intestinal-specific gene cdx2 in stomach leads to transdifferentiation of glandular epithelium to intestinal epithelium (Silberg *et al.,* 2002). To investigate whether the ectopic expression of *Vsig1* in intestine can induce the transdifferentiation of intestinal epithelium, we have generated Vill-*Vsig1* transgenic mice. Analysis of transgenic mice revealed the overexpression of *Vsig1*in intestine. However, histological analysis did not reveal any obvious changes in histological structure of intestine of transgenic mice.

4.5-The role of *Vsig1* in spermatogenesis

The seminiferous epithelium in adult testis is composed of germ cells and polarized Sertoli cells that provide nutrients for germ cells. There are two cell junction complexes between testicular cells. The inter-Sertoli cell junctions are tight junctions (Tjs) that are formed between adjacent Sertoli cells (Sertoli-Sertoli Tj) and compose the blood-testis barrier (BTB) (Cheng and Mruk, 2002). The other cell adhesion junction (Aj) is formed between Sertoli cells and spermatids. The major role of Sertoli-spermatid adhesion junctions is to orientate developing spermatids in the epithelium, with their heads located toward the basement membrane of the seminefrous tubules. Sertoli-spermatid Ajs are loosened when spermatids are released into the lumen of seminiferous tubule (Fig. 4.3) (Mruk and Cheng, 2004). Disruption of Sertoli-spermatid Ajs by inactivation of genes coding adhesion molecules leads to misoriented spermatids and spermatid depletion from the epithelium (Ozaki-kurada *et al*., 2002).

Cell adhesion molecules of JAM/CTX and nectin family are highly expressed in testis. JAM/CTX and nectin family molecules are involved in the Sertoli-Sertoli Tjs and Sertoli-spermatid Ajs through homotypic and heterotypic interactions. Nectin-2 is expressed on both Sertoli and germ cells, whereas nectin-3 is only expressed in spermatids (Ozaki-kurada *et al.*, 2002).

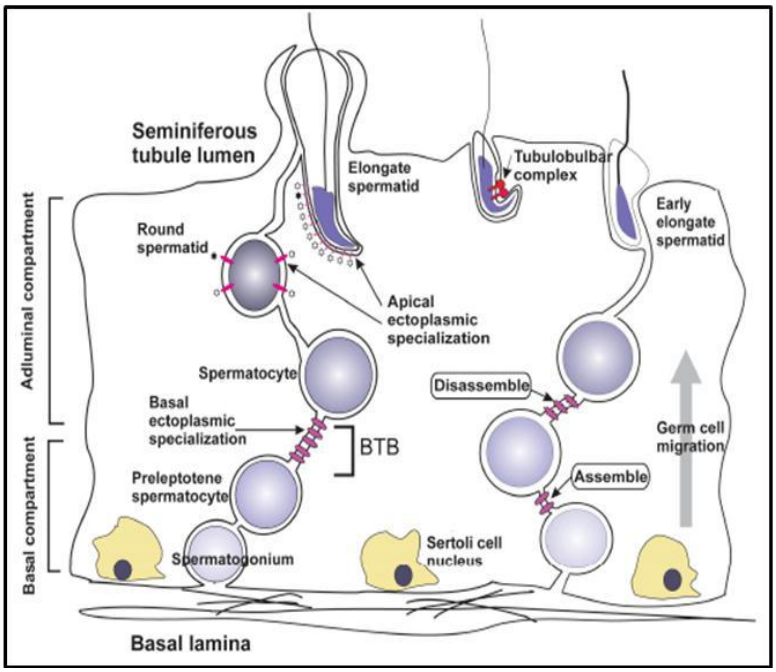

Figure 4.3: *Movement of developing germ cells in the seminiferous tubule of the adult testis. Germ cells first have to break through the tight junctions at the BTB with minimal disruptions. After the opening of the BTB, the progression of germ cells relies solely on series of transient adherens junctions at the Sertoli–germ cell interface. Assembly and disassembly of junctional complexes at the basal and apical ectoplasmic specialization occurs continuously (Wang and Cheng, 2007).*

Immunohistolgical analysis showed that nectin-2 is localized at the inter-Sertoli cell junction. At the Sertoli-spermatid adhesion junctions, nectin-2 and -3 forms heterotypic binding. In testes of nectin-2 and -3 knockout mice, the Sertoli-spermatid Ajs have not been formed properly. Both knockout mice exhibited defective sperm morphology and male infertility (Mruk and Cheng, 2004; Inagaki *et al.*, 2006). JAM-B is located at the membrane of Sertoli cells and interacts in heterotypic manner with JAM-C, which is present at plasma membrane of spermatids (Gliki *et al*., 2004). Analysis of JAM-B and –C knockout mice showed that both are required for the differentiation of round spermatids into spermatozoa (Gliki *et al*., 2004).

Analysis of testis of *Vsig1*$^{F/Y}$*CreERT* mice after 20 day of TAM treatment revealed the spermatogenesis is arrested at round spermatids stage. However, these results require further analysis.

5-Summary

The aim of this study was to determine the expression pattern of *Vsig1* during testis development and analysis of the conditional *Vsig1*knockout mouse, transgenic Cyto-*Vsig1* and Villin-*Vsig1* mouse.

Expression analysis revealed that *Vsig1* gene transcribes two alternatively spliced mRNA variants, namely 2.4-kb *Vsig1A* and 1.6-kb *Vsig1B*. The *Vsig1A* transcript is regulated by sequences locating in 5' flanking region of exon1a, while the shorter transcript *Vsig1B* is presumably directed by sequence locating in the 5' flanking region of exon1b. Northern blot analysis showed that *Vsig1A* is expressed in Sertoli cells of testis and in glandular epithelium of stomach. RT-PCR analysis revealed the expression of *Vsig1A* during embryonic development of testis.

Expression of *Vsig1B* was first detectable in testis of postnatal day 20 suggesting that the expression of *Vsig1B* is restricted to haploid spermatids. Immunofluorescent analysis of testis sections and germ cell suspension revealed that VSIG1 is loclized in the centrosome of dividing germ cells and elongated spermatids. Western blot analysis showed the presence of the shorter VSIG1B protein in the cytoplasmic fraction of testis extract. The centrosomal localization of VSIG1 was also confirmed by immunofluorescent staining of primary fibroblast, NIH 3T3 embryonic fibroblast and embryonic stem cells (ESC). The VSIG1 was colocalized with γ-tubulin, a centrosomal marker, in centrosomes of all stages of mitotic division.

To study the role of VSIG1 in cell-cell adhesion and migration, a stable transfected HepG2 cell line overexpressing VSIG1 was generated. Results of migration and spreading assays revealed that overexpression of VSIG1 increases the migration and adhesion properties of cells.

To determine the consequence of *Vsig1* deletion, two conditional knockout mouse lines have been generated: *Vsig1-CreEIIa* and *Vsig1CreERT*. In *Vsig1-CreEIIa* mice showed the absence of VSIG1 protein in stomach of hemizygous $Vsig1^{\Delta/y}$ males, while *Vsig1* expression in stomach of heterozygous $Vsig1^{\Delta/f}$ females was in a chimeric pattern. Histological analysis of stomach from neonatal and adult $Vsig1^{\Delta/y}$ showed no overt structural abnormalities in comparison to that of wild-type mice. Immunostaining using anti-H^+/K^+ ATPase antibody, which is a marker of parietal cells of gastric gland, revealed that the number of parietal cell in wild-type stomach is significantly higher than that in cKO stomach.

To study the temporal deletion of *Vsig1* in the *Vsig1CreERT* mouse line, the animals were injected by TAM. H&E staining of stomach sections from cKO and wild-type mice showed no differences in histological structure or in the number of parietal cells in gastric units between wild-type and cKO stomachs after 10 and 20 days of TAM treatment. Analysis of $Vsig1^{\Delta/y}$ testes 10 and 20 days after TAM treatment showed that the number of round spermatids was markedly lower than that of treated controls at the same age. These results were confirmed by immunostaining of testis sections using anti-Apg1 antibody which is a meiotic and postmeiotic marker. These results suggest that *Vsig1*-deficiency leads to an arrest of spermatogenesis at round spermatid stage.

The ectopic expression of *Vsig1* in intestine under the control of villin promoter or in stratified squamous epithelium under the control of cytokeratin 5 promoter showed no overt structural differences between wild-type and transgenic animals.

6-References

Andreeva A.V., Kutuzov M.A., Thachuk V.a. and Voyno-Yasenetskaya T.A. (2009). T-cadherin is located in the nucleous and centrosome in the endothelial cells. *Am.Physiol.cell.Physiol.297:C11168-C1177.*

Ausubel FM, Brent R, Kingston RE, Moore DD, Seidman JG, Smith JA and Struhl K, (1994). "Current protocols in molecular biology." John Wiley & Sons Inc., USA.

Badano J. L., Teslovich T. M. and Katsanis N. (2005) The centrosome in human genetic disease. *Nature Rev.Genet. 6:194–205.*

Barclay A.N. (2003). Membrane proteins with immunoglobulin-like domains—a master superfamily of interaction molecules. *Sem.Immunol. 15: 215–223.*

Bazzoni G. (2003). The JAM family of junctional adhesion molecules. *CurrOpin Cell Biol; 15: 525-30.*

Bazzoni G., Dejana E.(2001). Pores in the sieve and channels in the wall: control of paracellular permeability by junctional proteins in endothelial cells. *Microcirculation.8:143-152.*

Beauchemin N., Draber P., Dveksler G, Gold P., Gray-Owen S., Grunert F., Hammarstrom S., Holmes K.V.,. Karlsson A., Kuroki M., Lin S. H., Lucka L., Najjar S.M., Neumaier M., Obrink B., Shively J.E., Skubitz K.M., Stanners C.P., Thomas P Thompson., J.A., Virji M., von Kleist S., Wagener C., Watt S., and Zimmermann W. (1999). Redefined nomenclature for members of the carcinoembryonic antigen family. *Exp. Cell Res. 252:243–249.*

Becker A,, Lucka L.. Kilian C., Knnnicht C. and Reutter W. (1993) Characterisalion of the ATP-depcnJent Iaurocliolat-cnrricr protein (gp 1 10) 01 the hcptitocyte canalicular mcmhrane. *EIU: J. Biorhom.214, 539- 548.*

Birnboim, H.C. and J. Doly (1979). A rapid alkaline extraction for screening recombinant plasmid DNA. *Nuc. Acid Res., 7:1513-1523.*

Black D.L. (2003). Mechanisms of alternative pre-messenger RNA splicing. *Annu.Rev. Biochem.72:291-336.*

Bornens M., Bailly E., Gosti F. and Keryer G. (1990) The centrosome: recent advances on structure and functions. *Prog.Mol.Subcell.Biol.11:86–114.*

Bradford M.M., (1976). "A rapid and sensitive method for the quantitation of microgram quantities of protein utilizing the principle of protein-dye binding. *Anal Biochem. **72**:248-54.*

Brittan M. and Wright N.A. (2002). Gastrointestinal stem cells. *J. Path. 197(4): 492–509.*

Cheng C.Y. and Mruk D.D. (2002). Cell junction dynamics in the testis: Sertoli-germ cell interactions and male contraceptive development. *Physiol.Rev.82:825–874.*

Clark JM, (1988). "Novel non-templated nucleotide addition reactions catalyzed by procaryotic and eucaryotic DNA polymerases." *Nucleic Acids Res.* **16**:9677-86.

Conduit P.T. and Raff J.W. (2010). Cnn Dynamics Drive Centrosome Size Asymmetry to Ensure Daughter Centriole Retention in Drosophila Neuroblasts. *Current Biology 20, 2187–2192.*

David B. (2004). Epithelial polarity and proliferation control: links from Drosophila neoplastic tumor suppressors. *Genes Dev.18: 1909-1925.*

Denhardt D. T. (1966). A Membrane-Filter Technique for the Detection of Complementary DNA. *Biochem. Biophys. Res. Commun, 23: 641-6.*

Dooley T.P., Miranda M., Jones N.C., DePamphilis M.L. (1989). Transactivation of the adenovirus EIIa promoter in the absence of adenovirus E1A protein is restricted to mouse oocytes and preimplantation embryos. *Development 107(4):945-56.*

Feil R., Brocard J., Mascrez B., LeMeur M., Metzger D. and Chambon, P. (1996). Ligand-activated site-specific recombination in mice. *Proc. Natl. Acad. Sci. USA 93: 10887-10890*.

Feinberg A.P. and Vogelstein B. (1984). A technique for radiolabeling DNA restriction endonuclease fragments to high specific activity. *Addendum Anal. Biochem., 137; 266-267.*

Fujii T, Takahashi Y, Ikari A, Morii M, Tabuchi Y, Tsukada K, Takeguchi N, and Sakai H, (2009). Functional Association between K^+-Cl^- Cotransporter-4 and H^+,K^+-ATPase in the Apical Canalicular Membrane of Gastric Parietal Cells. *J. Biol.Chem., 284: 619–629.*

Garrick D., Fiering S., Martin D.I.K., and Whitelaw E. (1998). Repeatinduced gene silencing in mammals. *Nat. Genet. 18: 56–59.*

Gershoni J. M, Palade G. E. (1982). Electrophoretic Transfer of Proteins from Sodium Dodecyl Sulfate-Polyacrylamide Gels to a Positively Charged Membrane Filter. *Anal. Biochem, 124: 396-405*

Gliki G, Ebnet K, Aurrand-Lions M, Imhof BA, Adams RH (2004). Spermatid differentiation requires the assembly of a cell polarity complex downstream of junctional adhesion molecule-C. *Nature 431:320–324.*

Gumbiner B.M. (1996). Cell adhesion: the molecular basis of tissue architecture and

morphogenesis. *Cell 84(3):345-57.*

Gumbiner B.M. (2000). Regulation of cadherin adhesive activity. *J.Cell Biol.148(3):399-404.*

Hemmila E., Turbide C., Olson M., Jothy S., Holmes K.V. and Beauchemin N. (2004). Ceacam1a$^{-/-}$ Mice Are Completely Resistant to Infection by Murine Coronavirus Mouse Hepatitis Virus A59. *J.Virol.78(18):10156-10165.*

Henikoff S. (1998). Conspiracy of silence among repeated transgenes. *Bioessays 20(7):532-5*
.

Hodge R, (1994). "Preparation of RNA gel blots." *Methods Mol Biol.* **28**:49-54.

Hu G, 1993. "DNA polymerase-catalyzed addition of nontemplated extra nucleotides to the 3' end of a DNA fragment. *DNA Cell Biol.* **12**:763-70.

Inagaki M., Irie K., Ishizaki H., Tanaka-Okamoto M., Miyoshi J. and Takai Y. (2006). Role of cell adhesion molecule nectin-3 in spermatid development. *Genes.Cells.(11):1125-1132.*

Jacobsen C.M., Narita N., Bielinska M., Syder A.J., Gordon J.I., Wilson D.B. (2002). Genetic mosaic analysis reveals that GATA-4 is required for proper differentiation of mouse gastric epithelium. *Dev.Biol.241(1):34-46.*

Johnson J.M., Castle J., Garrett-Engele P., Kan Z., Loerch P.M., Armour C.D., Santos R., Schadt E.E., Stoughton R. and Shoemaker D.D. (2003). Genome-wide survey of human alternative pre-mRNA splicing with exon junction microarrays. *Science 302: 2141-2144.*

Kim B.M., Miletich I., Mao J., McMahon A.P., Sharpe P.A., Shivdasani R.A. (2007). Independent functions and mechanisms for homeobox gene Barx1 in patterning mouse stomach and spleen. *Development 134(20):3603-13.*

Kim E., Lee Y., Kim J.S., Song B.S. Kim S.U., Huh J.W., Lee S.R., Kim S.H., Hong Y. and Chang K.T. (2010). Extracellular domain of V-set and immunoglobulin domain containing 1 (VSIG1) interacts with sertoli cell membrane protein, while its PDZ-binding motif forms a complex with ZO-1. *Mol.Cells.30(5):443-448.*

Kochanski R.S. and Borisy G.G. (1990). Mode of centriole duplication and distribution. *J Cell Biol. 110(5):1599-605.*

Kopera I.A., Bilinska B., Cheng C.Y. and Mruk D.D. (2010). Sertoli–germ cell junctions in the testis:a review of recent data. *Phil. Trans. R. Soc. 365, 1593–1605.*

Laemmli UK, (1970). "Cleavage of structural proteins during the assembly of the head of the bacteriophage T4. *Nature.* **227**:680-685.

Laird PW, Zijderveld A, Linders K, Rudnicki MA, Jaenisch R and Berns A, (1991). "Simplified mammalian DNA isolation procedure." *Nucleic Acids Res.* **19**:4293.

Lakso M., Pichel J.G., Gorman J.R., Sauer B., Okamoto Y., Lee E., Alt F.W., Westphal H. (1996). Efficient in vivo manipulation of mouse genomic sequences at the zygote stage. *Proc Natl Acad Sci U S A. 93(12):5860-5.*

Lander E.S., Linton L.M. and Birren B., (2001). Initial sequencing and analysis of the human genome. *Nature 409 (6822): 860–921.*

Lersch R., Fuchs E. (1988). Sequence and expression of a type II keratin, K5, in human epidermal cells. *Mol Cell Biol. 8(1):486-93.*

Lorthongpanich C., Yang S., Piotrowska-Nitsch K., Parnpa R. and Chan A.W.S. (2008). Development of single mouse blastomeres into blastocysts, outgrowths and the establishment of embryonic stem cells. *Reproduction 135:805–813.*

Lucka L., Cichocka I., Bäumler K., Bechler K. and Reuter W. (1995). A short isoform of carcinoembryonic-antigen-related rat liver cell-cell adhesion molecule (C-CAWgpllO) mediates intercellular adhesion Sequencing and recombinant functional analysis. *Eur.J.Biochem.234:572-535.*

Manandhar G., Moreno R.D., Simerly C., Toshimori K. and Schatten G. (2000a). Contractile apparatus of the normal and .bortive cytokinetic cells during mouse male meiosis. *J.Cell Sci. 113(23):4275-4286.*

Manandhar G., Simerly C. and Schatten G. (2000b). Centrosome reduction during mammalian spermiogenesis. *Curr.Top.Dev.Biol. 49:343–363.*

Manandhar G., Simerly C., Salisbury J.L. and Schatten G. (1999). Centriole and centrin degeneration during mouse spermiogenesis. *Cell Motil Cytoskeleton. 43:137–144.*

Manandhar G., Sutovsky P., Joshi H.C., Stearns T. and Schatten G. (1998). Centrosome reduction during mouse spermiogenesis. *Dev Biol 1998; 203:424–434.*

Matlin A.J., Clark F. and Smith C.W.J. (2005). Understanding alternative splicing: towards a cellular code. *Nature Rev.6(5):386–398.*

Matsuyama M., Chijiwa T., Inoue Y., Abe Y., Nishi M., Miyazaki N., Furukawa D., Mukai M., Suemizu H., Sekido Y., Ueyama Y., Nakamura M. (2009). Alternative splicing variant of vascular endothelial growth factor-A is a critical prognostic factor in non-small cell lung cancer. *Oncol Rep. 22(6):1407-13.*

Modrek B. and Lee C. (2002) A genomic view of alternative splicing. *Nat. Genet., 30, 13-19.*

Mruk D.D. and Cheng C.Y. (2004). Sertoli-Sertoli and Sertoli-germ cell interactions and their significance in germ cell movement in the seminiferous epithelium during

spermatogenesis. *Endocr.Rev.25:747–806.*

Nigg E.A. (2002). Centrosome aberrations: cause or consequence of cancer progression? *Nature Rev.Cancer 2, 815–825.*

Oidovsambuu O., (2009) Expression and Functional Analysis of Vsig1 Gene. PhD thesis.

Ozaki-Kuroda K., Nakanishi1 H., Ohta H., Tanaka H., Kurihara H., Mueller S., Irie K., Ikeda W., Sakai T., Wimmer E., Nishimune Y. and Takai Y. (2002). Nectin couples cell–cell adhesion and the actin scaffold at heterotypic testicular junctions. *Curr. Biol. 12, 1145–1150.*

Palermo G.D., Colombero L.T. and Rosenwaks Z. (1997). The human sperm centrosome is responsible for normal syngamy and early embryonic development. *Rev.Rep2:19–27.*

Praetorius H.A. and Spring K.R. (2005). A physiological view of the primary cilium. *Annu.Rev Physiol. 67: 515–529.*

Que J., Okubo T., Goldenring J.R., Nam K.T., Kurotani R., Morrisey E.E., Taranova O., Pevny L.H., Hogan B.L. (2007). Multiple dose-dependent roles for Sox2 in the patterning and differentiation of anterior foregut endoderm. *Development 134(13):2521-31.*

Ramalho-Santos M., Melton1 D.A., and McMahon1 A.P. (2000). Hedgehog signals regulate multiple aspects of gastrointestinal development. *Development 127, 2763-2772.*

Raschperger E., Engstrom U., Pettersson R.F., and Fuxe J. (2004). CLMP, a Novel Member of the CTX Family and a New Component of Epithelial Tight Junctions. *J.Biol.Chem.279(1):796–804.*

Resch A., Afonyushkin T., Lombo T.B., Mcdowall K.J., Bläsi U. and Kaberdin V.R. (2008). Translational activation by the noncoding RNA DsrA involves alternative RNase III processing in the rpoS 59-leader. *RNA 14:454–459.*

Resch A., Xing Y., Modrek B., Gorlick M., Riley R., Lee C. (2004). Assessing the impact of alternative splicing on domain interactions in the human proteome. *J. Proteome Res. 3(1):76-83.*

Rieder Cl., Faruki S., Khodjakov A. (2001). The centrosome in vertebrates: more than a microtubule-organizing center. *Trends in cell biology 11 (10): 413–9.*

Sanger F, Nicklen S and Coulson AR, (1977). DNA sequencing with the chain terminating inhibitors. *Proc Natl Acad Sci U S A. 74:5463-7.*

Scanlan M.J., Ritter G., Yin B.W.T., Williams C.Jr., Cohen L.S., Coplan K.A., Fortunato S.R., Frosina D., Lee S., Murray A.E., Chua R., Filonnenko V.V., Old L.J. and Jungbluth A.A. (2006). Glycoprotein A34, a novel target for antibody-based

cancer immunotherapy. *Can.Immunol. 6:1-6.*

Schatten G. (1994). The centrosome and its mode of inheritance: the reduction of the centrosome during gametogenesis and its restoration during fertilization. *Devel.Biol.165:299–335.*

Semb H. and Christofori G. (1998). INSIGHTS FROM MODEL SYSTEMS The Tumor-Suppressor Function of E-Cadherin. *Am. J. Hum.Genet. 63:1588-1593.*

Silberg D.G., Sullivan J. , Kang E. , Swain G.P., Moffett J., Sund N.J., Sackett S.D., Kaestner K.H. (2002). Cdx2 ectopic expression induces gastric intestinal metaplasia in transgenic mice. *Gastroenterology 122(3):689-696.*

Sorek R., Lev-Maor G., Reznik M., Dagan T., Belinky F., Graur D. and Ast G. (2004). Minimal conditions for exonization of intronic sequences: 5´splice site formation in alu exons. *Mol. Cell, 14, 221–231.*

Southern E. M. (1975). Detection of Specific Sequences among DNA Fragments Separated by Gel Electrophoresis. *J. Mol. Biol, 98: 503-17.*

Takai Y., Irie K., Shimizu K., Sakisaka T., and Ikeda W. (2003). Nectins and nectin-like molecules: Roles in cell adhesion, migration, and polarization. *Can.Sci,94:655-667.*

Takamoto N., You L., Moses K., Chiang C., Zimmer W.E., Schwartz R.J., DeMayo F.J. M.Tsai1 and Tsai1 S.Y. (2005). COUP-TFII is essential for radial and anteroposterior patterning of the stomach. *Development 132, 2179-2189.*

Van den Brink G.R, de Santa Barbara P., Roberts D.J. (2001). Development. Epithelial cell differentiation--a Mather of choice. *Science 7;294(5549):2115-6.*

Van den Brink G.R. (2007). Hedgehog signaling in development and homeostasis of the gastrointestinal tract. *Physiol.Rev.87(4):1343-75.*

Volkmer H., Zacharias U., Nörenberg U., Rathjen F.G. (1998). Dissection of Complex Molecular Interactions of Neurofascin with Axonin-1, F11, and Tenascin-R, Which Promote Attachment and Neurite Formation of Tectal Cells. *J.Cell.Biol.142(4):1083-1093.*

Vooijs M., Jonkers J., Berns A. (2001). A highly efficient ligand-regulated Cre recombinase mouse line shows that LoxP recombination is position dependent. *EMBO Rep. 2(4):292-7.*

Wegmann F., Petri B., Khandoga A.G., Moser C., Khandoga A., Volkery S., Li H., Nasdala I., Brandau O., Fässler R., Butz S., Krombach F. and Vestweber D. (2006). ESAM supports neutrophil extravasation, activation of Rho, and VEGF-induced vascular permeability. *J Exp Med.203(7):1671–1677.*

Wells J.M, Melton D.A. (1999). Vertebrate endoderm development. *Annu.Rev.Cell Dev.*

Biol.15:393-410.

Woolley D.M. and Fawcett D.W. (1973). The degeneration and disappearance of the centrioles during the development of the rat spermatozoon. *Anat.Rec.177:289–301.*

Zahler A.M. (2005). Alternative splicing in C. elegans. WormBook, ed. The C. elegans Research Community, WormBook, doi/10.1895/ wormbook.1.31.1, http://www.wormbook.org

Curriculum Vitae

Personal details:

Name:	Maiada Moustafa
Permanent address:	Am Vogelsang 1,
	37075 Göttingen
E-mail:	maiada112000@yahoo.com
Date of birth:	11.01.1979
Place of birth:	Cairo
Nationality:	Egyptian

Educational background:

1991 –2000:	Primary and secondary school and university
2000 –2001:	Course of premaster: Biology (embryology) Faculty of Science, Helwan University, Egypt
2001 –2004:	Master thesis: "Effect of Xenobiotics on Embryonic Development of Fish" Faculty of Science, Helwan University, Egypt Supervisor: Prof. Dr. med. Amany Tohamy, Prof. Dr. Ibrahim Abdelkader and
Since Nov. 2006:	Doctoral thesis: "Studies on Expression and Function of Vsig1 Gene'' Institute of Human Genetics, Georg-August-University Göttingen, Germany Supervisor: Prof. Dr. med. Dr. h. c. Wolfgang Engel

18.01.2010

ACKNOWLEDGEMENTS

I would like to express my deep and sincere gratitude to my supervisor, Prof. Dr. med. Wolfgang Engel, Director of Institute of Human Genetics, University of Göttingen. His wide knowledge and his logical way of thinking have been of great value for me. His understanding, encouraging and personal guidance have provided a good basis for the present thesis.

I am heartily thankful to my group leader, Prof. Dr. Ibrahim M. Adham, whose encouragement, guidance and support from the initial to the final level enabled me to develop an understanding of the subject.

I owe my most sincere gratitude to Professor Sigrid Hoyer-Fender who accepted to be my co-referee in this study.

During this work I have collaborated with many colleagues for whom I have great regard, and I wish to extend my warmest thanks to all those who have helped me with my work in the "Institute of Human Genetics".

I owe my loving thanks to my parents, family and friends. Without their encouragement and support it would have been impossible for me to finish this work.

The financial support of the Egyptian Government is gratefully acknowledged.

Göttingen, Germany, 2010

Maiada Moustafa